

THE DEFORMATION PROPERTIES OF CLAD  
SHEET METALS

BY

R. HAWKINS, B.Sc. (Hons)., Grad. I.M.

A thesis for consideration for the degree of Doctor of Philosophy of the University  
of Aston in Birmingham.

AUGUST, 1970.

621.77 HAW  
22 MAR 71 136162



## SUMMARY

The techniques commonly used to produce clad sheet metals and the properties of these materials are reviewed.

Experimental work is described for a range of two and three layer copper—steel composites produced by adhesive and roll bonding, the materials being processed to give a range of copper—steel thickness ratios. The tensile, plane strain compression, deep drawing and stretch forming properties of the composites were determined, the experimental results being compared with those calculated theoretically by means of the equal stress or equal strain hypothesis.

The results showed that the stress—strain behaviour of the composites in both tension and compression; proof stress; ultimate tensile strength and the maximum punch loads for both deep drawing and stretch forming could be accurately predicted using the equal strain hypothesis. Properties such as uniform elongation and 'R' value could not be predicted with the same degree of accuracy; this being attributed to the accuracy with which these properties could be experimentally determined. The 'n' values for the composites could not be simply predicted by means of the equal strain hypothesis, but a relationship has been derived, and experimentally verified, to enable 'n' to be predicted from the stress—strain characteristics of the individual components. The stretch formability of the composites could not be predicted by the equal strain hypothesis because stretch formability was dependent upon the ductility of the component on the outermost surface during deformation.

The existing theory for calculation of draw stress in the drawing of cylindrical flat bottomed cups has been modified so that the draw stress for composites may be calculated from the stress—strain characteristics of the individual components. The results from the modified theory have been shown to be as accurate as the results obtained for single metals calculated by the conventional theory.



## CONTENTS

	Page No.
1.0 INTRODUCTION	1
2.0 CLAD MATERIALS	2
2.1 THE PRODUCTION OF CLAD MATERIALS	2
2.1.1 Roll Bonding	3
2.1.2 Adhesive bonding	5
2.1.3 Summary of cladding techniques	7
2.2 THE MECHANICAL PROPERTIES OF CLAD MATERIALS	8
2.2.1 Concluding summary	20
3.0 THE PRESS FORMING OF SHEET METAL	21
3.1 STRETCH FORMING	21
3.2 DEEP DRAWING	21
4.0 THE ASSESSMENT OF PRESSFORMING PROPERTIES OF SHEET METAL.	26
4.1 THE USE OF SIMULATIVE TESTS	26
4.1.1 Stretch forming tests	27
4.1.2 Deep drawing tests	28
4.2 THE USE OF NON-SIMULATIVE TESTS AND THEIR CORRELATION WITH SIMULATIVE TESTS AND PRESSING BEHAVIOUR	29
4.2.1 Hardness tests	30
4.2.2 Tensile test	30
4.2.3 Plane strain compression test	35
5.0 THE PRESS FORMING PROPERTIES OF CLAD MATERIALS	37
6.0 EXPERIMENTAL PROCEDURE	38
6.1 MATERIALS USED	38
6.2 PRODUCTION OF COMPOSITES	39
6.2.1 Adhesive bonded composites	39
6.2.2 Roll bonded composites	41
6.3 ELECTRON PROBE MICROANALYSIS	42
6.4 X-RAY DIFFRACTION	43
6.5 TENSILE PROPERTIES	43



	Page No.	
6.6	<i>DEEP DRAWING PROPERTIES</i>	
6.6.1	<i>Equipment</i>	46
6.6.2	<i>Test variables</i>	48
6.6.3	<i>Determination of critical blank diameters</i>	52
6.6.4	<i>Earing measurements</i>	52
6.6.5	<i>Thickness surveys on drawn cups</i>	52
6.7	<i>STRETCH FORMING PROPERTIES</i>	52
6.8	<i>PLANE STRAIN COMPRESSION TESTS</i>	53
6.9	<i>TESTS ON THE STEEL AND COPPER COMPONENTS OF THE COMPOSITES</i>	55
6.10	<i>DEEP DRAWING OF UNBONDED COMPOSITES</i>	56
7.0	<b>EXPERIMENTAL RESULTS</b>	58
7.1	<i>ELECTRON PROBE MICROANALYSIS</i>	58
7.2	<i>X-RAY DIFFRACTION</i>	59
7.3	<i>TENSILE PROPERTIES</i>	62
7.4	<i>DEEP DRAWING AND STRETCH FORMING PROPERTIES</i>	68
7.5	<i>PLANE STRAIN COMPRESSION</i>	77
7.6.	<i>TESTS ON THE STEEL AND COPPER COMPONENTS OF THE ROLL BONDED COMPOSITES</i>	85
7.6.1	<i>Tensile properties</i>	85
7.6.2	<i>Deep drawing and stretch forming properties</i>	85
7.7	<i>DEEP DRAWING OF UNBONDED COPPER/STEEL COMPOSITES</i>	93
8.0	<b>DISCUSSION</b>	98
8.1	<i>CURLING OF TESTS PIECES IN THE TENSILE TESTS</i>	98
8.2	<i>THE COMPARISON OF CALCULATED AND EXPERIMENTAL STRESS-STRAIN CURVES</i>	100
8.2.1	<i>Application of the equal stress hypothesis</i>	101
8.2.2	<i>Application of the equal strain hypothesis</i>	101
8.2.3	<i>Graphical interpretation of the equal stress and equal strain hypotheses.</i>	102
8.2.4	<i>Stress-strain analysis for roll bonded composites</i>	102
8.2.5	<i>Stress-strain analysis for adhesive bonded composites</i>	105



	Page No.
8.3. <i>COMPARISON OF CALCULATED AND EXPERIMENTAL MECHANICAL PROPERTIES</i>	108
8.3.1 <i>Properties of the roll bonded composites</i>	110
8.3.2 <i>Properties of the adhesive bonded composites</i>	114
8.3.3 <i>Summary of the comparisons of calculated and experimental mechanical properties.</i>	118
8.4 <i>GENERAL DISCUSSION OF THE DEEP DRAWING AND STRETCH FORMING RESULTS</i>	123
8.4.1 <i>Limiting draw ratios</i>	123
8.4.2 <i>Earing</i>	124
8.4.3 <i>Deep drawing of unbonded composites</i>	130
8.4.4 <i>Stretch forming</i>	131
8.5 <i>APPLICATION OF THE EQUAL STRAIN HYPOTHESIS TO THE DEEP DRAWING AND STRETCH FORMING PROPERTIES.</i>	134
8.5.1 <i>Calculation of the punch loads for the composites</i>	135
8.5.2 <i>Calculation of the earing properties of the composites</i>	135
8.6 <i>THE THEORETICAL CALCULATION OF MAXIMUM DRAW STRESS</i>	142
8.7 <i>THE PLANE STRAIN COMPRESSION PROPERTIES OF THE ROLL BONDED COMPOSITES</i>	145
8.7.1 <i>The relationship between true stress and true strain</i>	145
8.7.2 <i>Anisotropy in plane strain compression</i>	153
8.7.3 <i>Optimum clad ratio</i>	155
8.8 <i>APPLICATION OF THE EQUAL STRAIN HYPOTHESIS TO THE PLANE STRAIN COMPRESSION PROPERTIES</i>	158
9.0 <b>SUGGESTIONS FOR FURTHER WORK</b>	161
10.0 <b>CONCLUSIONS</b>	162
11.0 <b>ACKNOWLEDGMENTS</b>	164
12.0 <b>REFERENCES</b>	165
<b>APPENDICES:</b>	
1. <i>Analysis of the deep drawing process for the drawing of flat bottomed cylindrical cups.</i>	168
2. <i>Selection of an adhesive for the production of the adhesive bonded composites.</i>	173
3. <i>The theoretical calculation of draw stress.</i>	176



## UNITS

This work was commenced at a time of transition from Imperial to S.I. units and for this reason both units are used in this work. For simplicity, particularly in tables of results, Imperial units have been omitted where the initial measurements were made in S.I. or metric units e.g. for the tensile and press forming properties.

At the commencement of this work, the metallurgical industries preferred the hectobar to the S.I. unit of  $\text{GN/m}^2$  or  $\text{kN/mm}^2$  for stress and this unit has been adopted for this work.

To aid conversion of hb to Imperial units, or vice versa, a nomogram is included. For more accurate conversions the following conversion factors may be used.

$$1 \text{ t.s.i.} = 1.5444 \text{ hb}$$

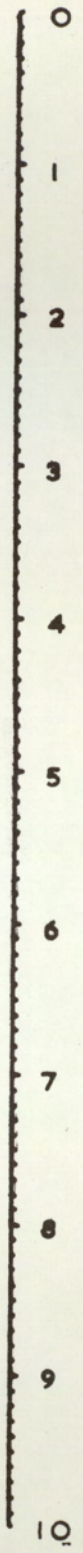
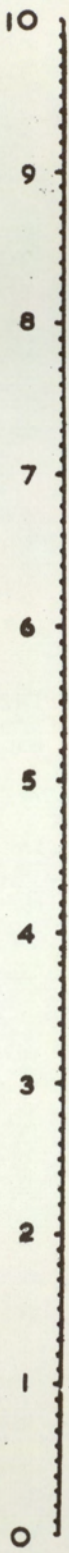
$$1 \text{ hb} = 1.02 \text{ kg/mm}^2$$

$$1 \text{ hb} = 100 \text{ kN/mm}^2 = 1\text{kN/cm}^2$$



hb

tsi



$$1 \text{ hb} = 1.5444 \text{ tsi}$$



## 1.0 INTRODUCTION

It has for many years been realised that the common engineering materials do not possess ideal combinations of, for example, mechanical, physical and corrosion properties. This, along with the increased demands placed on materials by technological advances, has led to the use of composite materials. The use of composite materials may, however, be traced back to ancient Egypt where straw was mixed with clay and hair added to plaster to produce stronger building materials. The extension of this principle to the strengthening of metals is a much more recent innovation, although early examples of "metallic" composite materials include Damascus steel, wrought iron and electro-plated articles.

The term "composite" material may be used to describe any material that is made up of various distinct components. For the purposes of this work the term "composite material" will be used to refer to any material in which at least one of the component parts is metallic. Within this definition of composite practically any desired combination of properties e.g. strength coupled with lightness or strength with oxidation resistance, may be obtained by careful selection of the basic components forming the composite.

There are several types of composite material even within the limitations imposed by the above definition, but for convenience these may be roughly divided into two categories:

- Group 1. — those in which fibres, "whiskers" or second phase particles are distributed within a, usually ductile, matrix e.g. fibre-re-inforced, dispersion and precipitation hardened materials.
- Group 2. — layered materials which consist of layers of one or more metals. These may alternatively be known as clad, coated, sandwich or bimetals.

It is with this second group of composites that this work is concerned and, for this reason, the discussion will be confined to these. Throughout this thesis group 2 composites will simply be referred to as clad materials.



## 2.0 CLAD MATERIALS

### 2.1 *THE PRODUCTION OF CLAD MATERIALS*

There are numerous techniques used for producing clad material, but a review of all these techniques is beyond the scope of this thesis. The techniques that are, or in the author's opinion, could be used to produce clad flat plate or strip include: roll, explosive, diffusion or adhesive bonding, casting, hot dipping, metal spraying, weld deposition, electrodeposition and powder compaction.

For the experimental work, clad material having an extensive diffusion or alloy layer was considered undesirable because the mechanical properties of this layer would be difficult, if not impossible, to determine. However, in practically all cladding techniques diffusion plays an important part in the formation of a bond.

Diffusion processes may be classified into two groups:

- a. high pressure, low temperature
- b. low pressure, high temperature

It is this second group of diffusion processes that would produce material having an extensive diffusion or alloy layer. Of the techniques previously listed, roll and explosive bonding may be classified in group (a), and casting, hot dipping, metal spraying and weld deposition in group (b), diffusion playing little, or no part, in the bonding process for adhesive bonding, electrodeposition and powder compaction.

Electrodeposited coatings are normally 0.002 – 0.005" thick, although thicker coatings may be produced. A wide range of clad ratios was required for the experimental work, the clad thickness ranging from 0.01" to 0.06", so that electro-deposition was not considered suitable in these circumstances.

The mechanical properties of the individual components, making up the clads, were required for comparison purposes so that unbonded components were required in similar metallurgical conditions to those making up the clads. This condition would probably rule out the use of roll compacting of powders because this would necessitate the production of strip direct from powder, a process that is still largely in the experimental stages.

It may be seen that clad strip, suitable for use in the experimental work, could be produced by either roll, explosive or adhesive bonding. Of these three



processes only roll bonding is used commercially to produce clad material suitable for the experimental work. Explosive bonding is generally limited to the production of thick plate, the process only being competitive with other cladding techniques for clads greater than 2" thick<sup>(1)</sup>. Adhesive bonding, although usually used for specialised applications, such as the production of aircraft skin panels or helicopter rotor blades, may be used to produce clad strip. The bonding process is relatively simple and is easily performed in the laboratory with little specialised equipment or knowledge.

This thesis is not primarily concerned with the production of clad material, so that only the roll and adhesive bonding techniques are discussed.

### 2.1.1. *ROLL BONDING*

Roll bonding is the most common process used to produce clad metals. The process may be used to produce both plate and thin sheets, for the former hot rolling is generally employed, whereas cold rolling is generally used for the latter.

For the production of clad plates, sandwich packs are made up as shown in figure 2.1. The packs are usually hot rolled on normal production lines, being treated as homogeneous metal. Multi-layer packs may be used, provided that they are symmetrical, otherwise differences in thermal expansion and deformation characteristics will cause warping on rolling and on cooling.

A three stage process<sup>(2)</sup> is best used for the production of clad strip. The process consists of :—

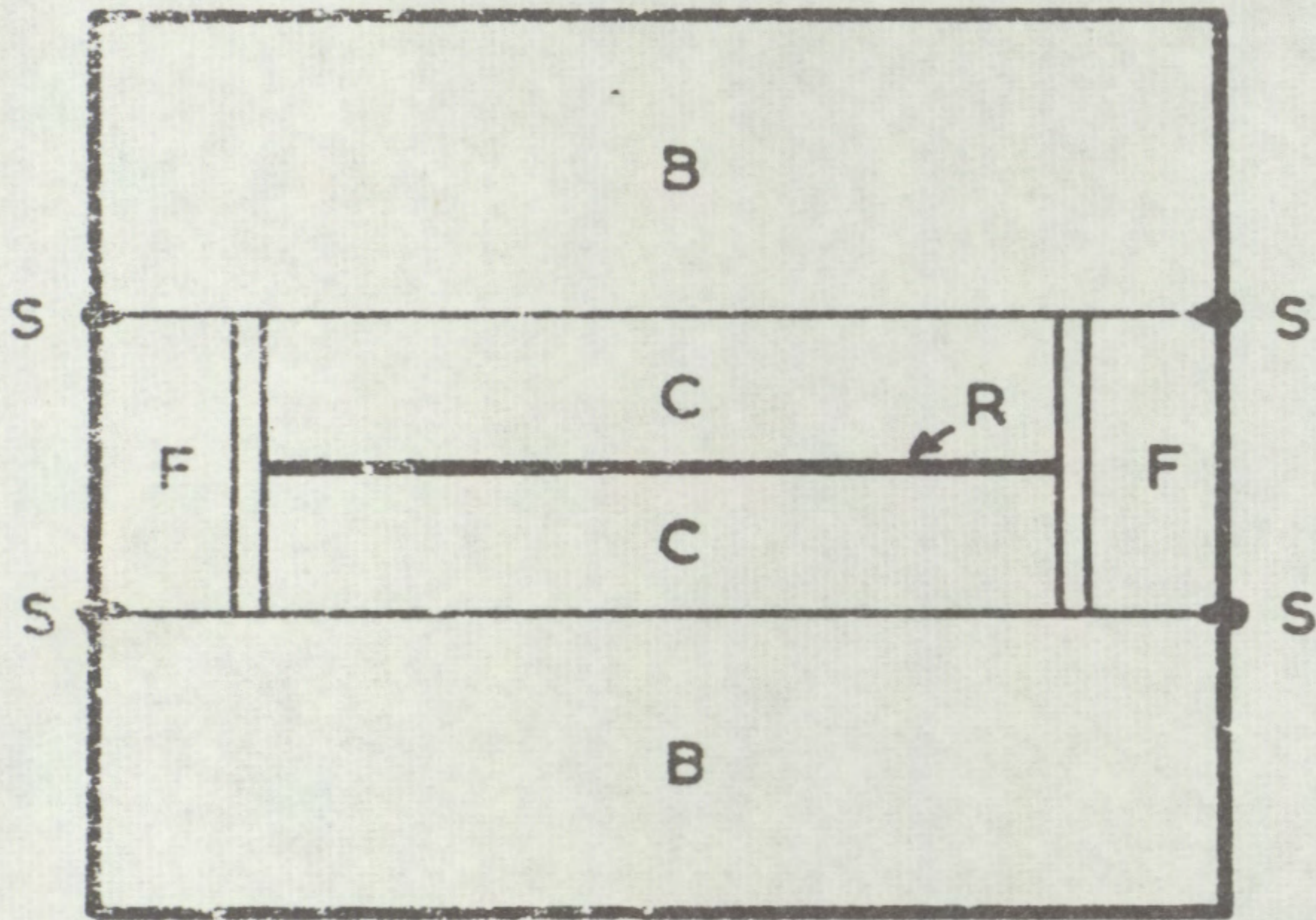
- i. cleaning of the faying surfaces
- ii. production of a green bond
- iii. sintering

In the cleaning stage all visible contaminants, e.g. oil and scale are carefully removed from the faying surfaces. Immediately after cleaning, the two or more strips are passed through a cladding mill and undergo at least a 50% reduction in thickness. Numerous discrete bonds are produced which grow laterally during sintering to produce a strong and substantially continuous bond.

For the production of sound bonds the first two stages of the process are critical. The incorporation of a heating cycle, during the cleaning operation, has been found advantageous in that any films escaping removal in other operations are



a)



B Base Metal  
C Cladding Metal  
R Refractory Separating Layer  
F Filler Strips  
S Sealing Welds

b)

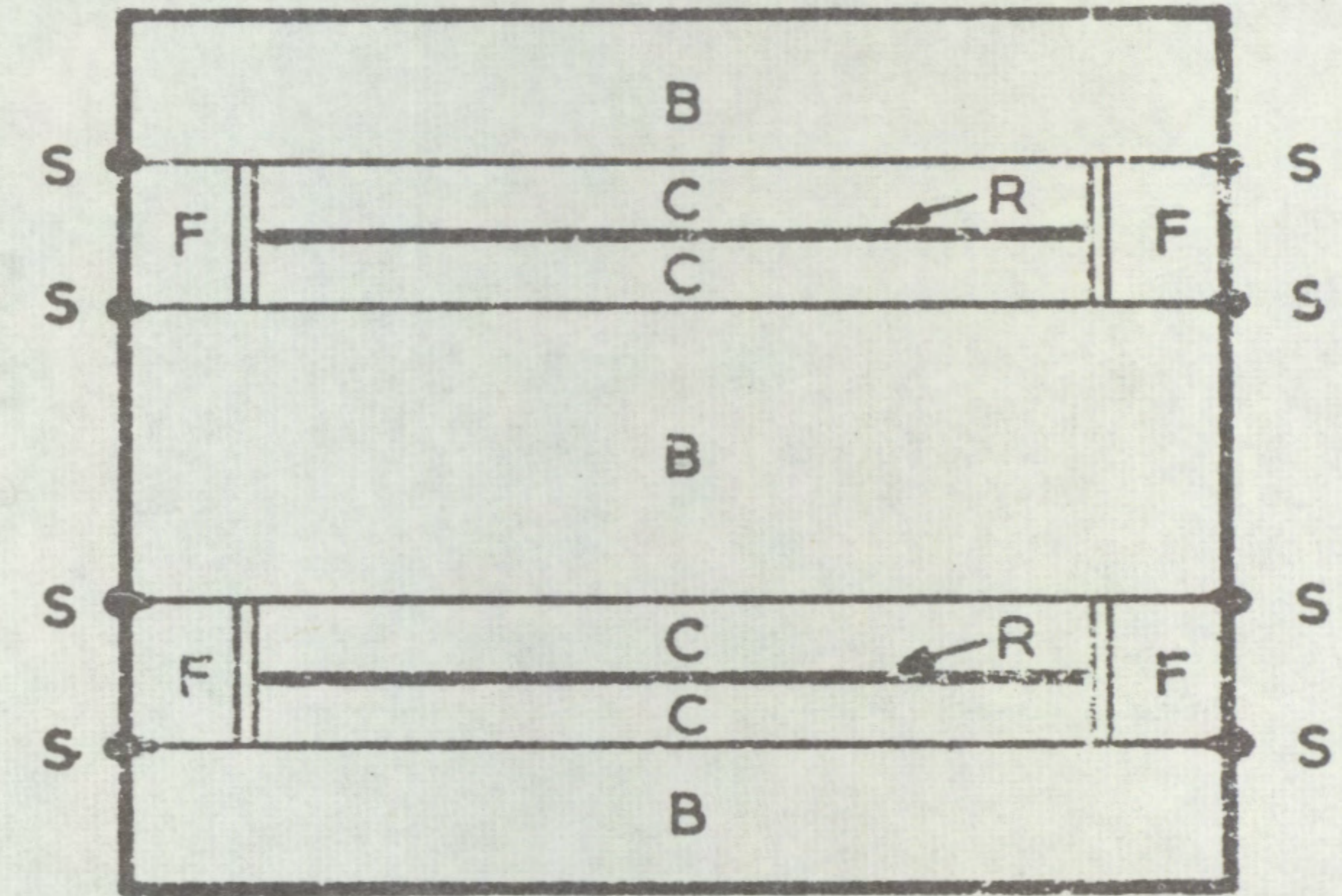


Figure 2.1. Sandwich packs, used to produce plates clad

(a) on one side only.

(b) on both sides.



dehydrated and, therefore, do not produce gaseous products during the sintering stage. In the second stage of the process, the production of a green bond, the deformation must exceed the threshold deformation necessary for bonding. Several workers<sup>(3-7)</sup> have attempted to establish the threshold deformation required to produce a bond, the results of their work being summarised in table 2.1. It may be seen from table 2.1 that reductions of at least 40% are necessary to achieve bonding when the process is carried out in air, although much lower reductions are required if the process is carried out in vacuum. An alternative to vacuum rolling is the use of evacuated packs which may be rolled on conventional rolling mills at elevated temperatures<sup>(8,9)</sup>.

The high reductions, necessary to achieve bonding, provides two limitations on the process :

- a. The annealing temperature of the clad metal, after bonding, is determined by the metal having the lowest melting point, unless differential hardening is acceptable.
- b. As the thickness of the metal increases the size of the mill also increases until a point is reached where other processes, e.g. explosive bonding, become more economical.

Despite its disadvantages roll bonding is the most common process used to produce clad metals. A wide range of metals are clad commercially, although some combinations, e.g. titanium and steel or stainless steel and carbon steel, may require a third metal to be interposed between the two base metals to prevent the formation of an alloy or intermetallic compound at the interface<sup>(10,11)</sup>.

#### 2.1.2. *ADHESIVE BONDING*

In the search for a more efficient method for structural assembling, the aircraft industry pioneered structural adhesive bonding. The high cost of the adhesives has tended to restrict the use of this technique except for specialised applications. Structural adhesives are used extensively by the aircraft industry, where the high cost of the adhesive is more than compensated by the weight saving the process affords over conventional mechanical joining techniques, e.g. welding, rivetting or bolting.

Adhesives are generally classified as thermoplastic or thermosetting. The thermoplastic polymers are flexible and have a tendency to creep, examples of such



Table 2.1 Minimum reduction required to produce a bond in roll bonding.

METALS USED	% REDUCTION	COMMENTS	REFERENCE
Copper	45	—	Agers <sup>(3)</sup>
Aluminium	40	—	"
Copper and Aluminium	65	—	Donelan <sup>(4)</sup>
—	40	Minimum to produce any bonding	Rollason <sup>(5)</sup>
—	70	To give 100% bonding	"
—	2	Small work rolls in vacuum	"
Niobium to Steel	30–40	10–15% per pass	Krivosov etal <sup>(6)</sup>
Refractory or Reactive metal combinations	5–40	Rolled in inert atmosphere	Bianchi <sup>(7)</sup>



adhesives are those based on acrylic, vinyl and polyvinyl resins. In contrast, the thermosetting polymers give permanence and rigidity, examples of such adhesives are those based on epoxy, phenolic and phenol-formaldehyde resins. Frequently adhesives are a blend of these two types to combine these properties, an example of such a blend being Redux\*.

Adhesives based on epoxy resins usually consist of two parts, the resin and a hardener to produce intermolecular cross-linking of the resin. The two components are mixed and hardening is usually accelerated by curing at an elevated temperature. During the curing process no volatiles are produced so that the pressure applied need only be sufficient to maintain the alignment of the components. There is a wide range of this type of adhesive available, because of the different combinations of resin and hardener, so that the cure temperature may range from below room temperature to above 200° C. One part adhesives are also available, hardening being effected solely by the application of heat.

Redux is a vinyl phenolic resin, the original adhesive consisting of a liquid resin and a thermoplastic powder which was cured by the simultaneous application of heat and pressure. For ease of application the adhesive is now often in the form of a thin film, although the two part variety is still widely used. During curing at elevated temperature (above 130° C) a small amount of water vapour is produced which necessitates the use of high pressures (up to 100 p.s.i.) during the cure cycle.

Structural adhesives are suitable for use under pure tension, shear and compression loadings but have poor strengths under peel or cleavage loadings. Provided the latter forms of loading are avoided adhesives may be used to produce strong bonds between a wide range of metals and non-metals.

### 2.1.3. SUMMARY OF CLADDING TECHNIQUES

Clad sheet metal, having a limited diffusion or alloy layer, may be produced by roll, or adhesive bonding. Roll bonding produces clad material having a direct metal to metal bond, the bond being effected by a combination of deformation and interdiffusion. With adhesive bonding, neither deformation nor interdiffusion are necessary to produce sound bonds.

\* Registered trade name of C.I.B.A. (A.R.L.) Ltd., Duxford, England.



Adhesives that are likely to be useful for the production of clad sheet metals are those based on thermosetting polymers or those produced by blending thermosetting and thermoplastic polymers. Thermoplastic polymers are not considered suitable as structural adhesives because of their tendency to creep. It is, however, possible that adhesives based on thermosetting polymers may be too brittle, although Davies <sup>(12)</sup> has successfully used this type of adhesive to produce aluminium clad copper, and subsequently deformed the material in plane strain compression.

Both cladding techniques may be used to clad a wide range of metals and alloys, with the roll bonding technique care must, however, be taken that brittle phases are not produced during the bonding process. The temperatures and pressures used in adhesive bonding, up to 200° C and 100 p.s.i. respectively, are such, that components may be bonded without appreciably changing their mechanical or crystallographic properties. The significance of this will be discussed in a later section of this thesis.

## 2.2 THE MECHANICAL PROPERTIES OF CLAD MATERIALS

The properties of composite materials may be determined using the rule of mixtures, i.e. the properties of the composite will be the weighted average of the properties of the individual components. The averaging of the properties may be made by either assuming that the strain in each component is equal or that the stress on each component is equal. These assumptions give rise to the following hypotheses :

### a. Equal strain hypothesis :

if it is assumed that the strain on each component is equal, then the stresses on the components must be dissimilar, the average stress i.e. the stress acting on the composite, being given by:

$$\sigma_{av} = \sigma_c = \sigma_1 f_1 + \sigma_2 f_2 \dots\dots\dots 2.1$$

where:  $\sigma$  = stress  
 $f$  = volume fraction  
 1,2 = components of the composite  
 $c$  = composite



With the equal strain hypothesis conditions are such that there is complete bonding at the interface and hence the two components deform together.

b. *Equal stress hypothesis :*

if it is assumed that the stress on each component is equal then it follows that the strains experienced by each component are dissimilar. The average strain of the composite is given by :

$$\epsilon_{av} = \epsilon_c = \epsilon_1 f_1 + \epsilon_2 f_2 \quad \dots\dots\dots 2.2$$

where  $\epsilon$  = strain

With the equal stress hypothesis the two components are free to deform more or less independently, with relative movement at the interfaces.

Idealised stress—strain curves illustrating the equal strain and equal stress hypotheses are shown in figure 2.2. (p.10). For any given strain the equal stress hypothesis predicts a lower average, or composite, stress than does the equal strain hypothesis as may be seen in figure 2.2c. The stress for a given strain would increase linearly with increasing volume fraction of the stronger component if the equal strain hypothesis was used to predict stress. However, the equal stress hypothesis does not produce a linear relationship between stress and volume fraction. Similar results have been obtained for the elastic properties of composites as shown in figure 2.3 :

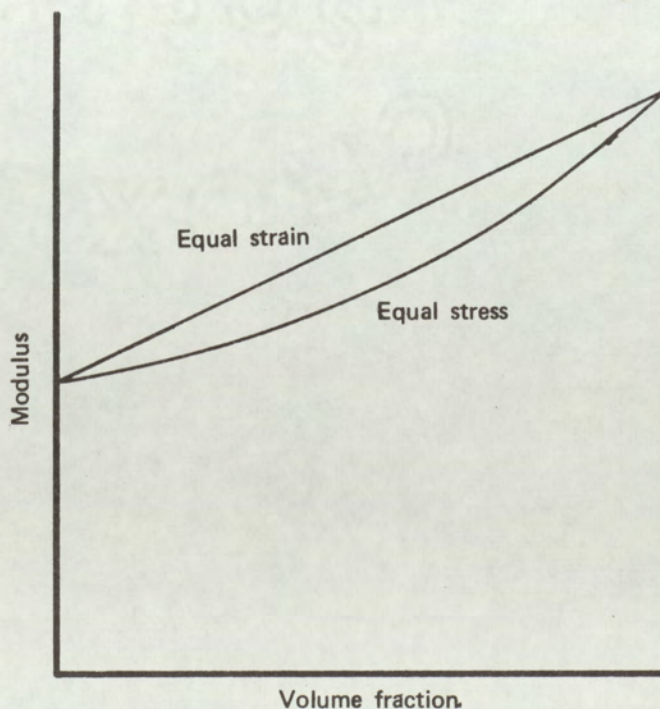


Figure 2.3. The relationship between modulus and volume fraction for the equal strain and equal stress hypotheses<sup>(13)</sup>



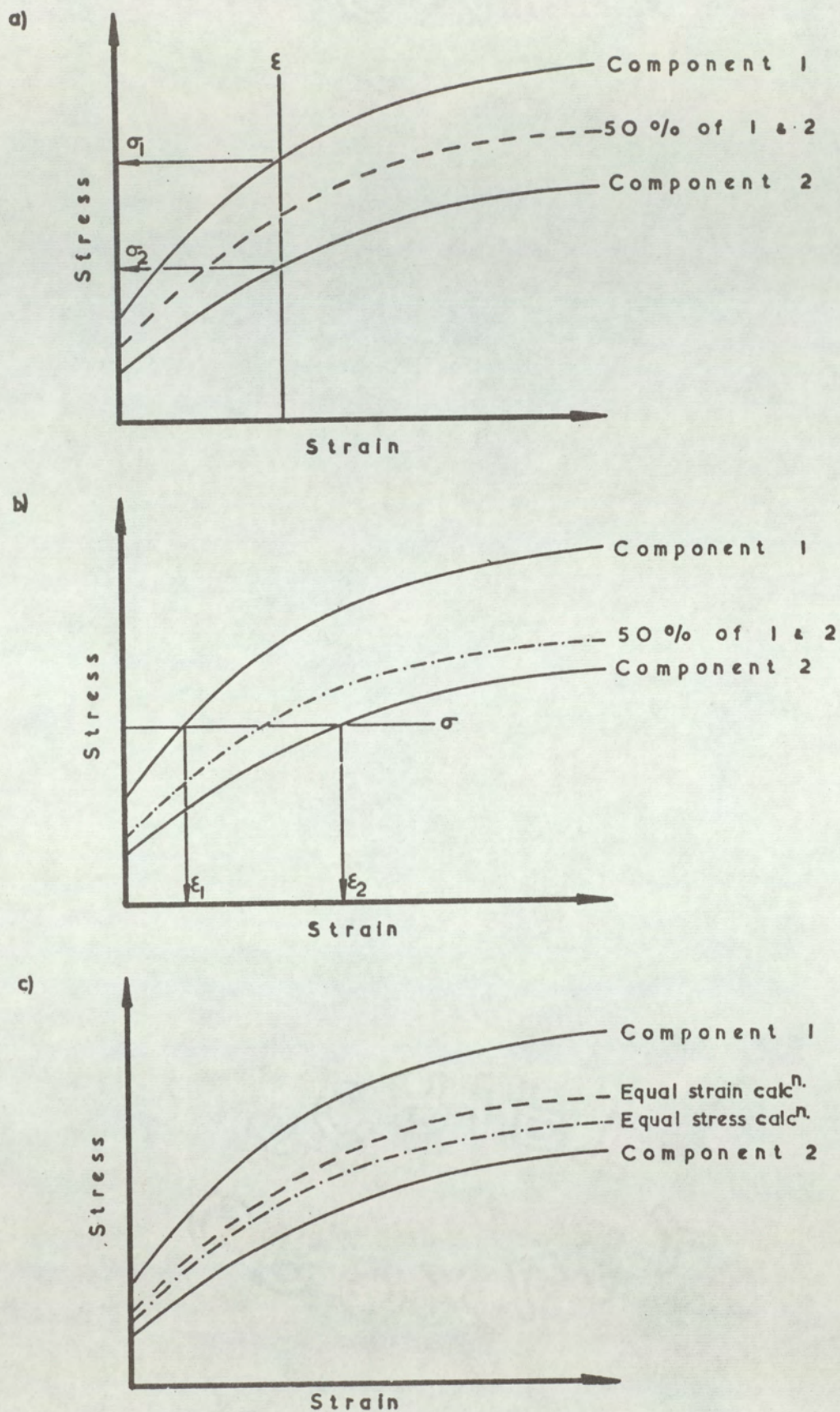


Figure 2.2. Idealised stress–strain curves for two components, 1 & 2, and for a composite of 50% 1 & 2 calculated using:

- The equal strain hypothesis.
- The equal stress hypothesis.
- A comparison of the two calculated stress–strain curves.



The rule of mixtures, therefore, predicts that the properties of composites fall between the two limits shown in figure 2.3, the precise position being dependent on the interfacial restraint between the two components. The upper limit is represented by :

$$E_c = E_1 f_1 + E_2 f_2 \quad \dots\dots\dots 2.3$$

where: E = Elastic Modulus

and the lower limit<sup>(13)</sup> by :

$$E_c = \frac{E_1 E_2}{E_1 f_2 + E_2 f_1} \quad \dots\dots\dots 2.4$$

The empirical equal strain and equal stress hypotheses have been experimentally verified for a wide range of composites. The properties of fibre-reinforced composites have been found best described by the equal strain hypothesis, examples being tungsten wires in a copper matrix,<sup>(14)</sup> fibre-reinforced plastics,<sup>(15)</sup> and aluminium reinforced with steel<sup>(16)</sup>. Dispersion hardened alloys would be expected to obey the equal stress hypothesis provided that there was no hydrostatic constraint between the particles and matrix. Dispersion hardened alloys investigated so far, e.g. tungsten-copper,<sup>(17)</sup> tungsten-iron-nickel,<sup>(18)</sup> & tungsten carbide-cobalt,<sup>(19)</sup> have yielded results that fall between the two hypotheses. This deviation from the equal stress hypothesis means that some degree of hydrostatic tension is generated in all of these materials<sup>(20)</sup>.

Although the use of the equal stress or equal strain hypotheses has been well established for group 1 composites i.e. fibre-reinforced composites, there is little experimental data available for group 2 composites, i.e. clad metals. Delagi<sup>(21)</sup> provides working equations for clad metal composites for such properties as modulus of elasticity, density, thermal conductivity and thermal expansion, that are based on the equal strain hypothesis, but for stress calculations he assumes that the material having the highest modulus of elasticity carries the total load. Several workers,<sup>(12, 22-27)</sup> have, however, utilised the equal strain hypothesis to predict the deformation properties of clad metal composites.

Holmes,<sup>(22)</sup> Arnold & Whitton,<sup>(23)</sup> and Afonja & Sansome,<sup>(24)</sup> confirmed both experimentally, and analytically, the validity of the equal strain hypothesis in their studies of the rolling of hard metal sandwiched between layers of a softer metal.



Both Holmes and Arnold & Whitton determined an equivalent yield stress,  $k$ , for the composite based on the equal strain hypothesis (equation 2.1) :

$$k = \frac{2t_c k_c + t_m k_m}{2t_c + t_m} \dots\dots\dots 2.4$$

where:  $t$  = thickness  
 $k$  = constrained yield stress

suffix  $c$  = clad metal  
 $m$  = core metal

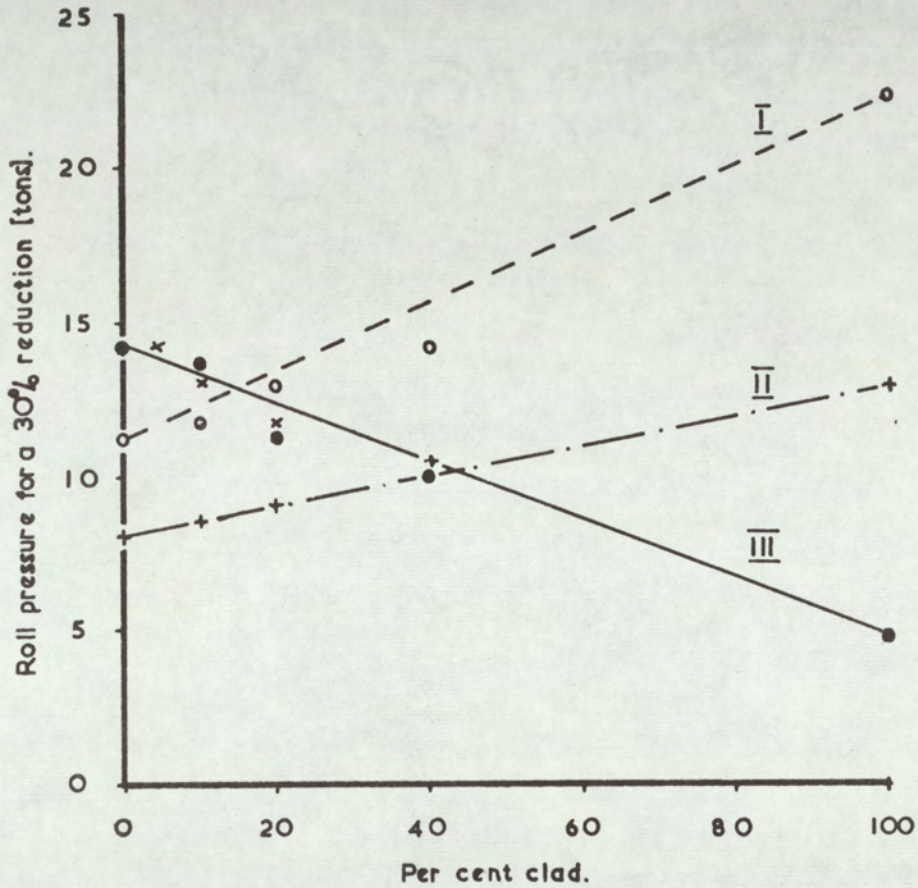
Arnold & Whitton substituted this equivalent yield stress into conventional rolling theories, <sup>(28-30)</sup> treating the sandwich pack as a single metal of yield stress,  $k$ . They found that the hardness ratio of the hard : soft metals was an important variable, their theory having limited application to composites having hardness ratios above about 3 (hardness being expressed as Vickers Diamond Pyramid values). For composites having hardness ratios less than 3, differential reduction of the composite components was small for rolling reductions above 15%, thus showing that the assumption of equal strain was valid. However, with hardness ratios greater than 3, the differential reduction increased and the assumption of equal strain was no longer valid. These conclusions were, however, derived from a study of only three clads having hardness ratios of 1.5, 2.5 and 4.0, hardly sufficient evidence for concluding that the theory is not applicable to hardness ratios greater than 3. Furthermore, the authors do not point out that this conclusion may be completely invalidated if frictional restraint between clad and core is increased with hardness ratio. Frictional restraint at the clad/core interface is more likely to control the degree of differential reduction obtained in sandwich rolling, and hence the validity of Arnold & Whitton's theory, than is hardness ratio.

The agreement between Arnold & Whitton's experimental and calculated rolling loads depended, to some extent, upon the rolling theory used in their calculations although the majority of the calculated results were within  $\pm 10\%$  of the experimental results.

Leug, in a communication to Arnold & Whitton's paper presented results of Pomp & Leug, <sup>(25)</sup> showing that roll pressure was reduced in hot rolling a core metal plated on both sides with a metal having a lower resistance to deformation, thus



substantiating Arnold & Whitton's results. Pomp & Leug deformed test pieces of pure copper, unplated steel and steel plated on one or both sides with copper and determined curves of roll pressure against per cent reduction. From these curves the authors constructed a graph of roll pressure against per cent clad for a 30% reduction as shown in figure 2.4. :



Steel plated on both sides with:

- copper and rolled at  $900^{\circ}\text{C}$
- 18/8 Cr/Ni " " "  $1000^{\circ}\text{C}$
- + 18/8 Cr/Ni " " "  $1100^{\circ}\text{C}$

Steel plated on one side with:

- x copper and rolled at  $900^{\circ}\text{C}$

Figure 2.4. The influence of clad thickness on roll pressure in hot rolling plated steel <sup>(25)</sup>.



From figure 2.4, Pomp & Leug concluded that the roll pressures for the clad metal lay approximately on the line connecting the roll pressures for the component metals (in other words the properties of the clad could be determined by the equal strain hypothesis). The authors also concluded that the same applied when the cladding metal had a higher resistance to deformation than had the core metal.

It may be seen from figure 2.4 that Pomp & Leug only studied composites containing up to 40% clad, so that their conclusions are really only valid up to this point. Although the deviation, between the experimental values and those predicted by the equal strain hypothesis (represented by lines I to III), appears to be less than 10%, the results for steel, plated on both sides with 18/8 chromium–nickel steel, and rolled at 1100° C seem to fit the equal stress hypothesis better, unless the result for 100% clad is incorrect.

Davies<sup>(12)</sup> and Walker<sup>(27)</sup> applied the equal strain hypothesis in their studies of the plane strain compression properties of copper–aluminium and copper–steel respectively and obtained similar agreement between experimental and calculated results as was obtained by Arnold & Whitton. Davies, however, found that the equal strain hypothesis only held for reductions less than 50%. Above this strain level the experimental values of stress decreased whilst the calculated values continued to increase (as shown in figure 2.5). Davies explained this behaviour by saying that the horizontal tensile stress, induced on the copper at the interfaces with the aluminium, eventually reaches a value where the overall stress deviator on the copper is tensile. When this stage is reached it is analogous to the behaviour of a specimen in tension with a super-imposed pressure on the sides of the test piece. Localised thinning and eventual failure of the core material takes place, hence the decrease in the curve shown in figure 2.5 until the curves for the composite and the aluminium coincide.

Walker, however, found that the equal strain hypothesis was applicable to true strain values of at least 1.0, and in none of his tests did the core of the composites fracture, as Davies observed. There were several pronounced differences, both in the materials used in the experimental work, and in the test procedures used by Walker and Davies. The important differences were :—



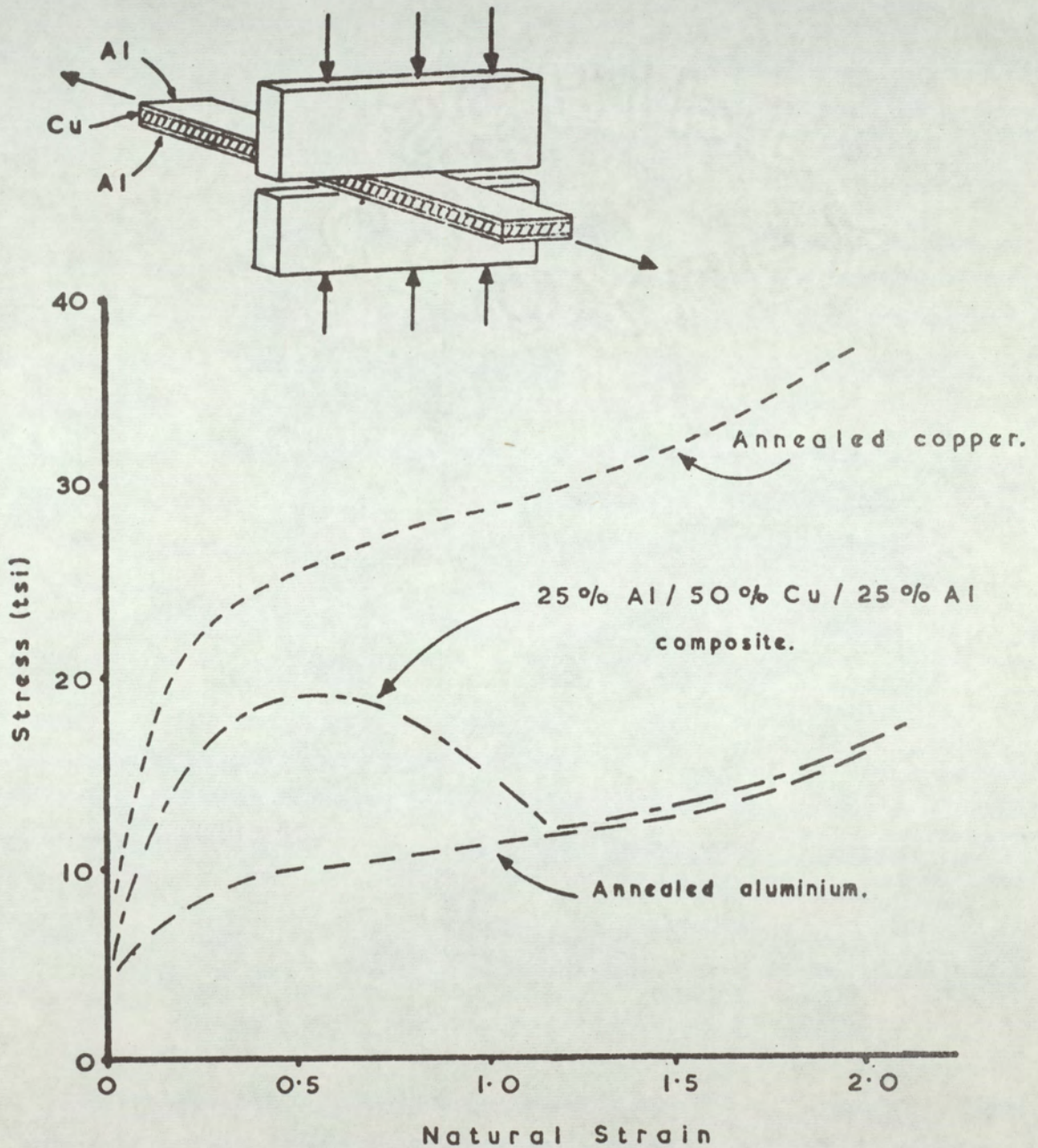


Figure 2.5. Plane strain compression curves for copper, for aluminium and for an adhesively bonded aluminium/copper/aluminium composite<sup>(12)</sup>.



1. Davies used epoxy resin bonded composites whereas Walker used roll bonded composites.
2. The "soft" component in Davies' composites (aluminium) had a lower rate of work hardening than the "hard" component (copper). In Walker's work the "soft" component (copper) had a work hardening rate approximately double that of the "hard" component (steel).
3. Davies used  $b/t$  ratios (i.e. die breadth: sheet thickness) ranging from 0.4 to 0.8, whereas Walker used  $b/t$  ratios of  $> 1.0$ , the majority of his tests being made with ratios of 2 – 4. Watts and Ford<sup>(31, 32)</sup> have shown that the  $b/t$  ratio should be maintained between 2 and 4 throughout the test. For ratios greater than 2, Watts & Ford showed that the yield stress increased only slightly above its true value, but for ratios greater than 4, the contact stress began to rise.

Walker did not satisfactorily resolve the anomalies between his and Davies' results, although he produced sufficient evidence to show that fracture of the core, observed by Davies, could have been a consequence of using  $b/t$  ratios less than the range recommended by Watts & Ford, rather than as a result of stresses generated at the clad-core interfaces.

In the discussion of Arnold & Whitton's analysis, Alexander,<sup>(33)</sup> pointed out that their analysis neglected the influence of interfacial friction, so that it was surprising that it gave such good agreement with their experimental results, but to allow for this in the analysis would produce such complications that the result would not be of great practical interest. The first comment of Alexander's would indicate that either the influence of interfacial friction was small, or their original assumption, that the percentage reduction in the soft and hard metal of the sandwich was the same, was valid. The second of these alternatives is the more likely because:

- (a) Arnold and Whitton observed little differential reduction of the components with hardness ratios less than 3.
- (b) The role of interfacial friction may be determined from equations 2.1 and 2.2, the equal strain and equal stress hypotheses. In the former, friction is high and the components deform together, and in the latter, friction is low and the components deform more or less independently of each other.



The analyses of Weinstein & Pawelski<sup>(26)</sup> and Afonja & Sansome<sup>(24)</sup> were more rigorous than that used by Arnold & Whitton, and an attempt was made to include the influence of friction. Weinstein & Pawelski studied the plane strain drawing of roll bonded (copper – steel) composites. The draw specimens were produced by clamping together, by means of the draw bench pulling head, two similar bimetal specimens with either the steel or the copper on the outside, so as to produce three layer composites. The geometry of the die and specimens was such that the deformation was confined to the thickness, the strip being merely constrained in the width direction.

In the mathematical model, Weinstein & Pawelski derived formulae for the prediction of the mean drawing stress, and the die pressure, the deviation between the theoretical and experimental values being less than 10% for the drawing stress but slightly greater for the die pressure. As Alexander suggested, the analysis was made much more complex by the inclusion of interfacial friction and, in order to simplify the analysis, Weinstein & Pawelski assumed that the bond was of sufficient strength to prevent relative movement and to transmit shear stresses of a magnitude at least equal to the shear strength of the weaker metal, i.e. conditions of equal strain were assumed. In their general analysis, Weinstein & Pawelski showed that the magnitude of the interfacial shear stress depended upon the clad to total sandwich thickness ratio, the relative difference between the yield stresses of the component metals, the die semi-angle and the friction between the die and clad material. It was also shown that the interfacial shear stress was a maximum at approximately 50% clad and that in the extreme case of frictionless drawing of a hard metal, clad with a metal having a very much lower plane strain yield stress, this maximum would be approximately 4% of the yield strength of the matrix.

A similar analysis to Weinstein & Pawelski's was made by Afonja & Sansome<sup>(24)</sup> for the sandwich rolling process. Briefly, Afonja & Sansome derived the normal stress on the clad along the arc of contact and the area under this curve was evaluated to determine the roll separating force. Afonja & Sansome compared the roll force, determined in this manner, with the experimental values, and with that determined using Arnold & Whitton's analysis. For aluminium/steel/aluminium, the maximum difference, based on the measured value, was – 8% using their analysis and – 14.3% using Arnold & Whitton's analysis. Both sets of workers made the same basic assumption that equal strain conditions were applicable, so that the differences in predicted rolling loads may be a reflection of the assumptions each made during the rolling analysis rather than to a difference from their techniques of determining the yield stress of the composite.

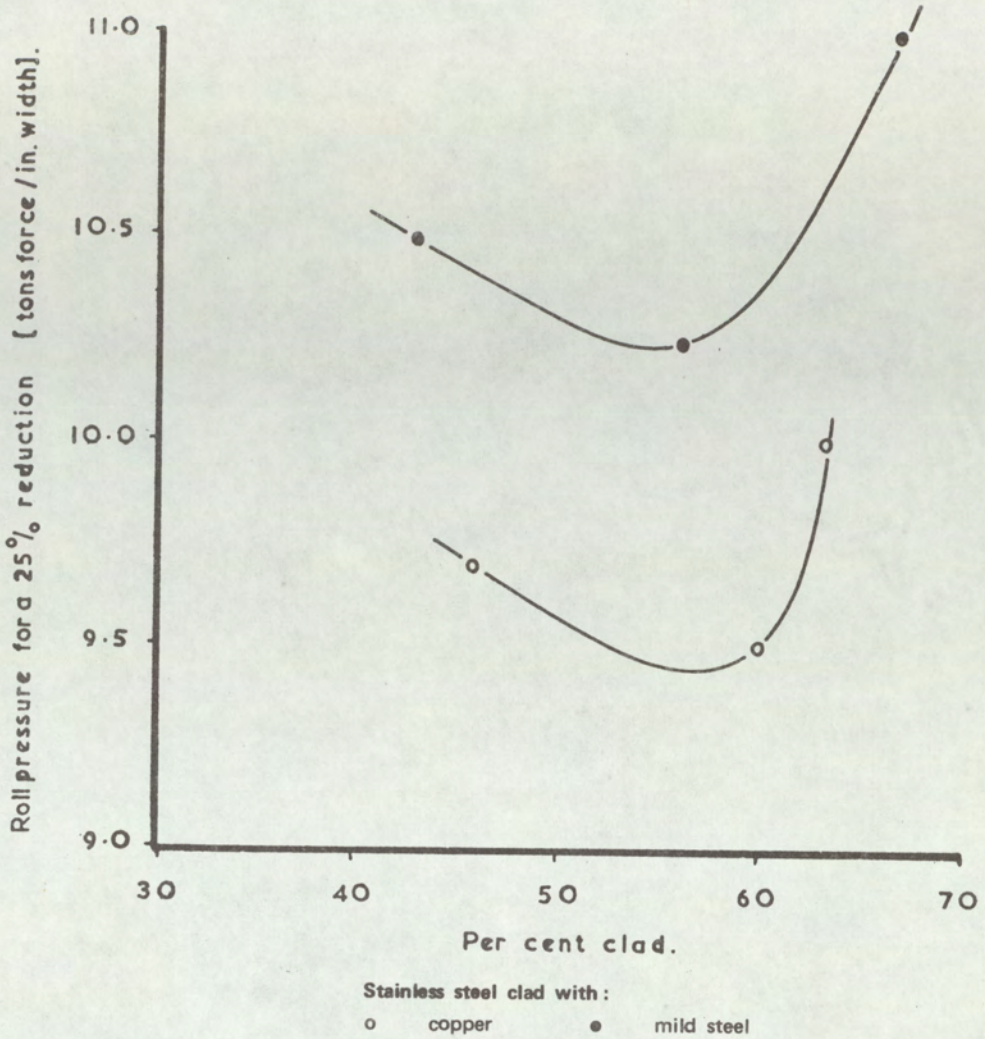


- Like Weinstein & Pawelski, Afonja & Sansome showed that the magnitude of the interfacial shear stress depended upon the reduction achieved, the differences in the yield stresses of the component metals, the clad to sandwich thickness ratio and the friction between the roll and the clad material. In their general analysis of the sandwich rolling process, the interfacial shear stress was shown to be a maximum at 50% clad, thus confirming Weinstein & Pawelski's analysis, but no attempt was made to quantitatively assess its magnitude. Afonja & Sansome did, however, show experimentally that the roll load, for a given reduction, was a minimum between 50 & 60% clad, indicating that there was an optimum clad : core thickness ratio to give maximum reduction in rolling load.

Examples of Afonja & Sansome's results are shown in figure 2.6. from which it may be seen that their conclusions are based on a study of only three clad : core ratios. It may also be seen that the difference between the maximum and minimum values for either curve is small, 0.5 and 0.75 tons/inch width for stainless steel clad with copper and mild steel respectively. It is possible that the minimum observed by the authors may be the result of either experimental scatter in measuring roll load or variation in mechanical properties of the clad components. Afonja & Sansome used 1" wide strip for all their experimental work so that accurate load measuring devices would be required to detect such small differences in load. Variations in the properties of the components of the clads are also likely, especially for the copper or mild steel cladding layers because of the different thicknesses of cladding used. The authors in fact state that the hardness of the copper components was 60 – 70 D.P.N. and that of the steel components 90 – 100 D.P.N., variations in hardness of this magnitude could easily produce variations in roll load of the observed magnitude.

Optimum clad : core thickness ratios have also been reported by Arnold & Whitton<sup>(23)</sup> and Davies<sup>(12)</sup> although their experimental evidence was as weak as Afonja & Sansome's. Arnold & Whitton, however, found that the conditions for determining this optimum ratio could not be simply stated. Some combinations, e.g. aluminium/brass, showed a minimum whereas others, e.g. brass/titanium, did not. Arnold & Whitton recommended that the optimum clad : core thickness ratio to give a minimum deformation load, for a given reduction, was 67: 33, whereas Davies and Afonja & Sansome obtained a ratio of approximately 50: 50.





Thickness of stainless steel (in.)	Thickness of clad (in.)	
	Copper	Mild Steel
0.047	2 x 0.0192	2 x 0.0174
0.047	2 x 0.0352	2 x 0.0287
0.047	2 x 0.0392	2 x 0.0436

Figure 2.6. The influence of clad thickness on roll pressure in cold rolling austenitic stainless steel clad with (I) copper and (II) mild steel.<sup>(24)</sup>



### 2.2.1. CONCLUDING SUMMARY

All of the analyses that have been outlined have made the basic assumption that the composite components were equally strained, although all of the workers, except Walker,<sup>(27)</sup> reported some relative movement of the composite components. When relative movement was small it was shown that the agreement between calculated and experimental values was better than  $\pm 10\%$ . Only Davies and Walker compared calculated and experimental values of flow stress, so it is difficult to assess from the published results the accuracy of the equal strain hypothesis in predicting flow stress, especially when there is no relative movement of the components i.e. the components are equally strained.

Published results show that there is some disagreement as to whether or not there is an optimum clad : core thickness ratio that will give a minimum deformation load for a given reduction and, even when there has been agreement, there has been disagreement over its value.

From this review it may be seen that, although clad metals are widely used, their mechanical and deformation properties have received little or no attention with, perhaps, the exception of sandwich rolling. The object of the work now reported was to examine the mechanical properties of clad metals, with particular reference to deep drawing and stretch forming. In the following section the deep drawing and stretch forming of single metals, and the relationships between simulative and non-simulative tests are discussed.



### 3.0 THE PRESSFORMING OF SHEET METAL

In the pressing of metals two basic, and fundamentally different, processes are involved: stretch forming and deep drawing.

#### 3.1 *STRETCH FORMING*

In stretch forming the metal is clamped rigidly between the die and blank-holder so that, as the punch is advanced, the metal blank is prevented from drawing-in. The metal is deformed by biaxial stretching over the punch profile, failure occurring over the punch nose. The precise position of failure depends on the frictional conditions between the punch and metal, as the frictional conditions are reduced the fracture site will move nearer the pole of the punch.

The use of stretch forming is limited by the onset of plastic instability and, for maximum strain before instability, the material should have a high rate of work hardening. In biaxial stretching the onset of plastic instability occurs at higher strains than in uniaxial stretching, but even so only a quarter of the elongation figure measured in the conventional tensile test is available in the stretch forming process<sup>(34)</sup>.

#### 3.2 *DEEP DRAWING*

In deep drawing the metal blank is allowed to draw in as the punch is advanced. Drawing in of the metal gives rise to a hoop compressive stress in the flange and, in order to relieve this stress, the blank tends to wrinkle and/or thicken. The blank is, therefore, held between the die and blank holder by a pressure just sufficient to suppress wrinkling. The stress system, operative during deep drawing, is more complex than that in stretch forming, the stresses acting on any segment of the cup, being shown in figure 3.1.

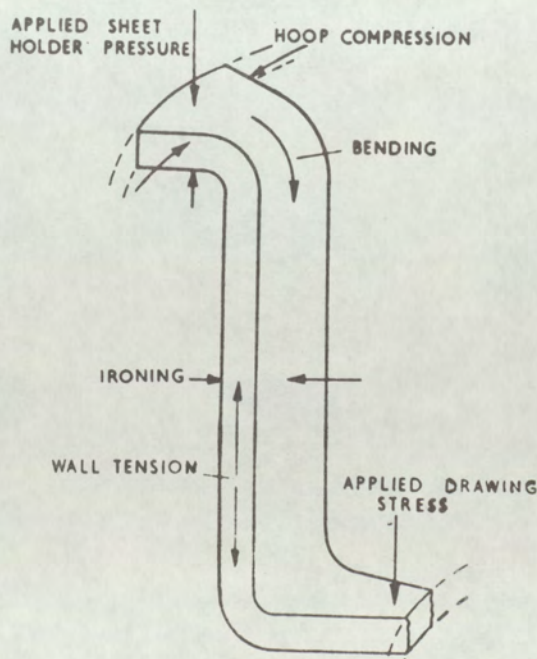


Figure 3.1. The stresses acting on a segment of a cup during deep drawing.



As a result of preventing the metal from wrinkling the flange will thicken during radial drawing, as shown in figure 3.2, so as to maintain constancy of volume.

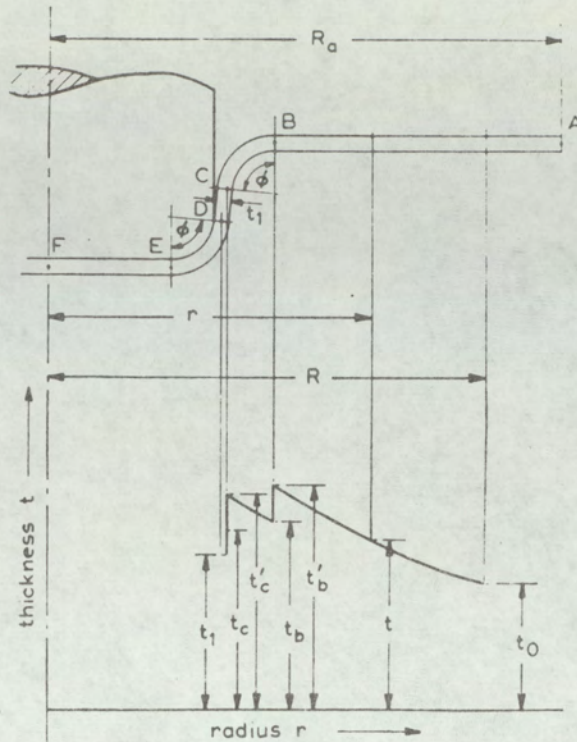


Figure 3.2. The thickness history of an element of the flange during deep drawing.<sup>(36)</sup>

Radial drawing, and hence thickening, continues until the material reaches the die profile radius (point B, figure 3.2) where it is plastically bent and subsequently unbent (point C, figure 3.2) whilst under a tensile stress in the radial direction. This bending and unbending under tension gives rise to a thinning of the metal and is influenced by the friction over the punch nose and the friction between the die and the blank holder.<sup>(37)</sup> High friction over the punch nose inhibits metal flow off the punch and thus reduces thinning and delays plastic instability. In addition, low friction between the die and the blank holder reduces the tendency to thin by reducing the applied tension. Between points B and C, in figure 3.2, radial drawing, and hence thickening of the material, occurs.

The metal may also thin in the cup wall during drawing if the tensile stresses are sufficient to cause plastic flow. Ironing, produced by tension in the direction of drawing and compression between the punch and die, may occur if the clearance between die and punch is inadequate to accommodate a "thickened" blank.



Elementary rings in the rim of a partially drawn cup are subjected to compressive thickness and hoop stresses and also to a radial drawing stress. The hoop compressive stress is a maximum at the periphery of the blank and decreases as the material nears the die throat, whereas the radial stress is a maximum at the die throat and zero at the periphery of the blank. The distribution of both the circumferential hoop stress and the radial drawing stress at various positions along the radius of the deforming blank may be calculated making due allowance for friction. The relative magnitude of these forces were derived by Wright<sup>(35)</sup> from the work of Chung & Swift<sup>(38)</sup> for an annealed mild steel blank and drawing ratio of 2.0, the results being shown in figure 3.3.

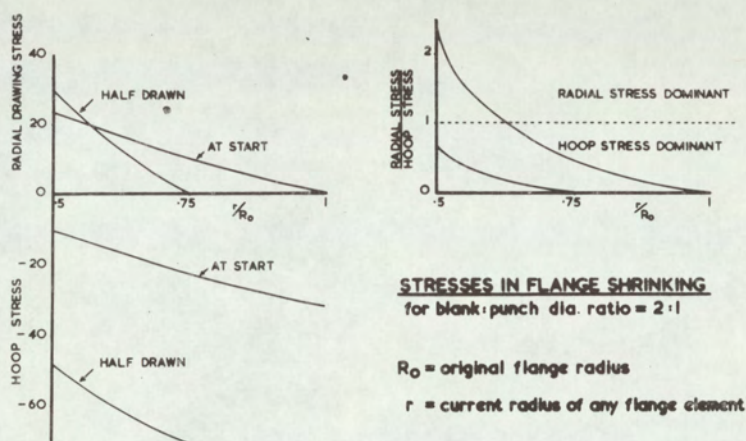


Figure 3.3. Relative stress magnitudes in flange shrinking.<sup>(35)</sup>

The compressive thickness stress acting on the blank is assumed to be concentrated at the periphery of the blank. As radial drawing proceeds, the radial stress increases towards the central axis of the cup, until the increment reaches point B (figure 3.2). Between points B and C the stress rises as the element thins on bending and unbending under tension, friction over the die profile further increasing the draw stress. Radial drawing proceeds up to point C (figure 3.2) and hence the radial stress continues to increase.



The drawing stress may, therefore, be calculated by summing the stresses necessary to produce :

- a. radial drawing of the flange
- b. bending over the die profile
- c. overcome friction over the die profile
- d. unbending over the die profile

Using this technique Chung and Swift<sup>(38)</sup> have calculated punch loads with great accuracy but their calculation is complex and lengthy. The agreement between calculated and experimental values, will be somewhat worse when frictional conditions, between punch and metal, are such that metal is drawn off the punch and/or the material, under examination, exhibits marked anisotropy. Chung & Swift's analysis accounts for neither of these two variables.

A much simpler analysis than Chung & Swift's was made by Barlow,<sup>(39)</sup> who used some of their results, made a number of approximations, and produced a fairly simple formula for calculating punch loads.

The assumptions made by Barlow were largely in the calculation of the stress increments necessary to produce bending and unbending and to overcome friction over the die profile. However, radial drawing accounts for some 70–75% of the total draw stress and hence Barlow's approximations do not introduce large errors in the calculations.

The calculation of draw stress is outlined in Appendix 1. In this analysis, a simplified form of Chung & Swift's approach for determining the stress increment due to radial drawing is used together with Barlow's approximation for those increments due to bending, unbending and friction over the die profile.

The maximum reduction attainable in deep drawing is that at which the maximum punch load equals the strength of the material in the cup walls. For good drawability a high resistance to thinning, i.e. a work hardenable material, is desirable. However, if the material in the flange, in addition to that in the cup wall, work hardens, the stress, necessary to draw in the flange will be greatly increased. Ideally, therefore, work hardening should be confined to the material in the cup walls.



This principle has been utilised by Mintz<sup>(40)</sup> to substantially improve the drawability of maraging steel. Mintz partially drew overaged material at room temperature, "maraged" the steel at 350° C for 28 hours and then completed the draw. This technique enabled the region round the punch nose, which thinned down most, to be strengthened by ageing without causing any corresponding increase in strength in the flange.



#### 4.0. THE ASSESSMENT OF THE PRESS FORMING PROPERTIES OF SHEET METAL

Manufacturers and users of sheet metal have, for many years, tried to quantitatively assess the likely press performance of a material, for a given application, without resorting to costly full scale trials. Three approaches to the problem have been used :

- a. the theoretical calculation of drawing stress, press capacity or the maximum reduction the sheet will withstand,
- b. the use of simulative tests,
- c. the use of non—simulative tests.

The theoretical approach has already been discussed in the preceding section and a simplified analysis is outlined in Appendix 1. From these it may be seen that even the simplified analysis is quite complex and the calculation lengthy. Furthermore the theoretical analyses have been confined to relatively simple pressings, such as flat bottomed cylindrical cups. The analysis for more complex pressings would, therefore, be so complex as to be of little practical interest and hence more attention has been paid to the use of simulative or non—simulative tests.

##### 4.1. *THE USE OF SIMULATIVE TESTS*

A large number of simulative tests have been devised, the entire field of sheet metal testing having been reviewed by Wright. <sup>(41)</sup> Simulative tests include wedge drawing, hole expanding, simple bending and the forming of conical shaped cups in addition to the more widely used stretch forming and deep drawing tests.

The advantage of simulative tests are that they are quick and reproducible. The test may not, however, be representative of the actual pressing operation and, in this case, the correlation between test and industrial conditions will be poor. Simulative tests tend to represent either stretch forming or deep drawing, whereas industrial pressings tend to be an indefinite ratio of stretch forming and deep drawing.



Simulative tests may be used industrially as a quality control check on incoming material, even when the test is not strictly representative of the actual pressing. The test results are compared with the test results and press performance of previous batches of material used and, with this information, it is possible to determine whether or not the incoming material is acceptable. In a similar manner, simulative tests may be used to evaluate process variables.

#### 4.1.1. *STRETCH FORMING TESTS*

Stretch forming tests include the Erichsen, Olsen and Jovignot tests, of which the Erichsen test is the most widely used.

Stretch forming tests consist of clamping the sheet between the die and blank holder and advancing a hemispherical ended punch into the sheet until fracture occurs. The depth of penetration at which fracture occurs is taken as the measure of stretch formability.

The depth of penetration may be significantly increased if drawing in of the material occurs. Kaftanoglu & Alexander,<sup>(42)</sup> in a detailed study of the Erichsen test, showed that drawing in of material could only be effectively prevented by using serrated blank holder and die faces, but the use of such tooling has not yet been adopted as standard procedure.

Examination of failed specimens may be used to obtain an estimate of the grain size of the sheet, roughening of the surface indicating a coarse grain size. King & Turner<sup>(43)</sup> point out that a quite accurate estimate of the grain size of aluminium may be obtained if the test piece is compared with a series of standard test pieces drawn from sheets of known grain size.

An indication of directionality may also be obtained from an examination of the fracture, a circular fracture indicating freedom from marked directionality, whilst straight line fractures will occur where there is planar anisotropy, the fractures being perpendicular to the direction of minimum elongation.

A better representation of biaxial stretching is obtained by use of the hydraulic bulge test, in which a circular disc of metal is deformed by hydraulic pressure until fracture occurs. Radial drawing in of the flange is prevented by a bead bulged in



the flange prior to commencing the test. The bulge test is of particular interest to research workers as it offers a fairly simple means of deriving the stress-strain curve under conditions of balanced biaxial stretching without the complications of friction between punch and metal.

#### 4.1.2. DEEP DRAWING TESTS

The simplest method of assessing deep drawability is to draw a cup from a standard sized blank, using standard tooling, lubrication and blank holder pressure, and measure the cup depth. A better technique, and the one most commonly used, is to determine the largest blank diameter that may be successfully formed into a cup, this diameter being known as the critical blank diameter (C.B.D.). The C.B.D. is often expressed as a ratio of blank to punch diameter and is referred to as the limiting draw ratio. (L.D.R.).

There are two tests commonly used to assess the C.B.D. : the Erichsen and the Swift tests, which differ only in the tools specified for the test, the Swift test having a more generous die entry radius than the Erichsen test. In addition, the latter controls the punch-die clearance in excess of sheet thickness more closely than does the Swift test. Both of the tests consist of drawing a circular blank to produce a flat bottomed cup.

Maximum punch load increases linearly with increasing blank diameter up to the C.B.D. and then remains constant. The C.B.D. may be determined by drawing a series of different sized blanks, some below and some above the estimated C.B.D., and plotting maximum punch load against blank diameter, the C.B.D. being read from the graph as shown in figure 4.1.

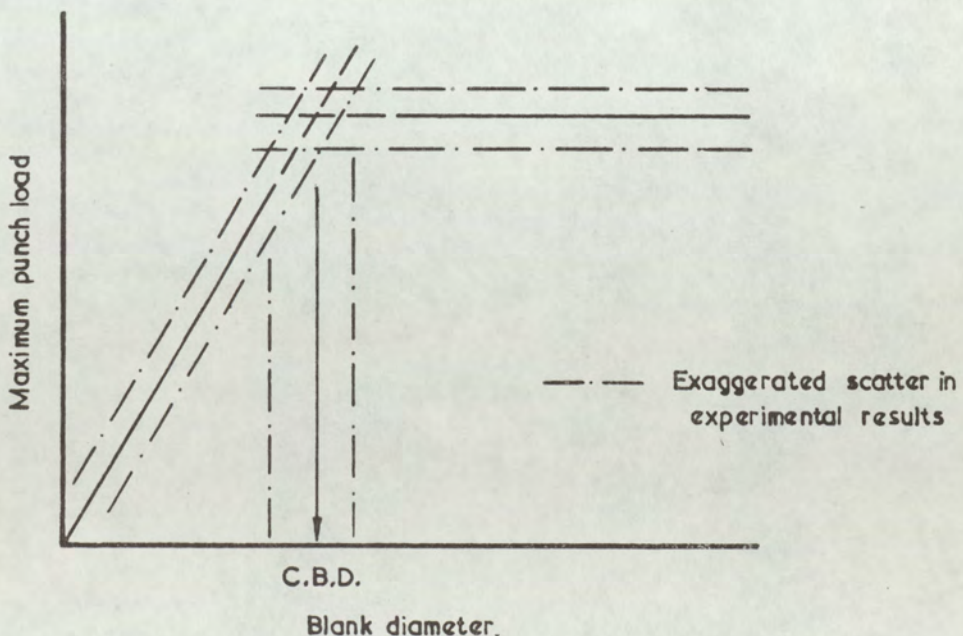


Figure 4.1. Graphical technique for the determination of C.B.D.



This technique is not often used because scatter in the experimental points makes accurate determination of the C.B.D. difficult, as shown in figure 4.1. A better technique is to test a series of blanks of different diameters, near to the estimated C.B.D., using a bracketing technique, until one too large and one too small is found. The mean of these is tested and, if it fails, the lower bracket is examined, otherwise the upper one is examined. This process is repeated until the C.B.D. is determined and this is then verified by repeated tests at the blank diameters adjacent to it. Svahn <sup>(44)</sup> states that an accuracy of 0.5% on the C.B.D. is possible by this technique if six blanks are used, but much larger numbers are required to significantly increase this accuracy.

Cup drawing tests are probably the most rapid means of assessing planar anisotropy (directionality) in sheet metals. Planar anisotropy gives rise to "ears" on the deep drawn cups and a semi-quantitative prediction of directionality may be made from the measurements of the heights of ears formed on cups during the test. With sheet exhibiting directionality it is important to remember that, in addition to the obvious variation in cup height at different angles to the rolling direction, there is also a variation in wall thickness in order to maintain constancy of volume. The material forming the ears of the cup will be thinner than that beneath the troughs so that, if ironing occurs in the latter stages of the draw, the troughs will be ironed preferentially and the apparent ear height will be reduced. If the primary purpose of the test is to study earing, tool geometry is of the utmost importance. Willis & Blade <sup>(45)</sup> have proposed a standard earing test where clearances range from 40% to 100%, although Plevy <sup>(46)</sup> showed that for steel, clearances at the upper end of this range led to the production of cups with "barrelled" walls. Plevy concluded that the optimum clearance for the accurate measurement of earing, conducive with the formation of a cup free from "barrelling" was 50-60%, but this would mean an even greater number of tools would be required than was originally proposed by Willis & Blade.

#### 4.2. *THE USE OF NON-SIMULATIVE TESTS AND THEIR CORRELATION WITH SIMULATIVE TESTS AND PRESSING BEHAVIOUR*

Much work has been done on non-simulative tests which give results useful in predicting the deep drawing or stretch forming qualities of a metal. Examples of such tests include simple indentation hardness measurements, the tensile test and the plane strain compression tests.



#### 4.2.1. *HARDNESS TESTS*

It is generally agreed <sup>(47, 48)</sup> that hardness is of little use in assessing deep drawability although it is a useful rapid test for stretch formability <sup>(49)</sup> and may be of use when used in conjunction with tensile data.

#### 4.2.2. *TENSILE TEST*

The tensile test is probably the most widely used non-simulative test in pressforming research. Limit of proportionality, yield point or proof stress, ultimate tensile strength and ductility are the most common parameters determined in the tensile test and, along with the ratio of yield to ultimate tensile strength, are useful in predicting the press performance of sheet metal. These properties, especially ductility, are of more use in predicting stretch formability than deep drawability as would be expected when the stress system operative during the test (uniaxial tension) is compared with that operative in stretch forming, (essentially biaxial tension) and deep drawing, (complex system).

Total elongation is generally used as a measure of ductility, but this parameter should be used with caution because of its dependence on test piece geometry, particularly the initial gauge length. For this reason values are only meaningful when the gauge length, used for the tests, is quoted. A better assessment of ductility may be obtained by measuring the uniform elongation, which is independent of gauge length.

Ultimate tensile strength is also of little fundamental significance because it is based upon the initial cross-sectional area of the testpiece. The relevance of U.T.S. increases as the material becomes more brittle because with such material there is little reduction in area, so that the initial and final areas do not differ greatly.

From the load-extension, or stress-strain curves, true stress-true strain curves may be derived if the instantaneous area of the test piece and the corresponding load are known. At the onset of necking the measurement of instantaneous area becomes difficult but, in any case, the stress state, once necking commences, does not correspond to uniaxial tension and, for this reason, the natural strain is effectively limited to 0.3 – 0.4 for metals such as mild steel and aluminium.



A plot of true stress against true strain on logarithmic scales generally produces a straight line so that the relationship between true stress and true strain may be represented by the power function :

$$\sigma = k\delta^n \quad \dots \dots \dots 4.1$$

where  $\sigma$  = true stress     $\delta$  = true strain  
            $k$  = constant         $n$  = work hardening coefficient

If the flow curve for a material is given by the power function, the true strain at instability is numerically equal to the work hardening coefficient. When the flow curve for a material is not given by the power function the true strain at instability may be derived by Considère's construction.(50)

There have been numerous objections to the validity of the power function particularly by Voce.(51) Voce has pointed out that the power function is purely empirical and that it suggests that all materials become infinitely strong with severe deformation. Voce proposes that the true stress-true strain curve obeys an exponential function rather than the power function :

$$\sigma = \sigma_{\infty} - (\sigma_{\infty} - \sigma_0) \exp\left(-\frac{\delta}{\delta_c}\right) \quad \dots \dots \dots 4.2$$

where  $\sigma_0$  = threshold stress at which deformation begins  
 $\sigma_{\infty}$  = asymptotic stress attained after severe deformation  
 $\delta_c$  = characteristic strain which determines the shape of the curve

A plot of the exponential function on logarithmic scales produces a curve where only the central portion is linear as shown in figure 4.2:

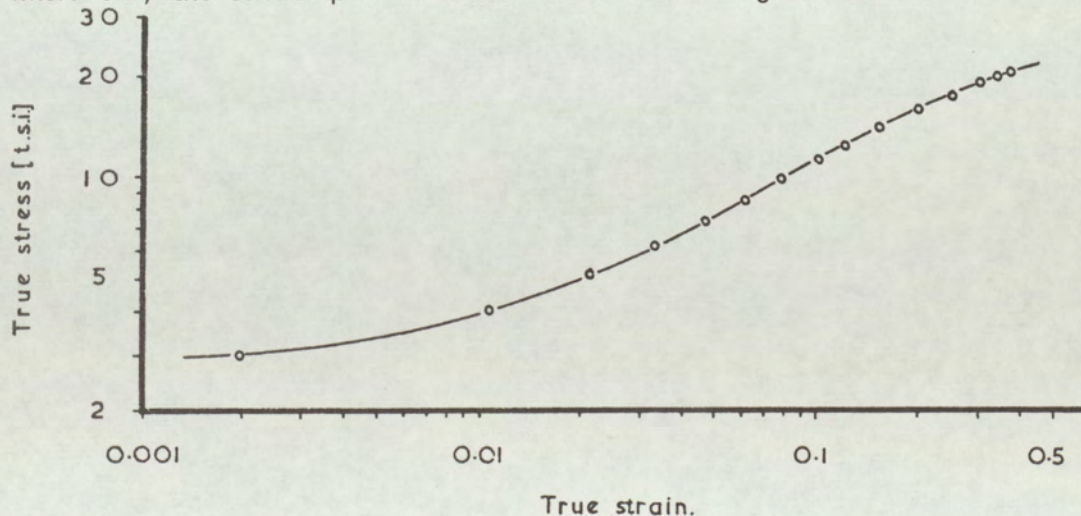


Figure 4.2. Tensile true stress-true strain curve for annealed high conductivity copper. (51)



There is considerable experimental evidence to support the validity of both the exponential and power functions. It appears fortuitous that the natural strain levels normally determined from a tensile test (0.03 – 0.3) fall in the central region of the exponential function. The use of the power function, between these limits, appears valid but if the range of natural strain levels is increased by, for example, determining the stress–strain curve in compression, the use of the power function is no longer valid.

The tensile test may also be used to quantitatively assess planar and normal anisotropy. Planar anisotropy is assessed by determining the mechanical properties at varying angles to the rolling direction, or some other reference direction. Normal anisotropy is generally assessed in the tensile test by the strain ratio, or R value, proposed by Lankford, Snyder and Bauscher.<sup>(52)</sup>

$$R = \frac{\ln W_o / W_f}{\ln t_o / t_f} \dots\dots\dots 4.3.$$

where W and t refer to width and thickness respectively, subscripts o and f refer to initial and final thickness respectively.

With thin sheet the accuracy in determining R may be increased by measuring width and length strains and, assuming constancy of volume, convert the latter to thickness strains :

$$R = \frac{\ln W_o / W_f}{\ln l_f W_f / l_o W_o} \dots\dots\dots 4.4.$$

where l refers to length.

Numerous attempts have been made to correlate the results obtained from the tensile test with press performance and/or simulative tests. For stretch formability the best correlations have been obtained with uniform elongation or work hardening index (n); stretch formability increasing with increasing ductility.

The correlation between mechanical properties and deep drawability is generally poor although several workers have used “performance functions” such as that proposed by Butler :<sup>(53)</sup>

$$\frac{\text{U.T.S.} \times R \times n}{20\% \text{ flow stress}} \dots\dots\dots 4.5.$$

Such functions are not widely used.



The best correlation, and the one that has been most widely investigated, is that between R value and L.D.R. The highest correlations between R and L.D.R. have been obtained with mild steel, although Whiteley<sup>(54)</sup> has shown that a general relationship exists between the average R value,  $\bar{R}$ , and L.D.R. for various metals.

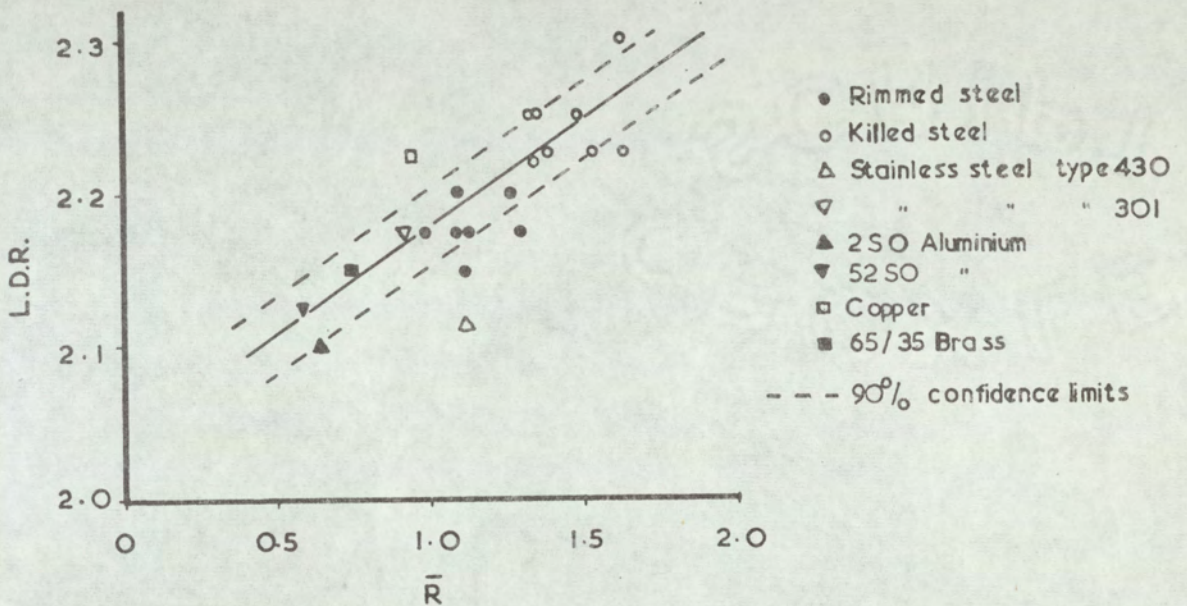


Figure 4.3. The relationship between L.D.R. and R value. <sup>(54)</sup>

The positions of ears, formed on deep drawn cups, may be predicted from the R values obtained in the tensile test; maximum ears forming in positions around the circumference of the blank where the R value, transposed tangentially, is a maximum. The actual heights of the ears are close to being proportional to the planar variation in R.



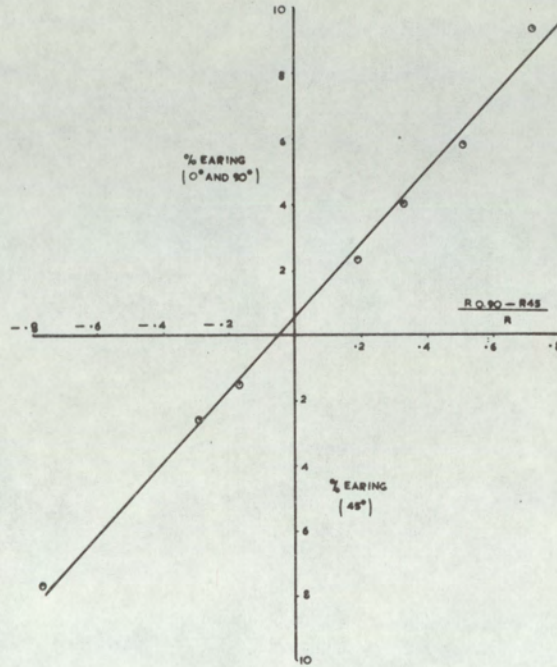


Figure 4.4. Variation in per cent earing and ear position with planar variations in  $R$  value.<sup>(40)</sup>

The importance of  $R$  value on drawability may be seen from figures 4.3 and 4.4. The former shows that L.D.R. increases with  $\bar{R}$ , the latter that earing increases with the planar variation in  $R$ , so that for good drawability with minimum earing, both  $\bar{R}$  and  $R$  (min) should be high.



### 4.2.3. PLANE STRAIN COMPRESSION TEST

The plane strain compression test, developed by Watts and Ford,<sup>(31,32)</sup> would be expected to more closely represent the stress system to which the flange and certain regions of the cup wall are subjected during radial drawing, than the tensile test. In addition it is possible to obtain R values, regardless of material temper, at higher strains than would be possible in the tensile test although their determination is much more difficult.

The test is not, however, widely used because it is a slow test to perform when compared with the tensile test, requires the use of low strain rates and does not give an indication of ductility unless the material is extremely brittle.

Normal anisotropy may be assessed using the technique developed by Holcomb & Backofen<sup>(55)</sup> in which the stress-strain curve is derived normal to the plane of the sheet (fig. 4.5a) and in the plane of the sheet using laminated specimens (fig. 4.5b). The laminated specimens were prepared by cutting strips from the sheet. These were then stacked and bolted and the centre section milled to the desired dimensions.

- (a) The plane-strain flow stress with  $d\epsilon_y = 0$  (numerator of Eq<sup>n</sup> 4.6) is determined by indenting strips cut from the sheet.
- (b) To obtain the denominator of Eq<sup>n</sup> 4.6 ( $d\epsilon_z = 0$ ) strips are cut, stacked, bolted and the centre section milled. The plane-strain flow stress is determined by indenting the test piece in the milled section. (For simplicity only the central region of the test piece is shown in the final illustration).

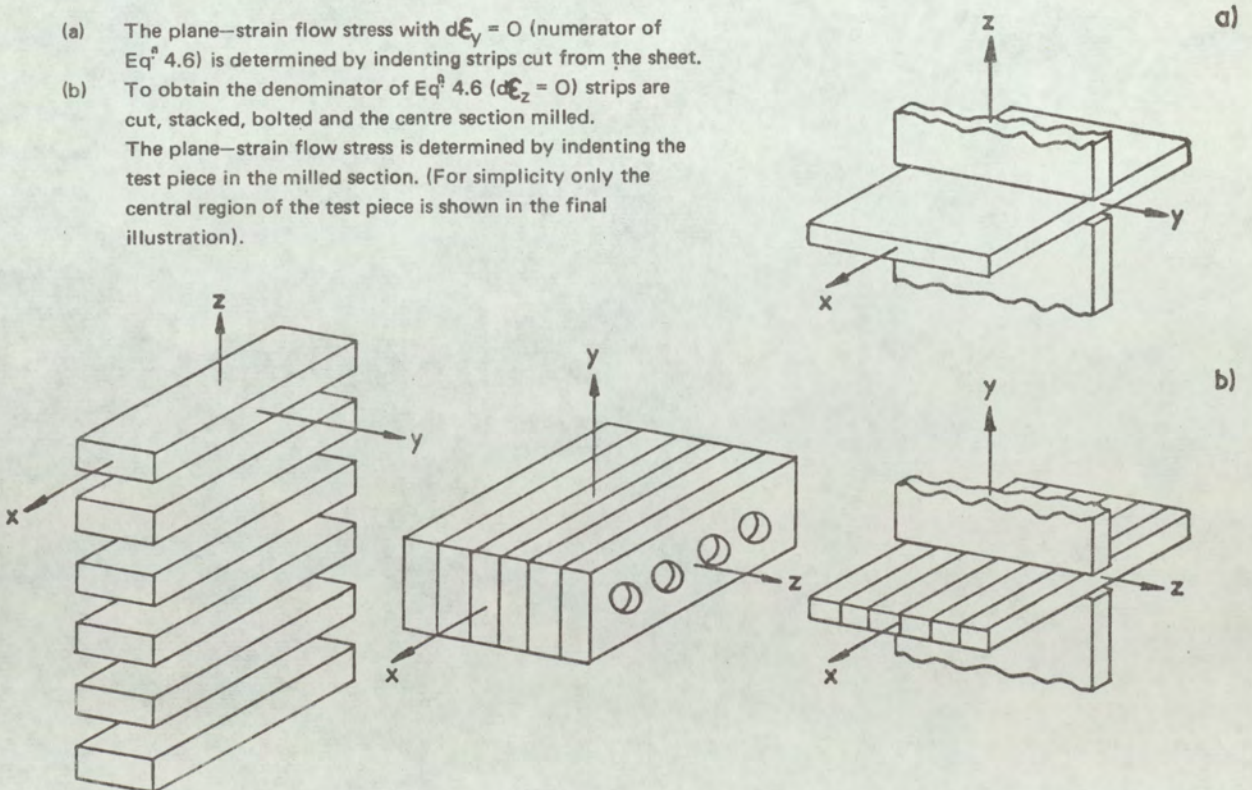


Figure 4.5. Schematic illustration of procedures used for the experimental determination of  $\beta$  by plane-strain indentation.<sup>(55)</sup>



Improvement in drawability may be obtained by increasing the ratio ( $\beta$ ), of the strength of the cup wall, where failure will generally occur, to the strength in the deforming flange. Holcomb and Backofen related the tests normal to the plane of the sheet (fig. 4.5a) to the behaviour of the material in the lower regions of the cup wall, and the tests in the plane of the sheet (fig. 4.5b) to the behaviour of the flange,  $\beta$  was then defined as :

$$\beta = \frac{\sigma_x \text{ (wall)}}{\sigma_y \text{ (flange)}} \quad \dots \dots \dots 4.6.$$

where  $\sigma_x$  = tensile stress for elongating a strip specimen without change in width direction ( $d\epsilon_y = 0$ )

$\sigma_y$  = compressive stress for squeezing in the plane of the sheet without thickening. ( $d\epsilon_z = 0$ )

Hosford and Backofen<sup>(56)</sup> have shown that  $\beta$  and R are related and for the special case of planar isotropy :

$$\beta = \sqrt{\frac{R+1}{2}} \quad \dots \dots \dots 4.7.$$

When the material exhibits planar anisotropy this relationship may be modified<sup>(55)</sup> to

$$\beta = \sqrt{\frac{R_{rd} (R_{td} + 1)}{R_{rd} + R_{td}}} \quad \dots \dots \dots 4.8.$$

where  $R_{rd}$  and  $R_{td}$  refer to R values in the rolling and transverse directions respectively.,  $R_{rd}$  being assigned to the "x" direction.

Whiteley<sup>(54)</sup> has expressed L.D.R. as a function of R value using the equation :

$$\ln(D/d) = \frac{1}{1+\mu} \sqrt{\frac{\bar{R}+1}{2}} \quad \dots \dots \dots 4.9.$$

where  $\frac{D}{d}$  = L.D.R.

$\mu$  = a friction parameter.

and it may be seen from equations 4.7 and 4.8 that L.D.R. may also be expressed as a function of  $\beta$ .

Holcomb and Backofen,<sup>(55)</sup> however, concluded that there was little value in accumulating " $\beta$  type" data on a routine basis, the measurements being time consuming, expensive and difficult to make with precision.



## 5.0. THE PRESSFORMING PROPERTIES OF CLAD MATERIALS

Information on the pressforming properties of clad materials is limited to technical data sheets issued by the producers of such material e.g. Texas Instruments, and to results on "coated" steel i.e. steel sheet coated with a thin layer of tin, zinc or copper. Substantial improvements in drawability, over conventional steel sheet, have been reported for tin <sup>(57)</sup> and zinc <sup>(58)</sup> coated steel, the improvement being attributed to the coating metal acting either as a solid-phase lubricant, or as an aid in retaining the lubricating oil film.

In none of the published work has an attempt been made to relate the performance of the composite to that of the components of the composite and their relative proportions, although Rathbone <sup>(59)</sup> concluded that for stretch forming mild steel-stainless steel, deeper penetrations were obtained when the thicker component (mild steel) was the outer one. Rathbone did not, however, indicate whether or not the deeper penetrations were obtained because the outer component was the thicker one or because it was mild steel rather than stainless steel.

In this work the mechanical and pressforming properties of two and three layer composites will be investigated and the results compared with the corresponding properties of the single components. From this data, it is hoped to calculate the mechanical and pressforming properties of the composite from a knowledge of the basic properties and thicknesses of the parent metals. The investigation will also include a study of the planar and normal anisotropy of composite material made up from metals of differing planar and normal anisotropy or of cross-matched planar anisotropy.

Roll bonded copper/steel composites were used for the investigation because roll bonded material was commercially available, a full range of copper/ steel combinations providing the producer, Texas Instruments, with fewer production problems than would other combinations, e.g. copper/aluminium. Adhesive bonded composites were also used because the bonding process, being independent of diffusion and deformation enabled the production of material with matched or cross-matched planar anisotropies.



## 6.0. EXPERIMENTAL PROCEDURE

### 6.1. *MATERIALS USED*

The materials used for the experimental investigation were steel/copper composites produced by either adhesive bonding or cold roll bonding. Mild steel and tough pitch copper were used to produce the adhesive bonded composites and SAE 1006AK steel and deoxidised low phosphorus copper for the roll bonded composites. The chemical compositions of the steel and copper are shown in table 6.1.

Table 6.1 *Chemical composition of steel and copper (weight per cent)*

*Adhesive bonded composites:*

Steel	C	Si	S	P	Mn	Al
	0.06	trace	< 0.01	< 0.01	0.33	< 0.01
Copper	Ag	Si	Fe	Ni		
	0.006	trace	< 0.003	trace		

*Roll bonded composites:*

Steel	C	Si	S	P	Mn	Al
	0.05/.10	0.005/.011	0.014/.025	0.006/.007	0.32/.40	0.059/.064
Copper	Ag	Fe	Pb	Ni	B	P
	0.006	< 0.003	< 0.005	0.006	trace	0.008

### 6.2. *PRODUCTION OF COMPOSITES*

The range of composites produced by the two bonding techniques are shown in the table 6.2:



Table 6.2. Range of Steel/Copper composites produced

Bonding Technique	Type of Composite	Thickness of copper %
Adhesive	bilayer	20, 67
Roll	bilayer trilayer	20, 33, 50, 67, 80. 2 x 25, 2 x 33, 80, 50, 34.

The Composites were processed as follows:

#### 6.2.1. Adhesive bonded composites

Bilayer composites were produced with steel : copper thickness ratios of 80/20 and 33/67, the total thickness in both cases being 1.83 m.m. (0.072"). The rolling and annealing schedules, used to obtain the necessary thicknesses of steel and copper, are shown in figure 6.1.

The schedules were arranged so that the steel or copper components of both composites, although of different textures, had similar mechanical properties.

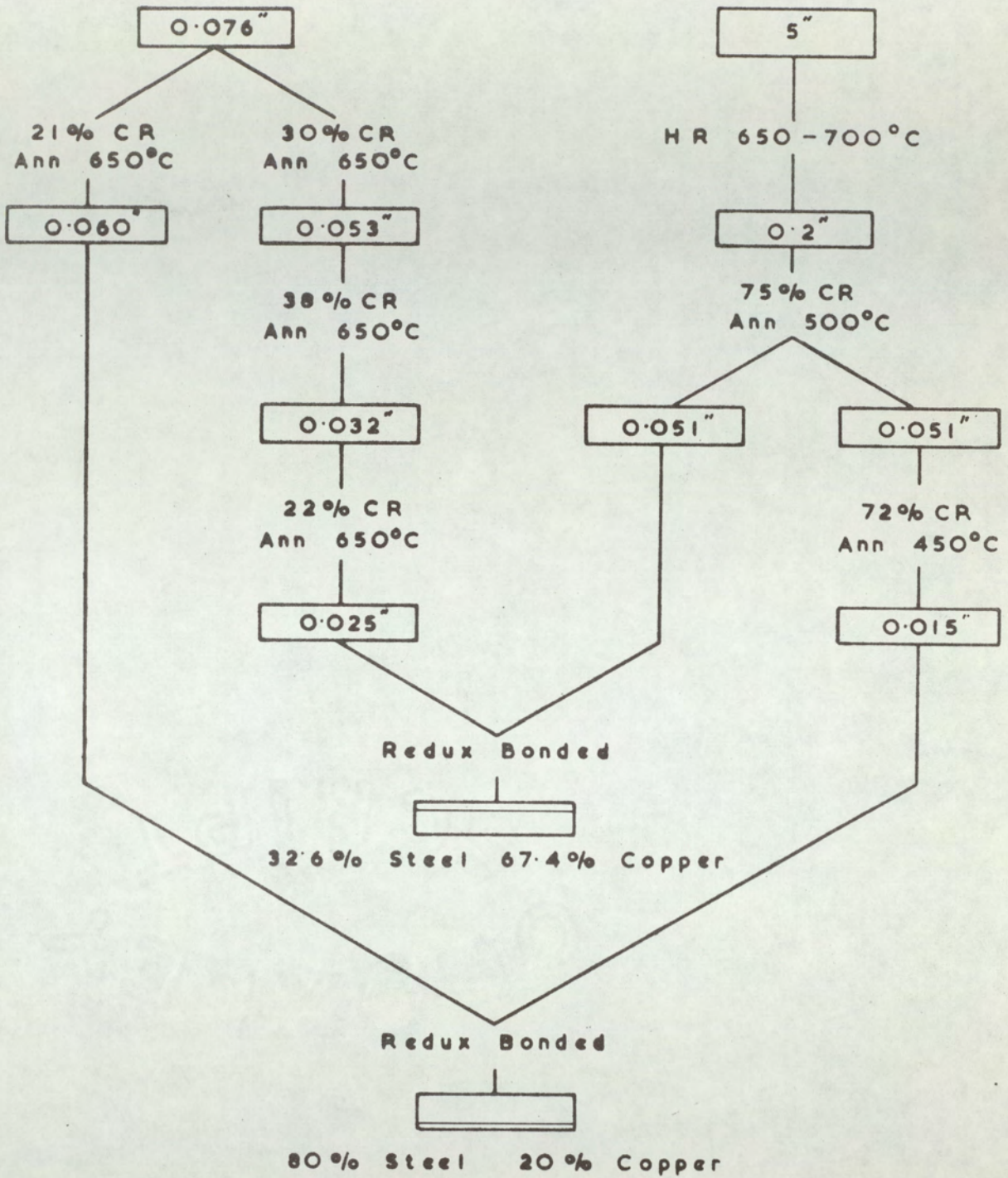
The composites were bonded by CIBA Ltd., Duxford, using 0.51 m.m. (0.020") thick Redux film. The selection of Redux, a vinyl phenolic resin, for the experimental work is discussed in Appendix 2. Prior to bonding, the composite components were degreased in a trichlorethylene vapour bath, the faying surfaces of the steel and copper were cleaned by means of shot blasting and fine emery respectively, and again degreased. The Redux was cured at 150° C for thirty minutes at a pressure of 100 p.s.i.

Both composites were produced with the respective rolling directions of the steel and copper matched and also mismatched by 45°. The thickness of the bond was approximately 0.25 m.m. (0.01") so that the total thickness of the composites was 2.03 – 2.16 m.m. (0.08 – 0.085").



Temper Rolled Mild Steel

Tough Pitch Copper



Abbreviations :

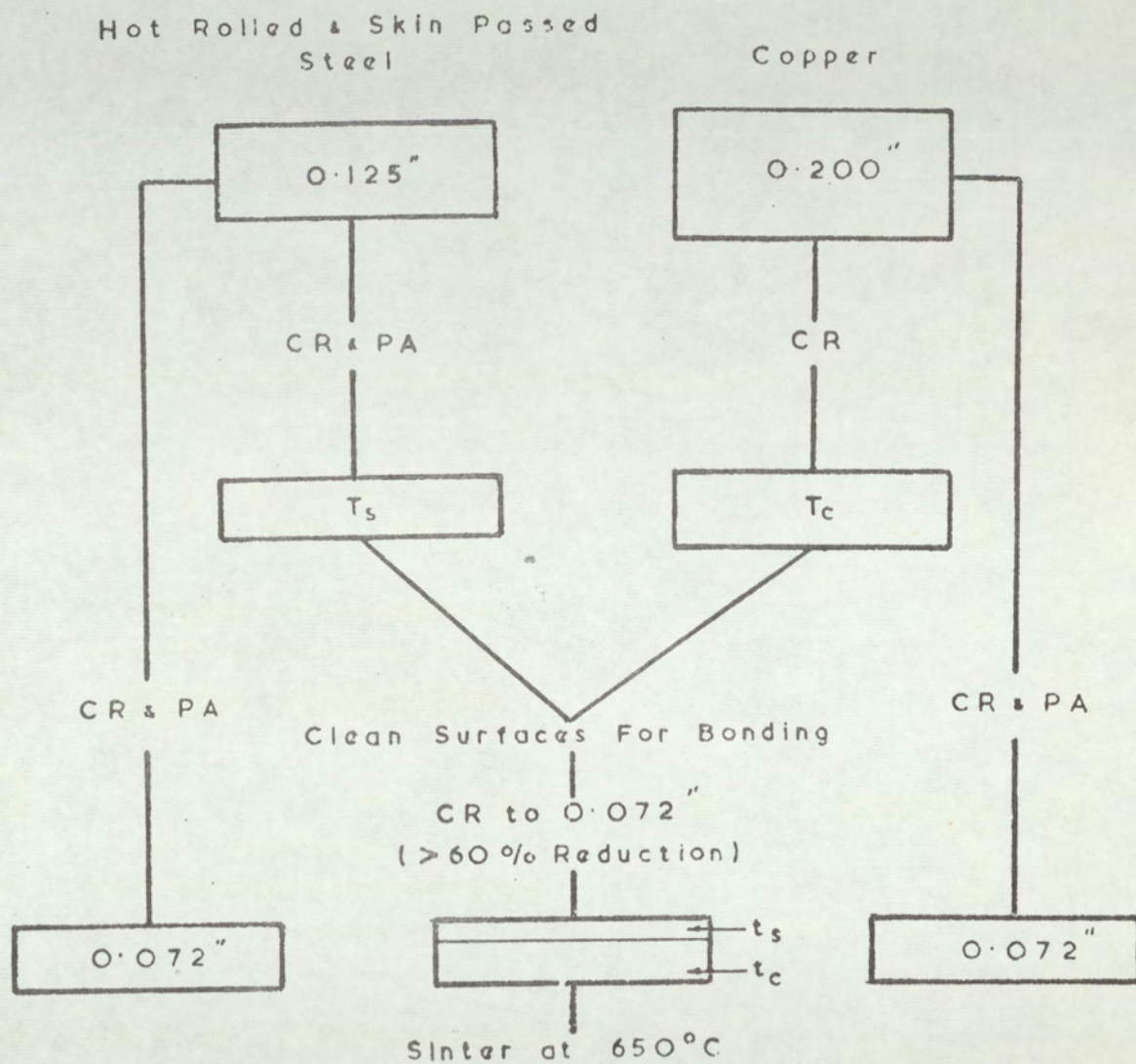
- HR — hot rolled
- CR — cold rolled
- Ann — 30 minute anneal

Figure 6.1. Production schedule for the adhesive bonded composites.



## 6.2.2. Roll bonded composites

The steel/copper composites were bonded by Texas Instruments using the three stage cladding process outlined in section 2.1.1. The composites were processed as shown in figure 6.2.



## Abbreviations:

- CR — cold rolled
- PA — process annealed at 650°C
- $T_s$  &  $T_c$  — intermediate gauge of steel & copper
- $t_s$  &  $t_c$  — final ratio of steel : copper ( $t_s + t_c = 1$ )

Figure 6.2. Production schedule for the roll bonded composites.



The intermediate gauges,  $T_s$  and  $T_c$  to which the steel and copper were rolled prior to cleaning and roll bonding, were dependent upon the required steel : copper thickness ratio (i.e.  $t_s : t_c$ ). It may be seen that each composite was processed slightly differently, so that the final thickness was 1.83 m.m. (0.072") in each case.

The roll bonded material was received in the process annealed condition but preliminary hardness tests revealed a wide variation both in the hardnesses of the steel, and of the copper components, as shown in table 6.3.

Table 6.3. *Hardnesses and steel : copper hardness ratios of the as-received and of the annealed material*

MATERIAL		HARDNESS (D P N)				Hd. (steel)	
		As Received		Annealed		Hd. (copper)	
% Copper	% Steel	Copper	Steel	Copper	Steel	As received	Annealed
—	100	—	132	—	108	—	—
100	—	112	—	48	—	—	—
20	80	86	146	44	103	1.71	2.3
33	67	76	114	42	112	1.50	2.6
50	50	75	106	43	103	1.42	2.4
67	33	77	108	39	103	1.41	2.6
80	20	73	121	42	104	1.66	2.5
80	2 x 10	54	112	47	101	2.06	2.2
50	2 x 25	69	110	47	103	1.59	2.2
34	2 x 33	69	110	50	109	1.59	2.1
2 x 25	50	77	115	45	109	1.50	2.4
2 x 33	34	60	93	45	97	1.55	2.1

In order to obtain an approximately constant steel to copper hardness ratio, for later comparisons, the composites were reannealed at 650°C in an argon atmosphere. The annealing time was varied to obtain an approximately constant steel to copper hardness ratio of 2.5. The hardness ratios obtained are shown in table 6.3.

### 6.3. ELECTRON PROBE MICROANALYSIS :

One of the problems encountered in annealing clad materials is interdiffusion across the interface. The extent of diffusion across the interface was, therefore, assessed, using the Cambridge Microscan II, on samples of the bilayer and trilayer roll bonded composites, in both the as received and the annealed condition. The samples were approximately 5 mm (0.2") long and were mechanically polished using standard metallographic techniques.



The intensity of the characteristic X-rays, emitted from the specimen,  $I_A$ , were compared with the intensity from the pure metal,  $I_{(A)}$ , the count ratio ( $k$ ) being approximately equal to the weight fraction of A :

$$k = \frac{I_A}{I_{(A)}} \quad \text{--- wt\%A} \quad \dots\dots\dots 6.1$$

The characteristic X-rays for both iron and copper were, in turn, monitored. At least two scans per element were made on all specimens, the accelerating voltage being selected to give sufficient accuracy and sensitivity.

#### 6.4. X-RAY DIFFRACTION :

Quantitative pole figures were determined by a counter technique using a Siemens texture goniometer with a Phillips X-ray generator and counting equipment.  $\{111\}$  pole figures were determined on the copper samples using a copper target operating at 40 kV and 18 mA with a Nickel filter. On the steel samples  $\{110\}$  and  $\{200\}$  pole figures were determined using a cobalt target, operating at 35kV and 14mA, with an iron filter.

The samples were chemically thinned to remove the surface layers, so as to eliminate any spurious surface effects. The normal Schulz reflection technique was employed, the samples being simultaneously rotated about the rolling plane ( $\beta$  rotation) and the normal to the rolling plane ( $\alpha$  rotation), such that  $360^\circ \alpha$  rotation was accompanied by  $5^\circ \beta$  rotation. Using this technique the centre of the pole figure outwards was covered by a spiral upto approximately  $70^\circ$  from the centre. The peripheral regions of the pole figures, which require a transmission technique, were not determined.

#### 6.5. TENSILE PROPERTIES :

The copper/steel composites, and the copper and steel used to produce these composites, were tested in tension. Duplicate tensile testpieces were cut from the sheets in direction at 0, 45 and  $90^\circ$  to the rolling direction, the dimensions of the testpieces being shown in figure 6.3.



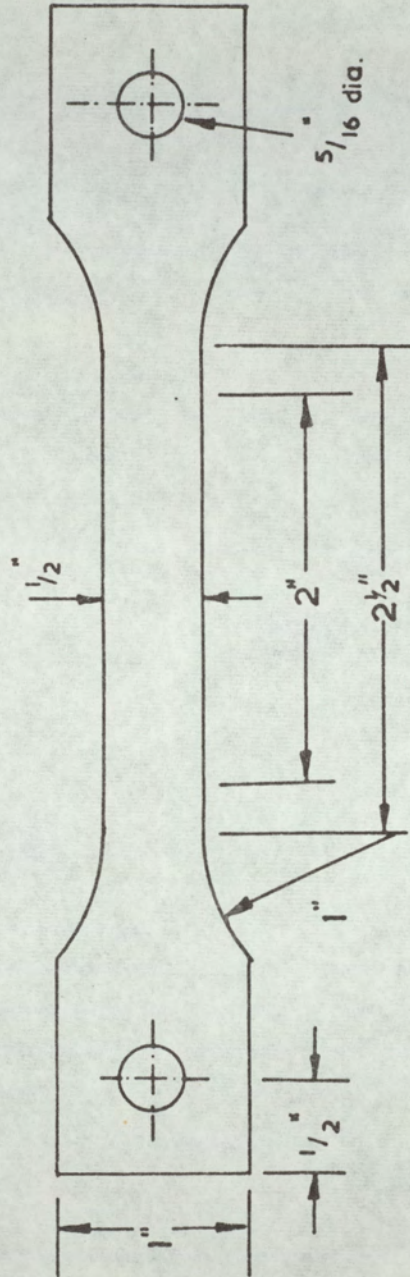


Figure 6.3 Dimensions of tensile test pieces.



Using a Hounsfield tensometer, yield stress or 0.5% proof stress, ultimate tensile strength, total elongation to fracture on a 50.8 m.m. (2'') gauge length, uniform elongation 'n' and 'R' values were determined. Where the material did not show a definite yield point, 0.5% proof stress was determined since the normal 0.1% proof stress could not be accurately measured. While the standard mercury column load measuring device of the tensometer was used for the load measurements, the standard graphical technique for measuring strain was not considered sufficiently accurate for the present work. Measurements of strain were, therefore, made by means of a cathetometer sighted on the scribed gauge marks on the testpieces.

The speed of cross-head travel was 1.6 m.m./min., the test procedure being as follows :

- i Width and thickness were measured at 4 evenly spaced intervals within the parallel section using a micrometer reading to 0.01 m.m.
- ii The testpiece was coated with Engineer's blue
- iii Gauge marks were lightly scribed within the parallel section at 6.3 m.m. (0.25'') intervals.
- iv The gauge marks were measured using a travelling microscope reading to 0.01 m.m.
- v The testpiece was assembled in the Hounsfield and the load measuring device zeroed.
- vi A 50.8 m.m. (2'') gauge length was measured using a cathetometer reading to 0.01 m.m.
- vii The testpiece was loaded and the load-extension curve plotted. The test was stopped after approximately 5% extension.
- viii The width and gauge length of the testpiece were remeasured as under (i) and (vi) respectively. Load, average width and gauge length were recorded.
- ix The test was recommenced, step viii being repeated at increments of 2 - 3% extension upto the onset of plastic instability.
- x After fracture, the testpiece was removed from the Hounsfield and each gauge increment remeasured as in step iv.
- xi The properties already listed were calculated.



## 6.6. DEEP DRAWING TESTS :

### 6.6.1. Equipment

Deep drawing tests were made using an Erichsen electro-hydraulic test machine (model 123) that had been modified by Griffiths<sup>(61)</sup> so that a continuous record of punch load/punch travel could be obtained, the equipment being illustrated in figure 6.4.

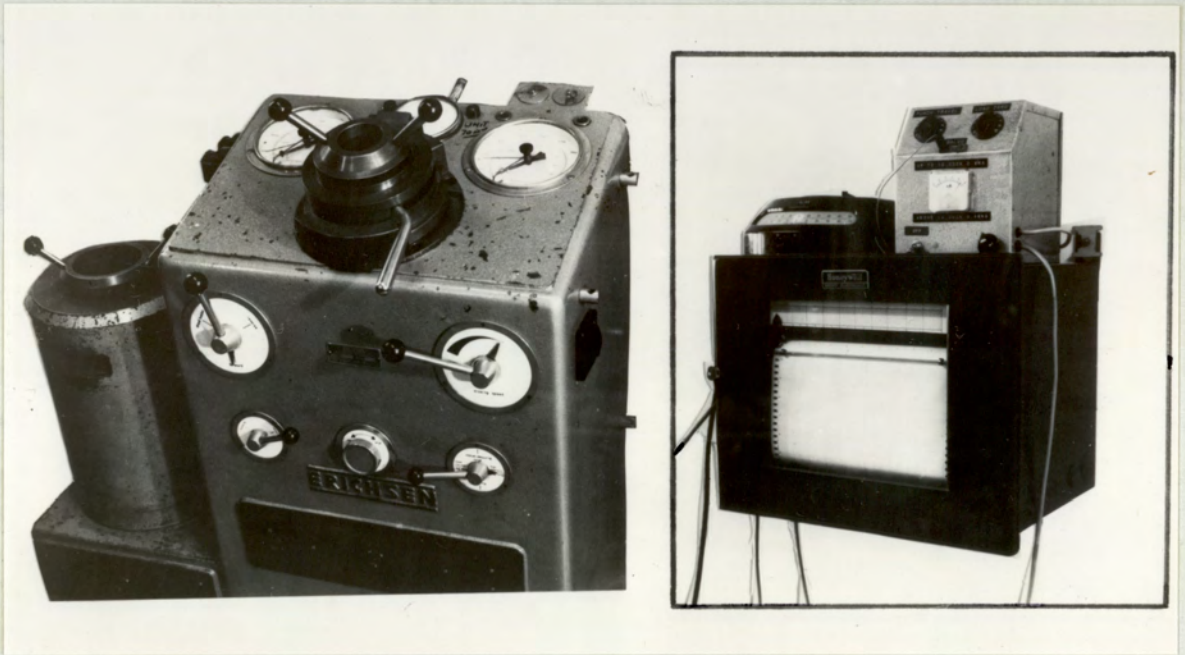


Figure 6.4. Photograph of the Erichsen press.  
Inset : close-up of the recording equipment.

The mechanism of the existing dial gauge was used to activate a transducer across which a voltage was applied, the output operating the chart drive of a Honeywell recorder. The punch load was determined by a load cell incorporated in the punch stem, the modified punch and load cell used by Griffiths is shown in figure 6.5.



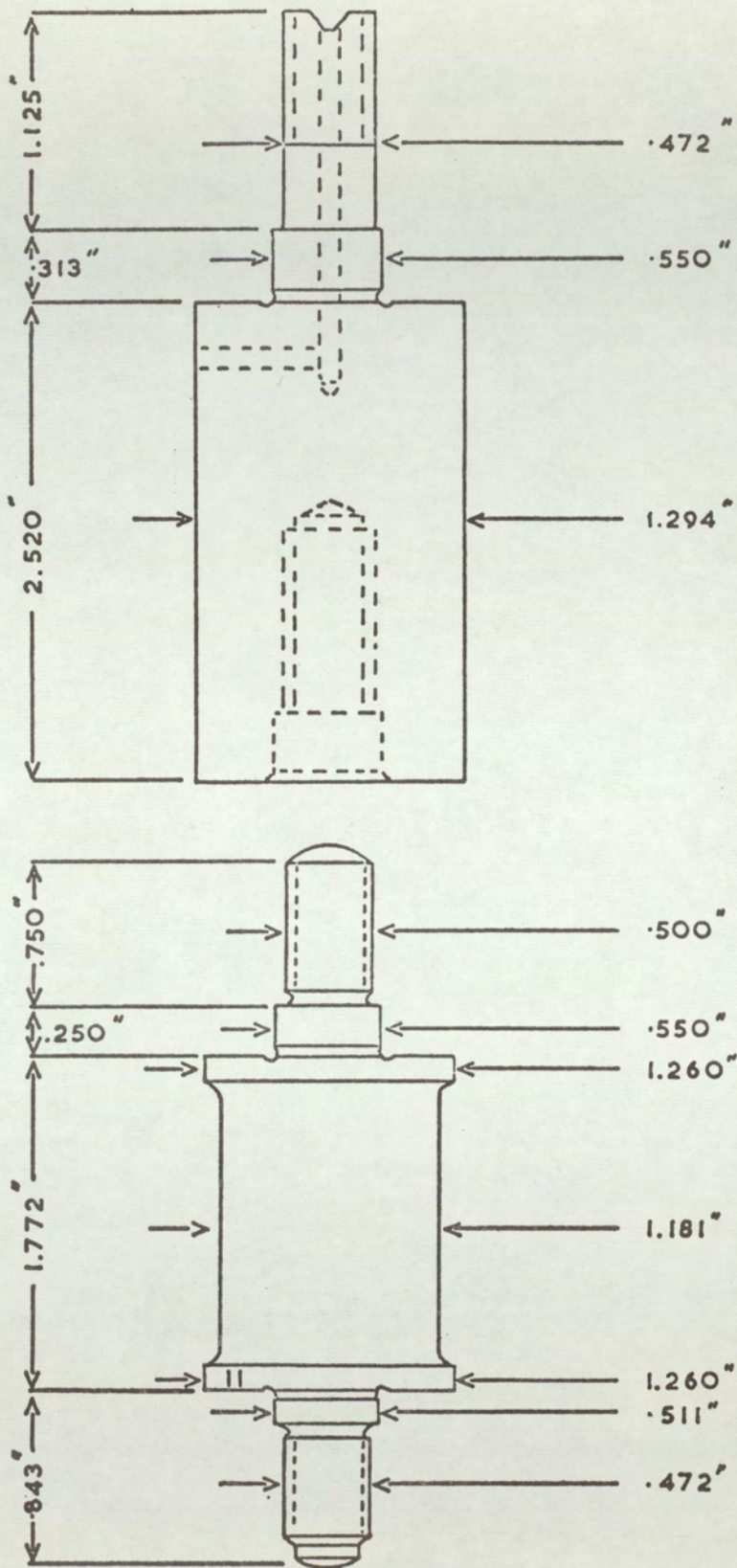


Figure 6.5. Modified Erichsen Punch and Load Cell.<sup>(61)</sup>



The system used by Griffiths had three major disadvantages :

- i balance of the circuit recording punch travel, such that 1 inch of chart travel corresponded to 10 m.m. punch travel, was difficult.
- ii the load, indicated by the recorder, varied with the batteries life.
- iii neither of the two circuits were stable and, during use, their zero positions tended to "drift".

The circuits used by Griffiths were modified so that these difficulties were overcome and more reliable results were obtained. The modified circuits are shown in figure 6.6.

After these modifications the load cell was recalibrated by incremental compressive loading, using the sub—press on a 50 ton Denison Universal Test machine. The load cell circuit was modified so that full scale chart deflections of either 10,000 or 20,000 kgs. could be obtained but neither of these produced a linear deflection on the recorder scale.

#### 6.6.2. *Test Variables :*

Cup drawing tests were reviewed in section 4.1.2. The results of these tests are influenced by punch—die clearance, blankholder load and friction. Preliminary tests were, therefore, made to determine suitable test conditions for assessing the deep drawabilities of the materials used in this work.

For all the deepdrawing tests the punch travel speed was 10 m.m./min. This strain rate was greater than that used in the tensile tests, but any associated temperature effects were considered to be negligible because of the large mass of the punch and die in contact with the blank throughout the test.

The tooling used in the standard Erichsen test has clearances of only 20%, whereas the optimum clearance for measurements of earing, has been shown to be 40 — 60% <sup>(46)</sup>. Preliminary tests revealed that clearances of 20% were insufficient to completely eliminate ironing. The degree of ironing obtained was not, however, considered to be sufficient to significantly affect measurements of ear



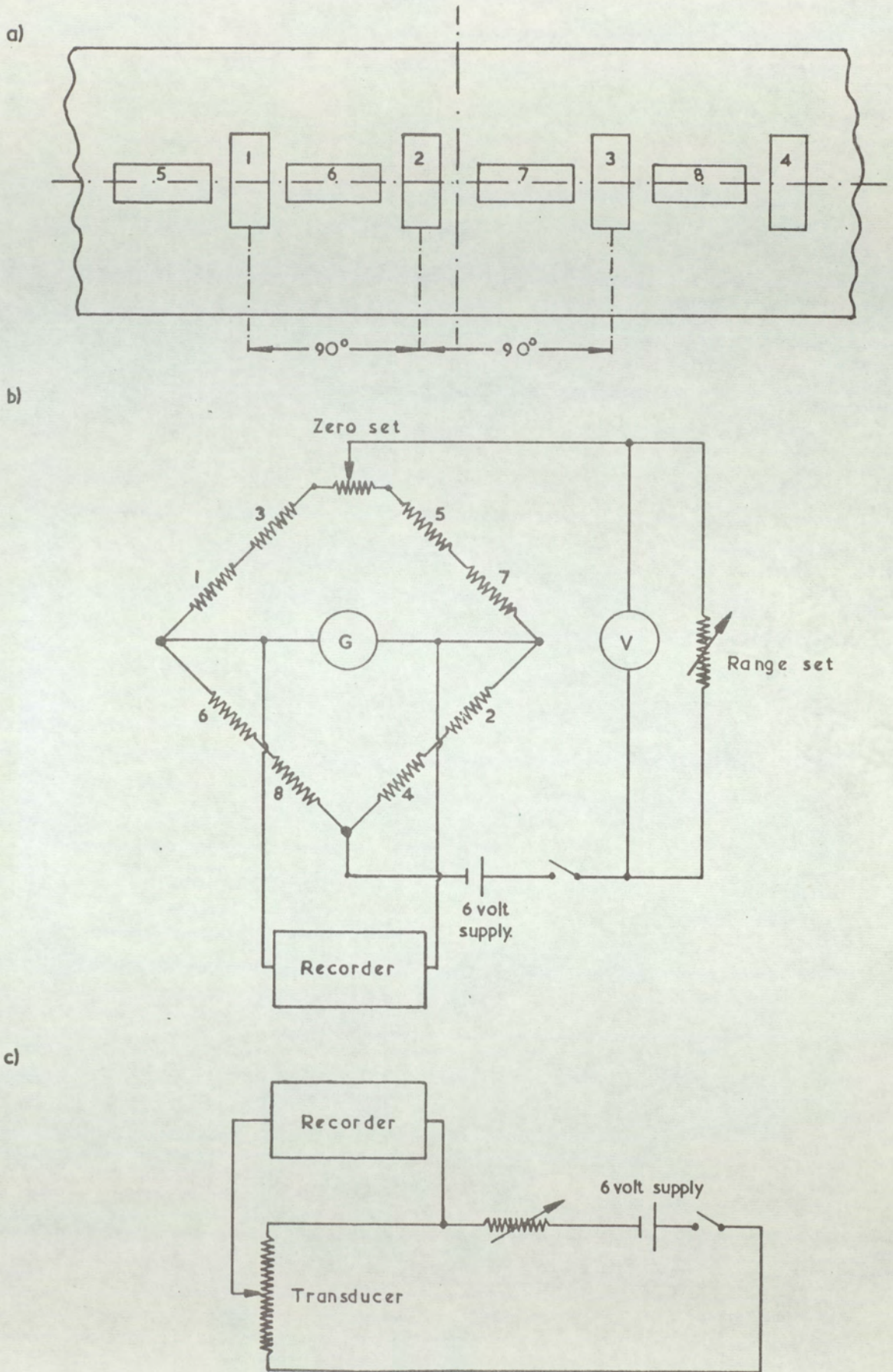


Figure 6.6.

- a. Arrangement of strain gauges
- b. Electrical circuit for the load cell
- c. Electrical circuit for the transducer



heights or to influence the maximum punch loads to such an extent that the C.B.D. would be affected. The standard Erichsen tooling was considered satisfactory for these tests, the tool dimensions being shown in table 6.4.

Table 6.4. Erichsen tooling details.

A.

Sheet Thickness		Die Diameter m.m.	Die Profile Radius m.m.	% Clearance
m.m.	ins.			
1.83	0.072	37.4	3	20.3
1.46	0.058	36.4	3	16.2
1.21	0.048	35.9	3	18.1
0.91	0.036	35.2	3	20.4
0.62	0.024	34.5	3	20.6
0.46	0.018	34.1	3	20.4
0.36	0.014	33.9	3	26.4

B.           Punch diameter     33 m.m.  
              Profile radius       4.5 m.m.

The blank holder load, necessary to suppress wrinkling during radial drawing— in of the flange, decreases as sheet thickness increases, but, for any particular sheet thickness, there is a wide range over which the blank holder load has little influence on the maximum punch load or on the quality of the cup. For a sheet thickness of 1.83 m.m. (0.072") a blank holder load of 500 kg. was found to be sufficient to completely suppress wrinkling. Unless otherwise stated the blank holder load was 500 kg. for all the deep drawing tests.

A suitable lubricant for the deep drawing tests was found by determining the maximum punch loads required to draw 62 m.m. diameter blanks of 1.83 m.m. (0.072") thick steel and copper using a range of lubricants commonly used in press work. Cups were also drawn without using a lubricant and the reduction in the punch load obtained with each lubricant was determined, the results being plotted in figure 6.7.



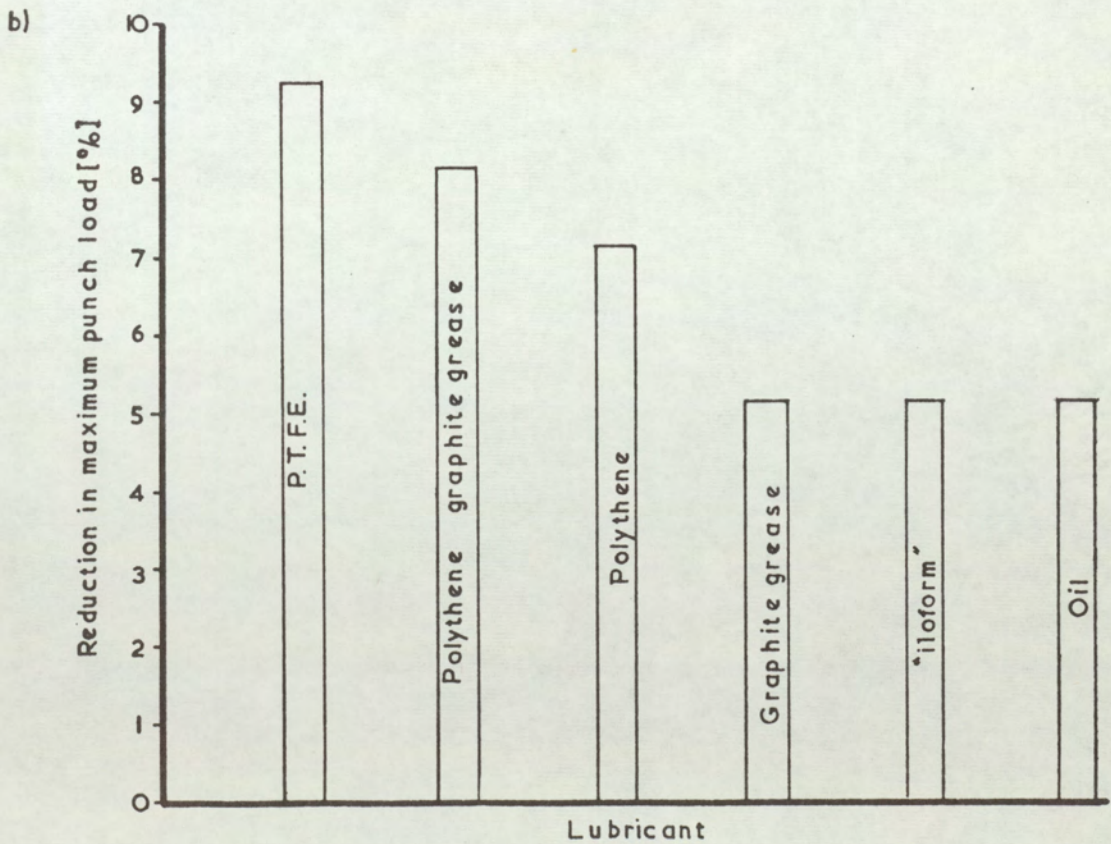
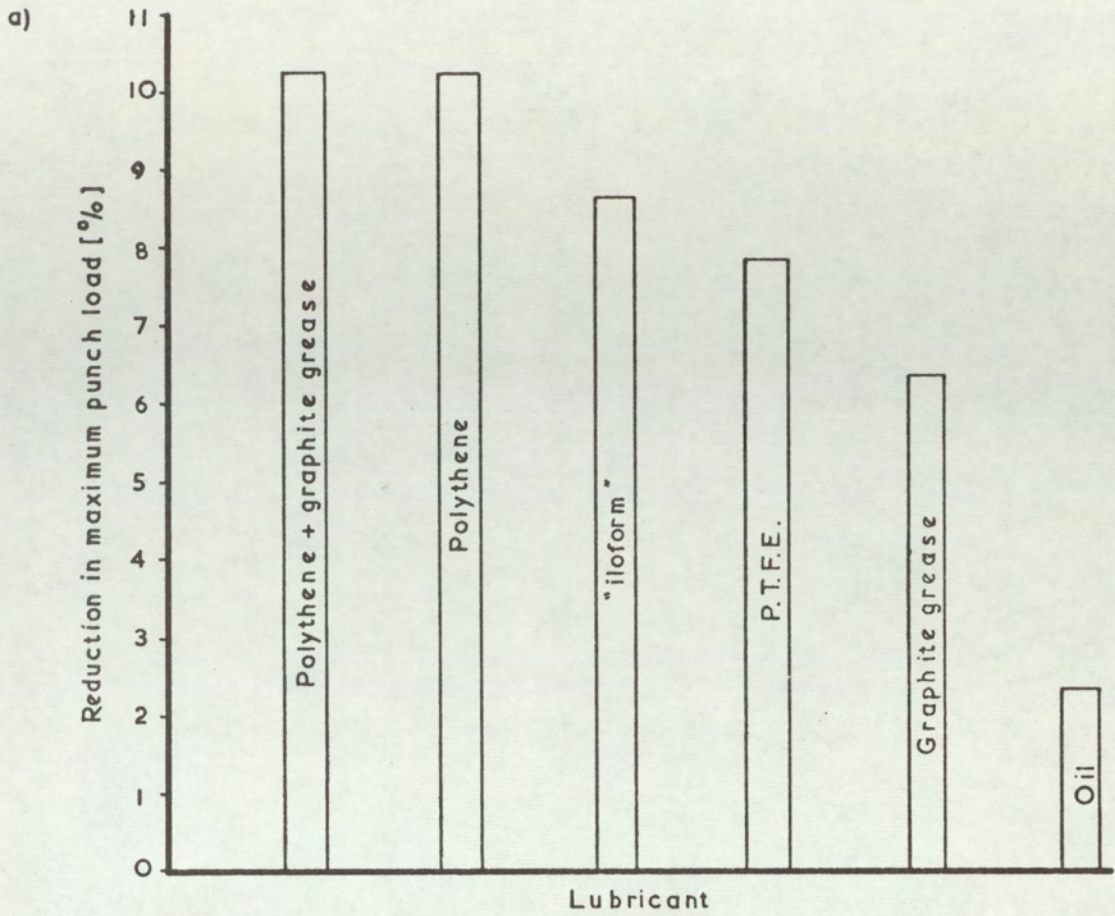


Figure 6.7. The influence of lubrication on the reduction in maximum punch load for drawing 62 m.m. diameter blanks of (a) steel and (b) copper.



The greatest reductions in punch load were obtained with polythene or polythene + graphite grease for the steel samples and with P.T.F.E. for the copper samples. The use of different lubricants for steel and copper would have also necessitated using appropriate lubricants for each side of the two layer composites, which was not considered practicable. Polythene + graphite grease was, therefore, used for all the tests, this being more convenient to use than was P.T.F.E.

#### 6.6.3. *Determination of critical blank diameters:*

The bracketing technique, outlined in section 4.1.2., was used to determine the critical blank diameters of the steel, copper and copper/steel composites. The C.B.D. determined by this technique, was that blank size at which at least three blanks formed complete cups whilst at a diameter 1 m.m. greater three cups failed.

#### 6.6.4. *Earing measurements*

Earing tests were made on all the materials using the same tooling and conditions as was used for the C.B.D. determinations. The tests were made in triplicate on a constant blank diameter, which was determined by that material having the lowest C.B.D., a diameter of 65 m.m. being used.

#### 6.6.5. *Thickness surveys on drawn cups:*

Thickness surveys were made on selected cups sectioned in the rolling direction, the measurements were made at intervals of 3 m.m. ( $1/8''$ ). The total thickness of the composites was measured using a micrometer with pointed anvils, whereas the thickness of the individual components of the composites was measured on a projection microscope.

#### 6.7. *STRETCH FORMING PROPERTIES:*

The stretch forming tests were made on the equipment used for the deep drawing tests, the punch travel speed being 10 m.m./min. and the blank holder load 1,000 kg. The tests were made in duplicate and in accordance with the Euronorm 14.58 specification<sup>(62)</sup> except that 0.03 m.m. (0.001'') thick polythene was used in conjunction with graphite grease as lubricant. The tool dimensions are shown in figure 6.8.



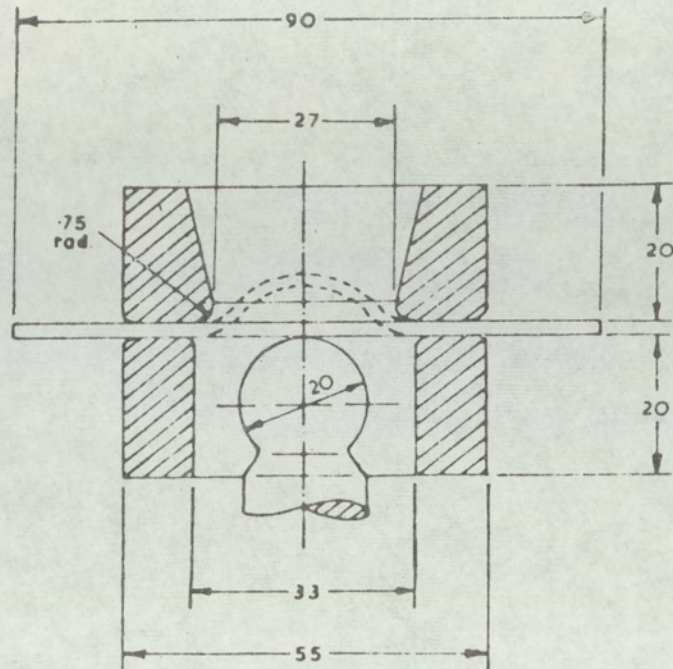


Figure 6.8. Tooling for the stretch forming tests (Dimensions in m.m's.)

#### 6.8. PLANE STRAIN COMPRESSION TESTS :

The plane strain compression tests were made using a sub-press fitted to a Denison Universal test machine, the sub-press being illustrated in figure 6.9. The dimensions of testpieces used are shown in figure 6.10.

It has been shown<sup>(31, 32)</sup> that for plane strain conditions the ratio of testpiece width to thickness should be greater than 6, and the ratio of die breadth ( $b$ ) to testpiece thickness ( $t$ ) should be 2–4. All of the testpieces used in this work had a ratio of width to thickness of 10–12 and the dies were selected such that the  $b/t$  ratio was 2–4 the range of dies available being shown in table 6.5.

The test pieces were deformed by increments of approximately 2% strain, the load being applied at the same point on the test piece for each increment. The load was held constant for 30 seconds, the test piece removed from between the dies and the width and thickness of the test piece, at the indentation, was measured using micrometers. The test pieces were relubricated between each indentation using either molybdenum disulphide or 0.03 m.m. (0.001") thick polythene, polythene being



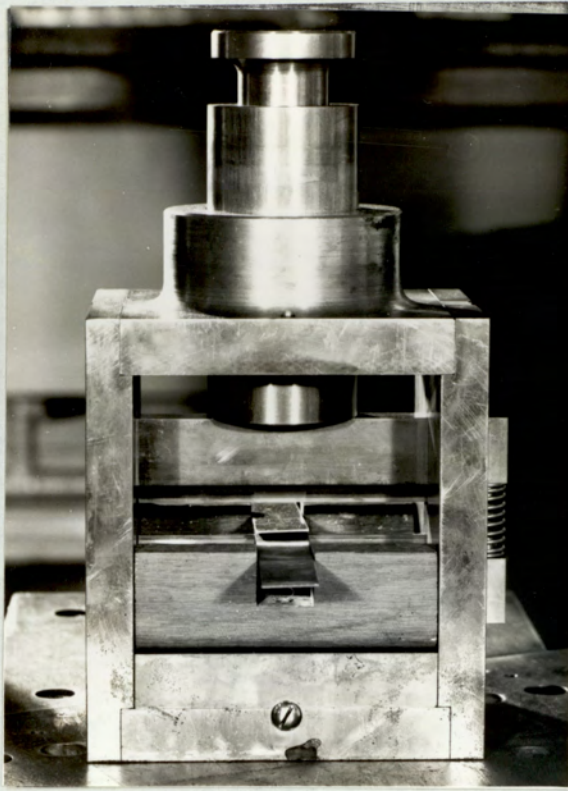


Figure 6.9 Sub-press for the plane strain compression tests.

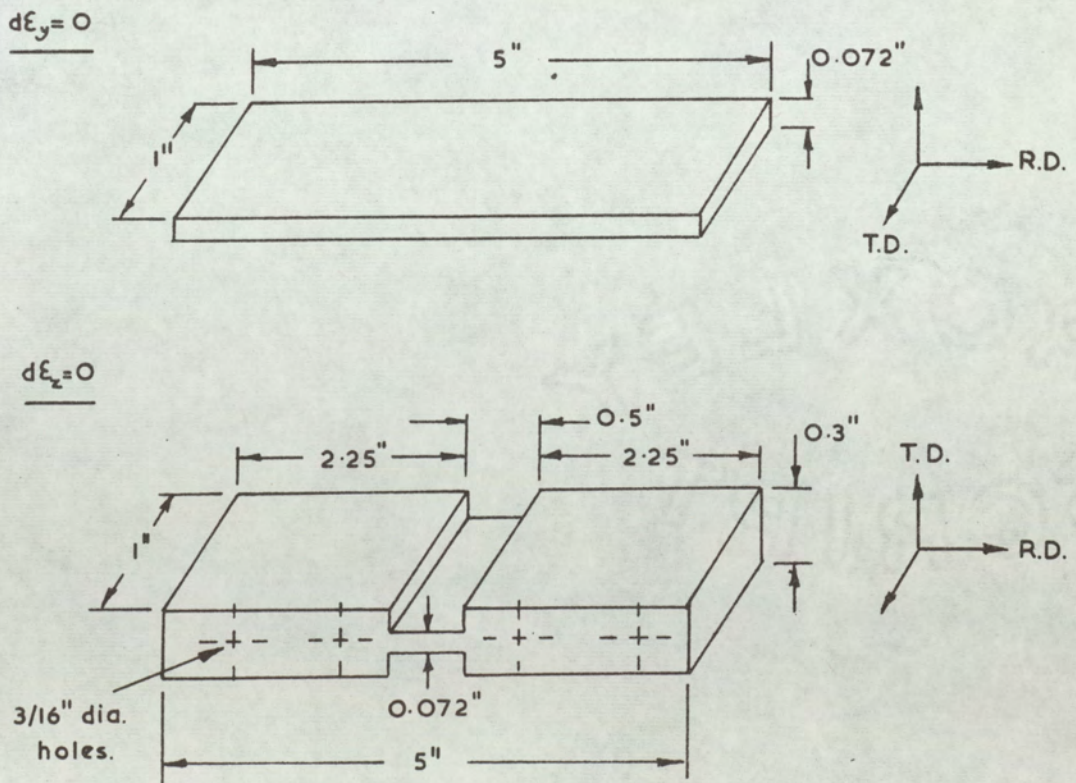


Figure 6.10 Dimensions of the plane strain compression test pieces.



used for the majority of the tests. The stress strain curve was derived up to a true strain of 1.5, this necessitating tool changes during the test to maintain the b/t ratio at 2–4 throughout the test.

Table 6.5. Dies available for the compression tests and the corresponding range of thicknesses for which b/t is 2–4.

DIE BREADTH		THICKNESS RANGE	
m.m.	ins.	m.m's.	ins.
18.14	0.7140	9.07 – 4.55	0.357 – 0.179
11.28	0.4440	5.64 – 2.82	0.222 – 0.111
7.01	0.2760	3.51 – 1.75	0.138 – 0.069
4.34	0.1710	2.18 – 1.09	0.086 – 0.043
2.93	0.1155	1.47 – 0.74	0.058 – 0.029
1.82	0.0715	0.91 – 0.46	0.036 – 0.018

#### 6.9. TESTS ON THE STEEL AND COPPER COMPONENTS OF THE COMPOSITES :

During the production of the adhesive bonded composites, samples of both the steel and the copper components were obtained that had been processed simultaneously with those of the composites, with the exception of the bonding schedule. The mechanical and press forming properties of the composite components would, therefore, be easily determined.

With the roll bonded composites, samples of the individual components of the composites were not available. The properties of these components could be determined by :

- (a) assuming that the properties of the 1.83 m.m. (0.072") thick steel and copper were comparable with those of the steel and copper components of each composite
- (b) by suitable rolling and annealing schedules process the 1.83 m.m. (0.072") thick steel and copper such that they are of similar thicknesses and properties as those of the composites



- (c) chemically or mechanically separate the composites into their individual components.

Reference to the processing schedules for the roll bonded composites, figure 6.2, shows that the 1.83 m.m. (0.072") thick steel and copper had received completely different processing histories from any of the composite components. These samples were, therefore, unlikely to be representative of those of the individual components of the composites and, furthermore, technique (b) was unlikely to yield results any more representative. Chemical or mechanical separation of the composite into its components was the only way of obtaining the properties of the individual components of the composites.

The copper components of the composites were electro-chemically removed using a 20% solution of ammonium nitrate at a current density of 0.5 – 1.0 amps./in<sup>2</sup>. Frequent additions of ammonia and/or ammonium nitrate were found necessary to prevent deposition of the copper salts. The steel components were removed using a 20% solution of sulphuric acid at a temperature of 50°C. In order to increase the rate of removal of copper from the steel – copper – steel composites, and of steel from copper – steel – copper composites, one of the outer components was first mechanically removed.

The components of the composites were tested in similar ways to the composites themselves to ensure that the results would be comparable. In the deep drawing tests the appropriate die from table 6.4 was selected such that the clearance was approximately 20%.

The copper : steel thickness ratios of the roll bonded composites were obtained by measuring the thicknesses of samples of the appropriate copper and steel components prepared using the techniques outlined in this section. The measured copper : steel thickness ratios did not significantly differ from those tabulated in table 6.3.

#### 6.10 *DEEP DRAWING OF UNBONDED COMPOSITES*

Samples of steel and copper were obtained from the roll bonded composites using the techniques outlined in section 6.9. The samples were assembled with varying degrees of frictional restraint at the interface and drawn using the tooling and techniques previously discussed. High interfacial friction was obtained by etching and



scoring the mating surfaces of the steel and copper. Low frictional restraint was obtained by polishing the mating surfaces and deforming the blanks with polythene sandwiched between the components.



## 7.0. EXPERIMENTAL RESULTS :

### 7.1. ELECTRON PROBE MICROANALYSIS :

Typical results of the electron probe micro-analysis are shown in figure 7.1 for the 20% copper/80% steel bilayer composite, the results having been calculated using equation 6.1. The position of the copper - steel interface of the samples could not be accurately detected with the micro-analyser because the copper tended to "smear" during mechanical preparation, thus making the interface diffuse.

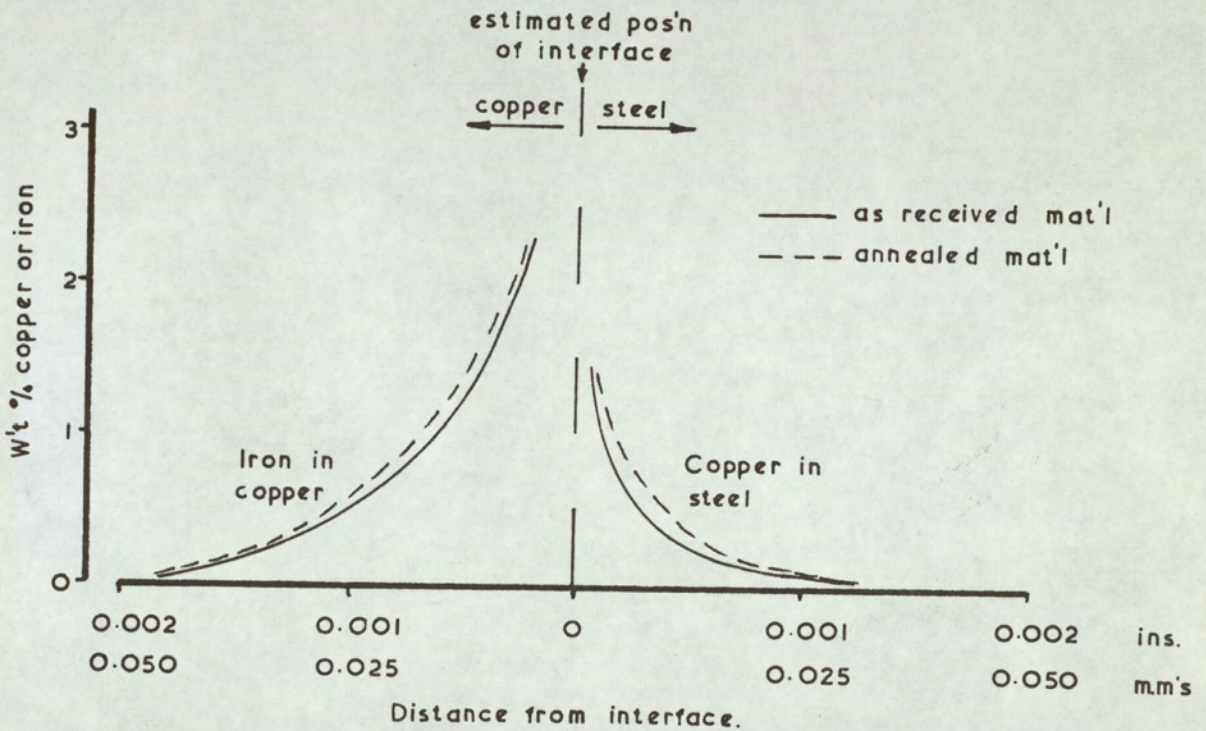


Figure 7.1. The extent of inter-diffusion of copper and iron in the 20% copper / 80% steel bilayer composite.

The results shown in figure 7.1 should be corrected to account for the effects of:

- differences in atomic number of the steel (iron) and copper
- differences in absorption characteristics
- fluorescence.



The penetration of the electron beam into the sample increases as the atomic number of the element decreases, this means that greater penetrations, and hence, a lower proportion of back scattered X-rays, are obtained with iron than with copper, the atomic numbers being 26 and 29 respectively. To compensate for this variation in back scatter, the results for iron in copper should be decreased when compared with the iron standard and those for copper in iron, increased when compared with the copper standard. Further corrections should be made to compensate for the differences in absorption, copper X-rays being heavily absorbed in iron whereas iron X-rays are only slightly absorbed in copper.

Fluorescence occurs when the X-rays emitted by one element, "excite" the second element causing X-rays of the second element to be emitted, this effect being greatest when the difference in atomic numbers is 2. Copper X-rays cause iron to fluoresce so that a proportion of the monitored iron X-rays arise from fluorescence, this proportion increasing exponentially as the beam nears the interface.

Quantitative corrections for the effects of atomic number, absorption and fluorescence may be made but the calculations, particularly for absorption, are complex. The purposes of the micro-analysis in this work was simply to determine the influence of the annealing treatment on the extent of inter-diffusion, so that qualitative corrections are adequate. The trace of iron in copper should be decreased to correct for the effects of fluorescence, and atomic number but increased slightly to compensate for absorption, whereas the trace of copper in iron should be increased to compensate for the effects of atomic number and absorption.

It may be seen, therefore, from figure 7.1, that the annealing treatment slightly increased the extent of diffusion. This increase was not considered to be sufficient to influence the properties of the composites.

## 7.2. X-RAY DIFFRACTION :

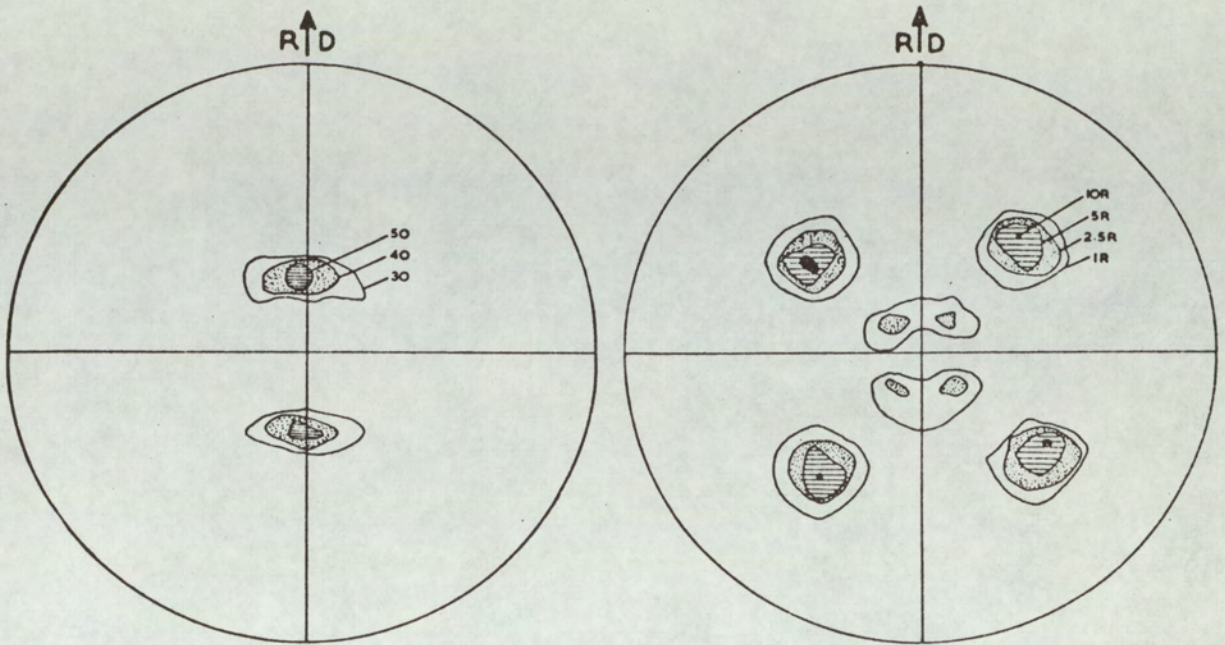
Examples of pole figures obtained on steel and copper components of the composites are shown in figure 7.2 for adhesive bonded composites and figure 7.3 for roll bonded composites. With the components of the roll bonded material all the textures, for a given type of component, were basically similar; the intensity levels varying as did the spread about the "ideal" texture.



a) 32.6 % Steel 67.4 % Copper bimetal

Steel (0.025" thk)

Copper (0.051" thk)



b) 80 % Steel 20 % Copper bimetal

Steel (0.060" thk)

Copper (0.015" thk)

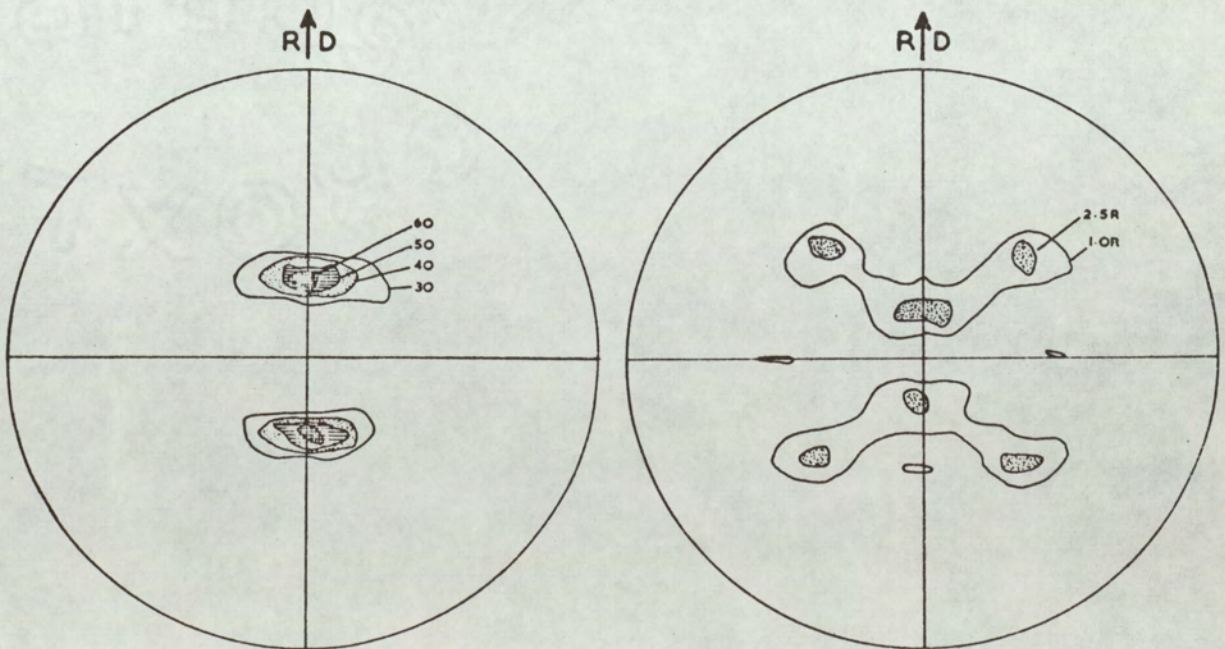


Figure 7.2. Examples of pole figures for the steel and copper components of the adhesive bonded composites.



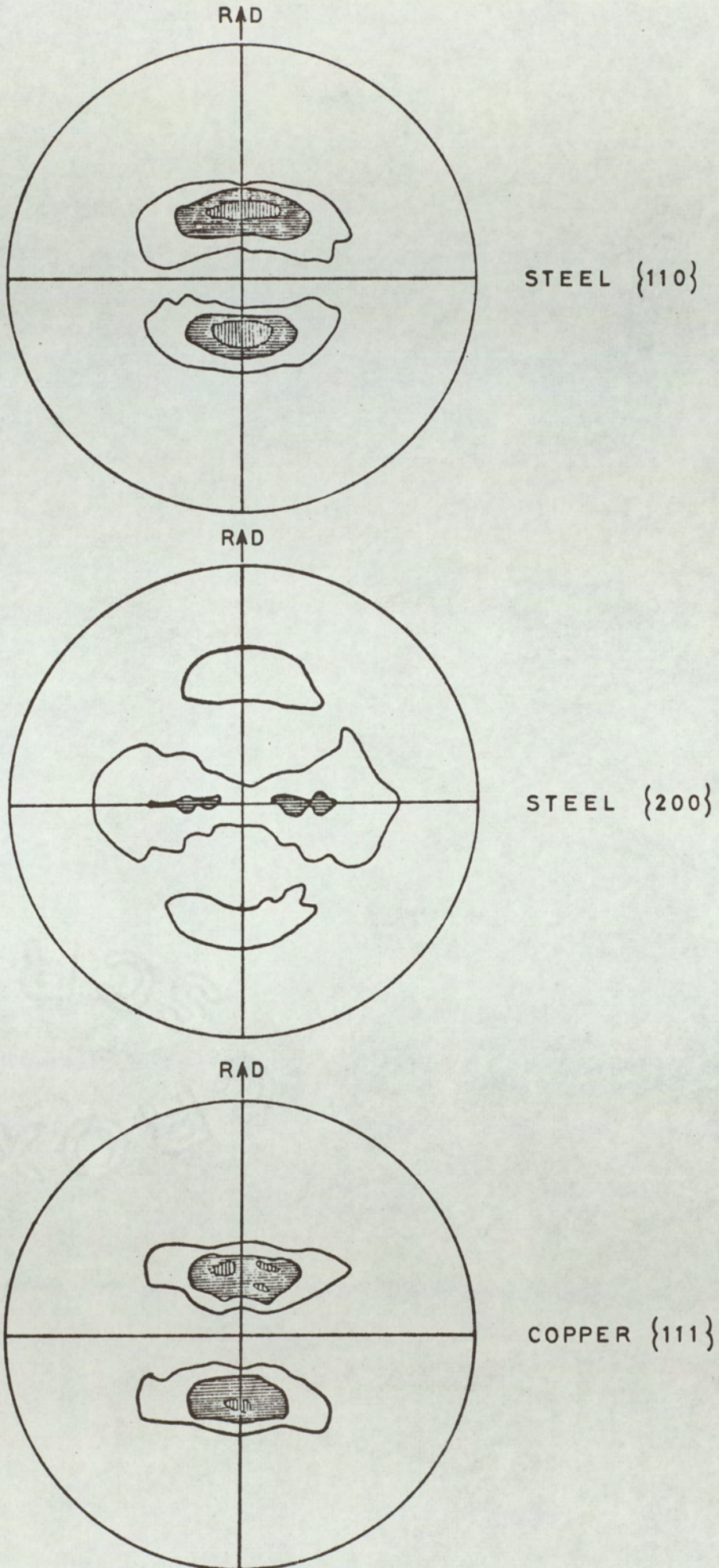


Figure 7.3. Examples of pole figures for the steel and copper components of the roll bonded composites.



The degree of spread, in the textures of the steel components, was such that the earing direction of these components could not be predicted with confidence. The  $\{111\}$  pole figures for copper show that the copper components of the adhesive bonded composites had slightly different textures; that of the 80/20 composite having a balanced texture, which would produce a flat topped cup, whereas that of the 33/67 composite had a texture which would be expected to produce  $0 - 90^\circ$  earing. All the copper components of the roll bonded composites would be expected to exhibit  $45^\circ$  earing.

### 7.3. TENSILE PROPERTIES :

The mechanical properties of the adhesive bonded composites are shown in tables 7.1 and 7.2 and those of the roll bonded composites in tables 7.3 and 7.4, the results being the mean of duplicate tests. The results for the adhesive bonded composites are arranged so that the results for a particular steel/copper composite immediately follow those of the components making up that composite.

The values of stress for the adhesive bonded composites were calculated in two ways; one using the cross-sectional area of the metal only, the other using the total cross-sectional area i.e. inclusive of the area of the adhesive. Both values are shown in the tables, those calculated using the total cross-sectional area being marked with an asterisk.

In the tensile tests several types of yield were observed as shown in figure 7.4. Types A and B were typical of the 100% copper and 100% steel respectively, and types C - E of the composites. It may be seen that yield strength may be calculated as limit of proportionality or proof stress for types A - E, upper or lower yield point for types B, D and E or as an "average" yield strength for types B - E. Only the limit of proportionality and proof stress were applicable to all types of yield but as calculation of limit of proportionality involved determining the point at which the stress-strain curve deviated from linearity, measurement of proof stress was preferred for the full range of materials.

The average properties quoted in the tables were calculated in the following manner:



TABLE 7.1A MECHANICAL PROPERTIES OF THE ADHESIVE BONDED 32.6% STEEL, 67.4% COPPER COMPOSITE (Rolling directions parallel)

Material	Direction	L.Y.P. (hb)	0.5% P.S. (hb)	U.T.S. (hb)	% Elongation		n	R
					Total	Uniform		
.025" Steel	0	20.5	20.1	30.9	30.5	25.5	0.260	0.78
.051" Copper		—	6.6	20.7	46.5	40.7	0.443	0.89
.085" Composite		+	11.6	23.3	47.6	40.9	0.319	0.72
		—	10.2*	20.5*				
.025" Steel	45	21.2	21.0	32.6	27.8	21.2	0.270	0.92
.051" Copper		—	6.6	19.9	60.7	52.8	0.419	0.47
.085" Composite		+	13.1	24.1	48.5	46.0	0.294	0.48
		—	11.6*	21.3*				
.025" Steel	90	19.6	20.4	30.7	34.7	24.0	0.258	2.00
.051" Copper		—	6.0	20.1	46.6	37.4	0.454	0.96
.085" Composite		+	12.5	23.9	41.2	33.3	0.303	0.86
		—	11.1*	21.2*				
.025" Steel	Ave	20.5	20.5	31.7	30.2	23.0	0.265	1.16
.051" Copper		—	6.5	20.2	53.6	45.9	0.434	0.70
.085" Composite		+	12.7	23.9	46.5	41.6	0.303	0.64
		—	11.1*	21.2*				

TABLE 7.1B. MECHANICAL PROPERTIES OF THE ADHESIVE BONDED 32.6% STEEL 67.4% COPPER COMPOSITE. (Rolling Directions mismatched by 45°)

Material	Direction	L.Y.P. (hb)	0.5% P.S. (hb)	U.T.S. (hb)	% Elongation		n	R
					Total	Uniform		
.025" Steel	45	21.2	21.0	32.6	27.8	21.2	0.270	0.92
.051" Copper	0	—	6.6	20.7	46.5	40.7	0.443	0.89
.085" Composite		+	13.1	24.7	40.8	34.7	0.290	0.93
		—	11.4*	21.5*				
.025" Steel	0	20.5	20.1	30.9	30.5	25.5	0.260	0.78
.051" Copper	45	—	6.6	19.9	60.7	52.8	0.419	0.47
.085" Composite		+	11.7	23.6	42.3	34.6	0.305	0.45
		—	10.2*	20.7*				

\* Calculated using total cross-sectional area.

+ No clear indication of 'steel type' yield elongation; a more gradual change of slope, type C; Figure 7.4.



TABLE 7.2A. MECHANICAL PROPERTIES OF THE ADHESIVE BONDED 80% STEEL  
20% COPPER COMPOSITE (Rolling directions parallel)

Material	Direction	L.Y.P. (hb)	0.5% P.S. (hb)	U.T.S. (hb)	% Elongation		n	R
					Total	Uniform		
.060" Steel	0	19.9	19.5	29.8	45.7	35.0	0.272	1.15
.015" Copper		—	6.3	21.9	44.7	40.5	0.460	0.80
.085" Composite		19.0	17.3	28.1	39.3	32.0	0.268	0.88
		16.8*	16.2*	24.9*				
.060" Steel	45	19.9	20.1	31.2	40.7	30.8	0.260	1.07
.015" Copper		—	6.5	20.7	52.2	44.5	0.450	0.92
.085" Composite		+	18.1	29.2	36.3	31.0	0.254	0.94
		—	15.8*	25.8*				
.060" Steel	90	18.8	20.2	30.9	42.4	29.6	0.248	1.77
.015" Copper		—	6.3	20.8	38.4	37.3	0.450	0.78
.085" Composite		17.8	17.6	29.0	36.9	28.7	0.249	1.09
		15.8*	15.6*	25.6*				
.060" Steel	Ave	19.6	19.9	30.7	42.4	31.5	0.260	1.27
.015" Copper		—	6.5	21.0	46.9	41.7	0.452	0.81
.085" Composite		—	18.1	28.9	37.2	30.7	0.256	0.96
		—	15.9*	25.5*				

TABLE 7.2B. MECHANICAL PROPERTIES OF THE ADHESIVE BONDED 80% STEEL,  
20% COPPER COMPOSITE (rolling directions mismatched by 45°)

Material	Direction	L.Y.P. (hb)	0.5% P.S. (hb)	U.T.S. (hb)	% Elongation		n	R
					Total	Uniform		
.060" Steel	45	19.9	20.7	31.2	40.7	30.8	0.260	1.07
.015" Copper	0	—	6.3	21.9	44.7	40.5	0.460	0.80
.085" Composite		18.4	18.8	30.0	32.9	25.4	0.252	0.86
		16.1*	16.1*	26.3*				
.060" Steel	0	19.9	19.5	29.8	45.7	35.0	0.272	1.15
.015" Copper	45	—	6.5	20.7	52.2	44.5	0.450	0.92
.085" Composite		18.5	19.2	28.1	39.2	30.1	0.253	0.95
		16.1*	16.5*	24.2*				

\* Calculated using total cross-sectional area.

+ No clear indication of 'steel type' yield elongation; a more gradual change of slope, type C, figure 7.4.



Table 7.3. Mechanical properties of roll bonded composites.

Material		0.5% P.S. (hb)			U.T.S. (hb)			% Elongation						n			R		
								Total			Uniform								
% Cu	% Steel	0	45	90	0	45	90	0	45	90	0	45	90	0	45	90	0	45	90
-	100	27.3	30.6	26.4	34.9	37.0	35.4	24.0	20.4	23.1	15.5	11.2	13.1	0.180	0.151	0.155	0.70	0.82	1.19
100	-	6.8	6.5	7.0	22.7	21.8	22.2	49.7	49.9	47.9	44.6	42.1	40.5	0.445	0.443	0.444	0.86	1.11	0.97
20	80	21.4	22.7	22.4	29.4	30.4	30.3	31.8	37.0	37.5	22.5	30.7	29.1	0.218	0.215	0.212	0.63	0.83	1.63
33	67	22.9	23.9	22.9	29.4	29.1	28.4	40.5	37.4	46.9	30.6	29.3	26.5	0.251	0.227	0.244	1.08	0.74	1.35
50	50	14.1	14.8	14.4	25.6	25.9	25.6	46.5	41.1	46.1	30.2	29.5	30.4	0.303	0.282	0.283	0.80	0.88	1.20
67	33	15.4	15.4	14.7	24.7	24.5	24.2	41.2	40.8	50.0	32.3	29.9	32.1	0.333	0.314	0.345	0.88	0.77	1.04
80	20	9.9	10.8	10.4	23.0	22.4	22.2	45.7	45.9	50.7	32.3	38.0	40.1	0.403	0.391	0.424	0.79	0.85	0.93
34	2x33	22.2	22.6	22.0	29.1	29.2	28.4	46.0	39.6	42.5	36.6	31.0	33.7	0.261	0.243	0.261	1.09	0.66	1.56
50	2x25	18.1	19.6	18.7	26.9	27.3	26.7	44.0	39.7	46.4	37.1	32.7	35.2	0.304	0.284	0.297	1.10	0.77	1.48
80	2x10	9.5	9.9	9.2	22.7	22.0	22.1	42.9	45.9	49.1	38.8	35.9	40.3	0.424	0.428	0.445	0.82	0.86	0.91
2x25	50	20.4	20.9	18.4	27.0	26.8	26.2	39.0	42.9	47.6	32.3	36.1	38.7	0.276	0.263	0.270	1.15	0.92	1.47
2x33	34	15.4	17.1	14.4	25.4	23.6	23.9	44.4	48.6	51.5	35.9	39.4	42.3	0.356	0.329	0.346	0.88	0.98	1.02



Table 7.4. Average mechanical properties of roll bonded composites.

Material		0.5% P.S. (hb)	U.T.S. (hb)	% Elongation		n	R	$\Delta R$
% Cu	% Steel			Total	Uniform			
-	100							
100	-	6.7	22.1	49.4	42.3	0.444	1.01	-0.193
20	80	22.3	30.1	35.8	28.3	0.215	0.98	0.306
33	67	23.4	29.0	40.6	28.9	0.237	0.98	0.486
50	50	14.5	25.8	43.6	29.9	0.288	0.94	0.128
67	33	15.2	24.5	43.2	31.1	0.327	0.87	0.220
80	20	10.5	22.5	47.1	37.1	0.402	0.86	0.012
34	2x33	22.4	29.0	41.9	33.1	0.252	0.99	0.670
50	2x25	19.0	27.1	42.5	34.4	0.292	1.03	0.505
80	2x10	9.6	22.2	46.0	37.7	0.431	0.86	0.006
2x25	50	20.1	26.7	43.1	35.8	0.268	1.12	0.350
2x33	34	16.0	24.1	48.3	39.3	0.340	0.97	0.031



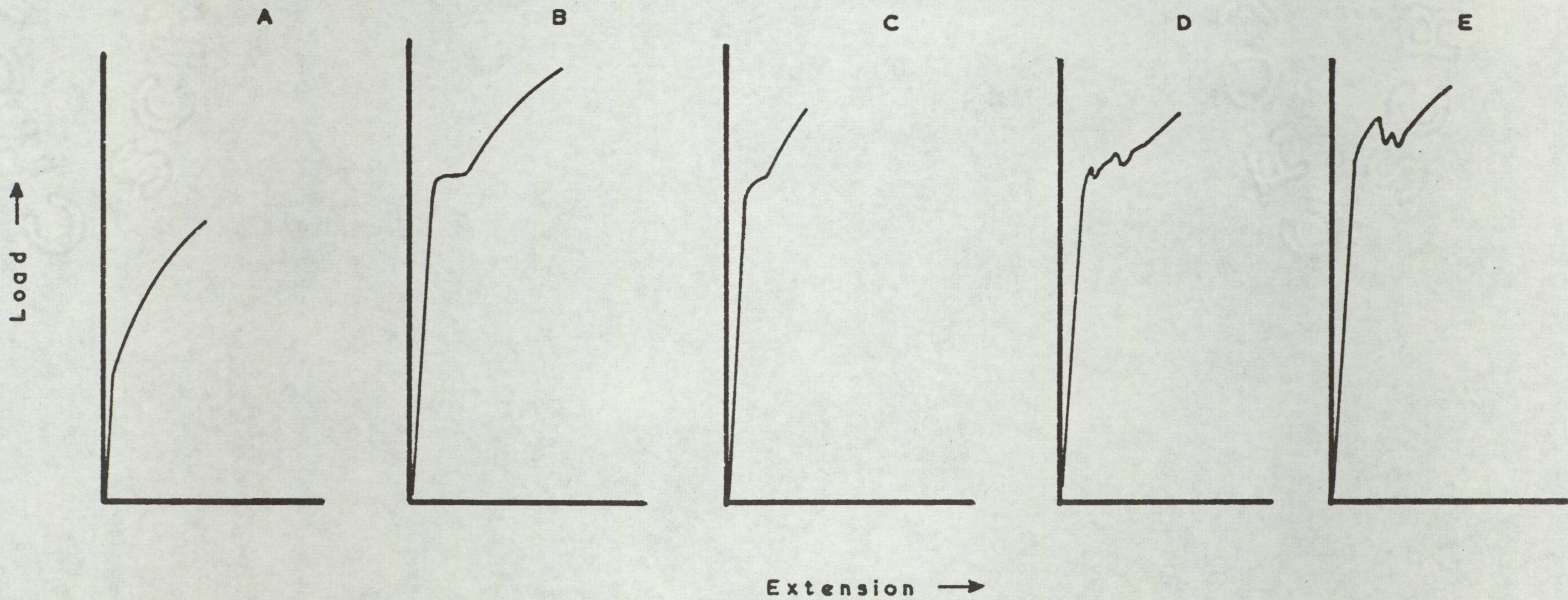


Figure 7.4 Load-extension curves illustrating the different types of yield observed in the experimental work.



e.g. ultimate tensile strength (M)

$$\bar{M} = \frac{(M_0 + 2M_{45} + M_{90})}{4} \dots\dots\dots 7.1$$

where  $\bar{M}$  = Mean U.T.S.

$M_{0,45,90}$  = U.T.S. at 0°, 45° or 90° to the rolling direction respectively.

R values were determined at strain levels varying from 5 to 25%, but were found to be approximately constant between 10 and 20% strain for all the materials examined. The tabulated R values are those determined at 15% strain.  $\Delta R$ , the planar variation in R, shown in table 7.4, was calculated using the formula :

$$\Delta R = \frac{R_0 - 2R_{45} + R_{90}}{2\bar{R}} \dots\dots\dots 7.2$$

where  $R_0, 45, 90$  = R value measured at 0°, 45° or 90° to the rolling direction respectively

$\bar{R}$  = mean R value

True stress – true strain data was determined from the experimental data using :

$$\sigma = \frac{P}{A_0} (1 + e) \dots\dots\dots 7.3$$

$$\delta = \ln (1 + e) \dots\dots\dots 7.4$$

where  $\sigma$  = true stress  
 $\delta$  = true strain  
 P = load  
 e = arithmetic strain  
 A<sub>0</sub> = original cross-sectional area



From the true stress – true strain data the work hardening index,  $n$ , was determined by calculating the slope ( $n$ ) of the true stress – true strain curve plotted on a logarithmic basis. The degree of correlation,  $r$ , about this line was also determined and in all tests  $r > 0.999$  ( $r = 1.0$  indicates a perfect fit) so that in all cases the true stress – true strain relationship may be represented by equation 4.1 :

$$\text{i.e.} \quad \sigma = k \epsilon^n$$

The values of the coefficients 'n' and 'k' are tabulated in tables 7.5 and 7.6.

Typical true stress – true strain curves for steel, copper and adhesive bonded copper/steel composite are shown in figure 7.5, the curve for the composite having been calculated using the cross-sectional area of the metal only.

#### 7.4. DEEP DRAWING AND STRETCH FORMING PROPERTIES :

The deep drawing and stretchforming results are summarised in tables 7.7 – 7.9 for adhesive bonded composites and tables 7.10 – 7.12 for roll bonded composites. The limiting drawing ratio (L.D.R.) was calculated as the ratio of the critical blank diameter to punch diameter (33 m.m.)

With the 20% copper/80% steel adhesive bonded composite failure of the copper component occurred, when the copper component was on the outer surface of the cups. Failure occurred even at blank diameters less than 50 m.m. although the C.B.D. for the copper component was 66+ m.m. The failure was similar to that shown in figure 7.12 (page 95 ) and was attributed to breakdown in adhesion at the periphery of the blank.

During radial drawing-in of the flange the copper component had a greater tendency to wrinkle than had the steel component because it was the thinner of the two, and, as a result, the adhesive at the periphery of the blank was subjected to a peel or cleavage type loading. Redux has a poor peel or cleavage strength and, in addition was probably weakened during the blanking operation, so that there was breakdown in the adhesion. The breakdown in adhesion allowed relative movement of the composite components and, hence, wrinkling of the copper to occur once the component was no longer restrained by the blank holder force. Failure of the copper occurred when the wrinkled flange of the copper was drawn into the die throat.



Table 7.5. Coefficient 'k' and 'n' for the adhesive bonded composites.

Material	% Copper	% Steel	k (hb)	n
0.060" Steel	—	100	57.1	0.260
0.015" Copper	100	—	49.8	0.452
0.085" Composite	20	80	53.2	0.256
0.025" Steel	—	100	60.3	0.265
0.051" Copper	100	—	46.8	0.434
0.085" Composite	67.4	32.6	46.3	0.303

Table 7.6. Coefficients 'k' and 'n' for the roll bonded composites.

Composite		k (hb)	n
% Cu.	% Steel		
—	100	57.3	0.159
100	—	52.5	0.444
20	80	52.0	0.215
33	67	51.7	0.237
50	50	49.3	0.288
67	33	49.3	0.327
80	20	50.5	0.402
34	2 x 33	52.7	0.252
50	2 x 25	52.0	0.292
80	2 x 10	51.7	0.431
2 x 25	50	49.6	0.268
2 x 33	34	49.4	0.340



Figure 7.5. Typical true stress - true strain curves for steel, copper and adhesive bonded steel/copper bilayer composite (longitudinal test pieces).

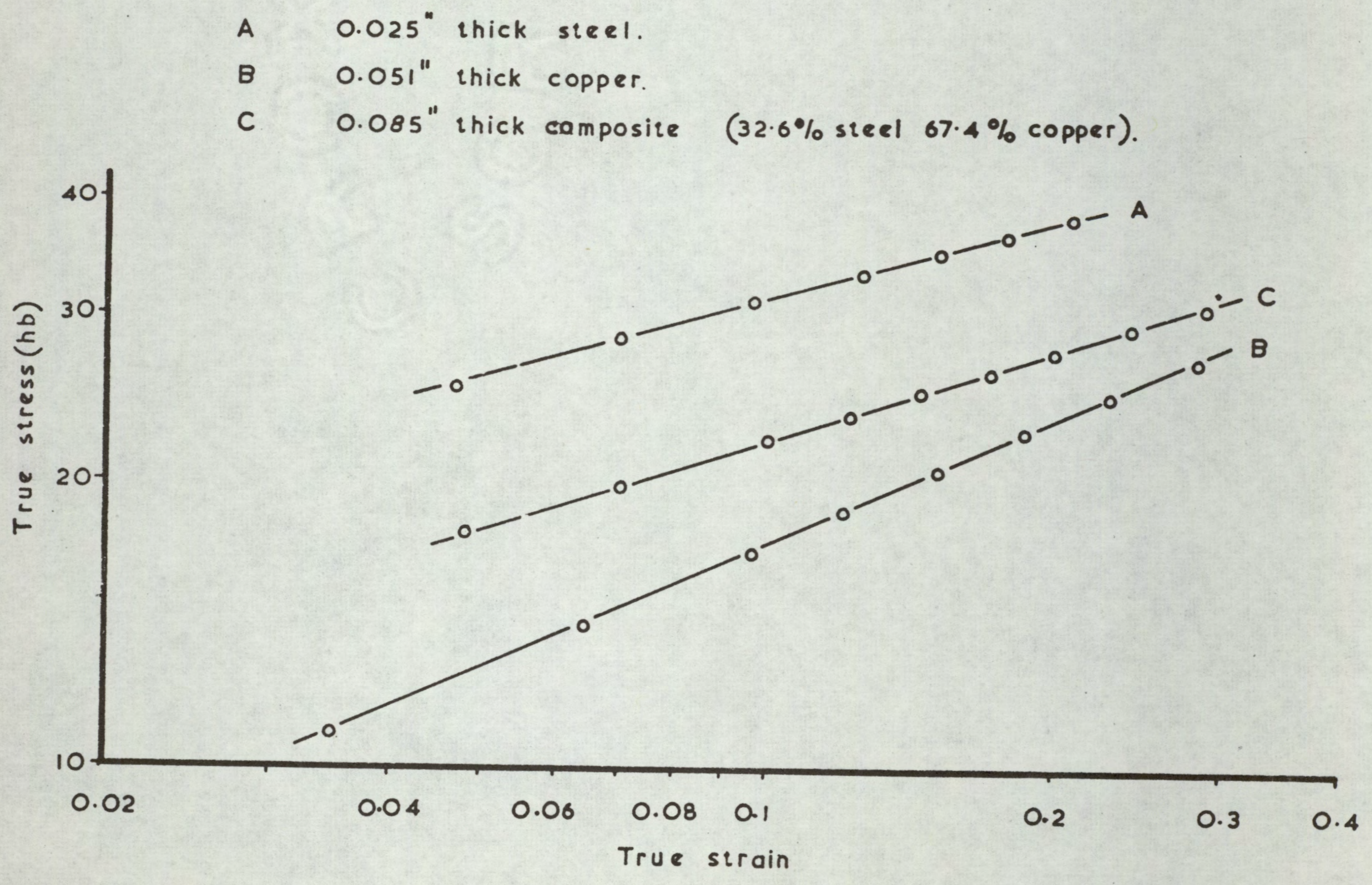




Table 7.7 Deep drawing results for the adhesive bonded composites.

Material	Per Cent		Rolling directions of steel & copper matched or mismatched by 45°	Copper on Outside			Steel on Outside		
	Copper	Steel		C.B.D.	L.D.R.	Maximum Punch Load (Kg)	C.B.D.	L.D.R.	Maximum Punch Load (Kg)
				(m.m.)			(m.m.)		
0.060" Steel	0	100	-	-	-	-	70	2.12	5300
0.015" Copper	100	0	-	66+	> 2.00 < 2.03	750	-	-	-
0.085" Composite	20	80	Matched	Failure of Adhesive			67	2.03	5600
" "	"	"	Mismatched	"	"	"	67	2.03	5650
0.025" Steel	0	100	-	-	-	-	72-	> 2.15 < 2.18	2300
0.051" Copper	100	0	-	67	2.03	2470	-	-	-
0.085" Composite	67.4	32.6	Matched	65	1.97	4500	65	1.97	4550
" "	"	"	Mismatched	65	1.97	4550	65-	1.97	4550



Table 7.8 Earing of cups drawn from 65 mm diameter blanks of the adhesive bonded composites. (The results are the mean of three tests).

Material	Per Cent		Rolling Directions of Steel and Copper matched or mismatched by 45°	Copper on Outside				Steel on Outside			
	Copper	Steel		Max. punch load (Kg)	Ear Height (m.m.)	% Earing	Mean Cup Height (m.m.)	Max. punch load (Kg)	Ear Height (m.m.)	% Earing	Mean Cup Height (m.m.)
0.060" Steel	0	100	-	-	-	-	-	4600	1.40	5.35	26.20
0.015" Copper	100	0	-	800	0.59	2.12	27.60	-	-	-	-
0.085" Composite	20	80	Matched	Failure of Adhesive				5420	0.71	2.70	26.23
" "	"	"	Mismatched	" " "				5420	0.68	-2.56	26.51
0.025" Steel	0	100	-	-	-	-	-	1900	1.06	4.18	25.31
0.051" Copper	100	0	-	2400	2.10	7.75	27.10	-	-	-	-
0.085" Composite	67.4	32.6	Matched	4500	1.05	3.83	27.38	4450	1.12	4.17	26.85
" "	"	"	Mismatched	4550	0.15	0.54	27.87	4450	0.85	3.06	27.61

N.B. Earing measurements on the composites with the rolling directions of the steel and copper components mismatched by 45° were made with respect to the rolling direction of the copper components.



Table 7.9 Stretch forming results for the adhesive bonded composites. (The results are the mean of duplicate tests).

Material	Per Cent		Rolling directions of Steel & Copper matched or mismatched by 45°	Copper on Outside		Steel on Outside	
	Copper	Steel		Erichsen Value (m.m.)	Maximum Punch Load (Kg)	Erichsen Value (m.m.)	Maximum Punch (Load Kg)
0.060" Steel	0	100	-	-	-	13.20	2350
0.015" Copper	100	0	-	10.75	200	-	-
0.085" Composite	20	80	Matched	10.50	2550	13.55	2550
" "	"	"	Mismatched	10.60	2650	13.40	2650
0.025" Steel	0	100	-	-	-	10.20	800
0.051" Copper	100	0	-	14.20	1250	-	-
0.085" Composite	67.4	32.6	Matched	13.75	2250	12.50	2250
" "	"	"	Mismatched	13.35	2200	11.80	2200



Table 7.10 Deep drawing results for the roll bonded composites.

Material		Copper on Outside			Steel on Outside		
% Copper	% Steel	C.B.D. (mm)	L.D.R.	Max. Punch Load (Kg)	C.B.D. (mm)	L.D.R.	Max. Punch Load (Kg)
-	100	-	-	-	65	1.97	6730
100	-	66	2.00	3800	-	-	-
20	80	66	2.00	5900	66(-)	> 1.97 < 2.00	5850
33	67	67	2.03	5200	67	2.03	5130
50	50	67	2.03	4750	66	2.00	4550
67	33	66	2.00	4300	66	2.00	4230
80	20	66	2.00	3920	66	2.00	3900
34	2x33	-	-	-	67(-)	> 2.00 < 2.03	5280
50	2x25	-	-	-	66	2.00	4830
80	2x10	-	-	-	66	2.00	3820
2x25	50	67	2.03	4800	-	-	-
2x33	34	66	2.00	4450	-	-	-



Table 7.11 Earing of cups drawn from 65 mm diameter blanks of the roll bonded composites.

Composite % Copper		Copper on outside				Steel on outside			
		Max. Punch Load (Kg)	Ear Height (mm)	% Earing	Mean Cup Height (mm)	Max. Punch Load (Kg)	Ear Height (mm)	% Earing	Mean Cup Height (mm)
-	100	-	-	-	-	6730	0.67	2.26	27.20
100	-	3800	0.05	-1.77	27.80	-	-	-	-
20	80	5600	1.54	5.65	27.34	5600	1.35	5.00	27.01
33	67	4960	1.43	5.14	27.15	5000	1.25	4.72	26.55
50	50	4610	0.44	1.90	27.74	4580	0.24	0.87	27.38
67	33	4275	0.78	2.82	27.65	4200	0.70	2.60	27.15
80	20	3925	0.10	0.27	28.21	3900	0.03	-0.12	27.70
34	2x33	-	-	-	-	5060	1.76	6.43	27.39
50	2x25	-	-	-	-	4650	1.16	4.19	27.53
80	2x10	-	-	-	-	3750	0.10	-0.32	27.83
2x25	50	4580	1.20	4.50	26.63	-	-	-	-
2x33	34	4360	0.10	-0.34	27.63	-	-	-	-

(Results are the mean of three tests).



Table 7.12 *Stretch forming results for the roll bonded composites.*

Material		Copper on Outside		Steel on Outside	
% Copper	% Steel	Erichsen (mm)	Maximum Punch Load (Kgs)	Erichsen (mm)	Maximum Punch Load (Kgs)
-	100	-	-	10.9	2700
100	-	14.9	1950	-	-
20	80	13.1	2575	12.3	2575
33	67	12.9	2350	12.5	2400
50	50	13.3	2200	12.4	2200
67	33	13.2	2050	12.4	2050
80	20	13.1	1875	12.3	1850
34	2x33	-	-	12.1	2350
50	2x25	-	-	12.4	2200
80	2x10	-	-	13.5	1825
2x25	50	13.1	2150	-	-
2x33	34	14.3	2100	-	-

(Results are the mean of duplicate tests).



The percentage earing, tables 7.8 and 7.11, was determined from measurements of ear and trough heights of cups drawn from blanks of 65 m.m. diameter using the formula:

$$E = \frac{\bar{h}_e - \bar{h}_t}{\frac{1}{2}(\bar{h}_e + \bar{h}_t)} \times 100 \quad \dots\dots\dots 7.5$$

where  $\bar{h}_e$  = mean ear height  
 $\bar{h}_t$  = mean trough height

In tables 7.8 and 7.11, and throughout the discussion, 0–90° earing has been designated positive and 45° earing negative.

Examples of the thickness surveys on cups sectioned in the direction of earing are shown in figure 7.6 for samples of the roll bonded composites. The degree of thinning over the punch nose was found to vary with per cent copper and, for the bilayer composites, was also found to vary with the component on the outer surface, as shown in figure 7.7.

#### 7.5 PLANE STRAIN COMPRESSION :

In the plane strain compression tests true stress and true strain were calculated as follows:

$$\sigma_p = \frac{p}{bW} \quad \dots\dots\dots 7.6$$

where  $\sigma_p$  = plane stress  
 $p$  = load  
 $b$  = die breadth  
 $W$  = width of testpieces after indentation

$$\delta_p = \ln t_o/t_x \quad \dots\dots\dots 7.7$$

where  $\delta_p$  = plane strain  
 $t_o$  = original thickness of testpieces  
 $t_x$  = thickness after indentation

$$\sigma = \sigma_p \times \sqrt{3}/2 \quad \dots\dots\dots 7.8$$

where  $\sigma$  = true stress

$$\delta = \delta_p \times 2/\sqrt{3} \quad \dots\dots\dots 7.9$$

where  $\delta$  = true strain



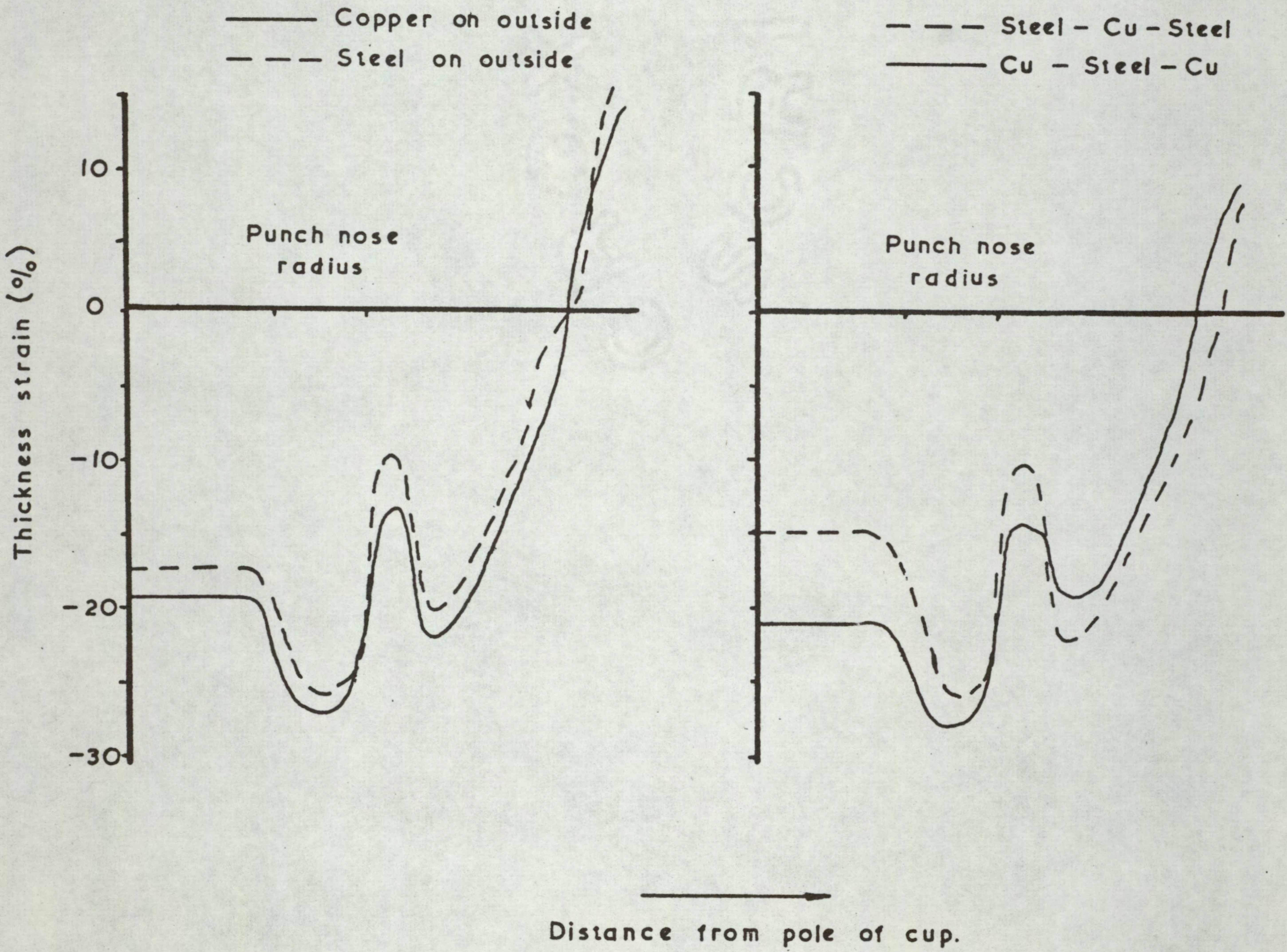


Figure 7.6

Thickness surveys on cups drawn from 65 m.m. diameter blanks:—

left: 50% Copper / 50% Steel bilayer composite

right: 25 / 50 / 25 three layer composite.



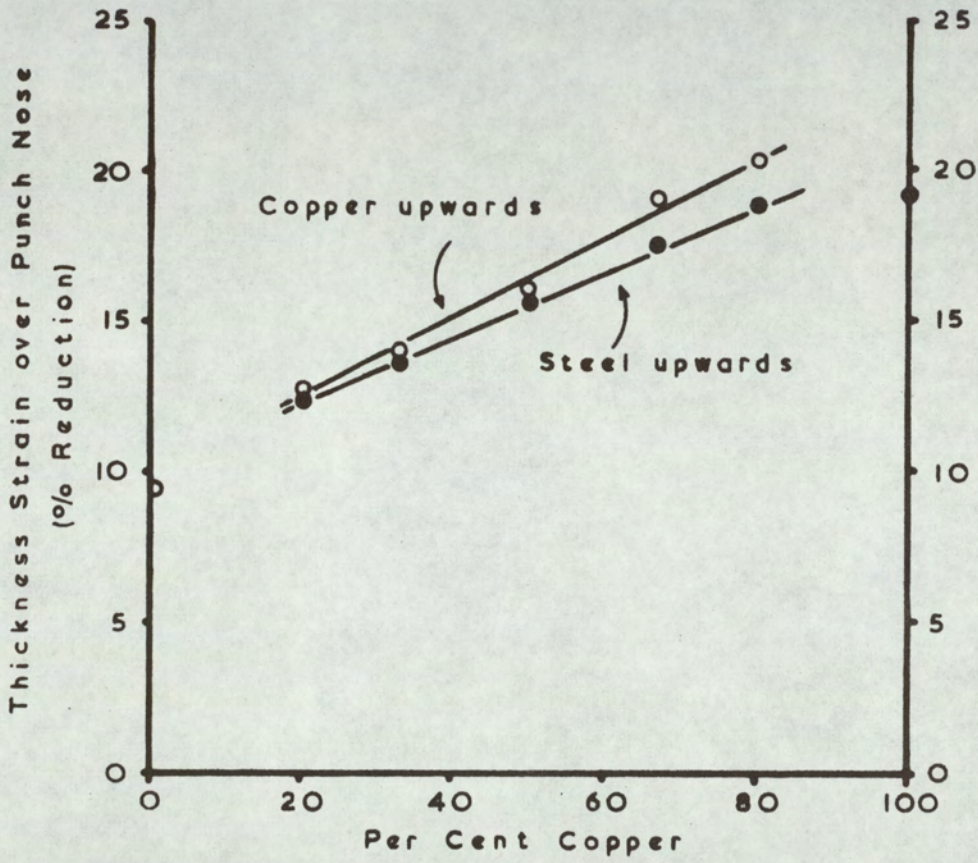


Figure 7.7 Variation of thickness strain over the punch nose with per cent copper.



Molybdenum disulphide grease is generally used as the lubricant in plane strain compression tests, but it was considered that the results of these tests would be more comparable with those of the deep drawing tests if polythene was used as the lubricant. To determine the influence of using polythene as lubricant, rather than molybdenum disulphide grease, the true stress – true strain curves for annealed copper and also steel, were derived using each lubricant in turn. A comparison of the two curves for the copper and for the steel revealed that, at any true strain, the corresponding true stress was approximately 7% lower when polythene was used as the lubricant instead of molybdenum disulphide, and so polythene was used for all the tests.

Only the roll bonded composites were tested in plane strain compression, the results being summarised in figures 7.8 and 7.9.

Normal anisotropy ( $\beta$ ) was assessed using the technique developed by Holcomb and Backfen <sup>(55)</sup> outlined in section 4.2.3, equation 4.6 being used for this purpose:

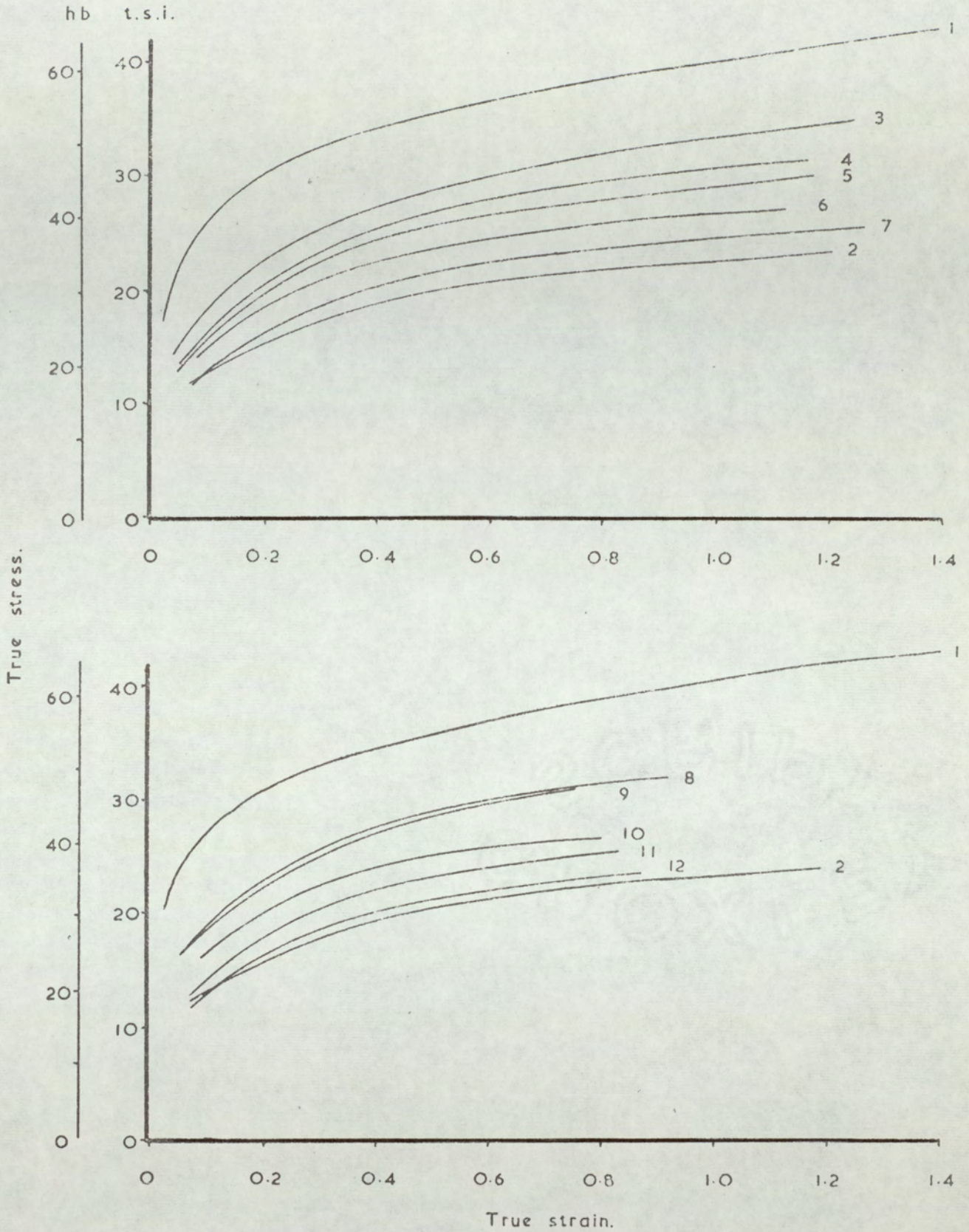
$$\text{i.e. } \beta = \frac{\sigma_x}{\sigma_y}$$

The results are tabulated in table 7.13 in which the variation of  $\beta$  with strain is illustrated.

The plane strain compression curves were derived upto true strain levels of 1.5 for the three layer composites, but the curves for the bilayer composites were not derived to such high strains because the specimens "bowed" during deformation to such an extent that, at strain levels of approximately 0.8 – 1.0, the regions outside the indenting dies began to engage on the die assembly. Figure 7.10 illustrates a sample that had been strained upto a true strain level of 0.9.

It was thought that "bowing" of the testpieces, especially when as severe as illustrated in figure 7.10, would affect the experimental curves. In order to prevent bowing, and hence to determine its influence on the experimental curves, three layer composites were made by bolting together two similar bilayer composites to form either steel/copper/steel or copper/steel/copper composites. The results for a 50% copper /50% steel composite are shown in figure 7.11 :



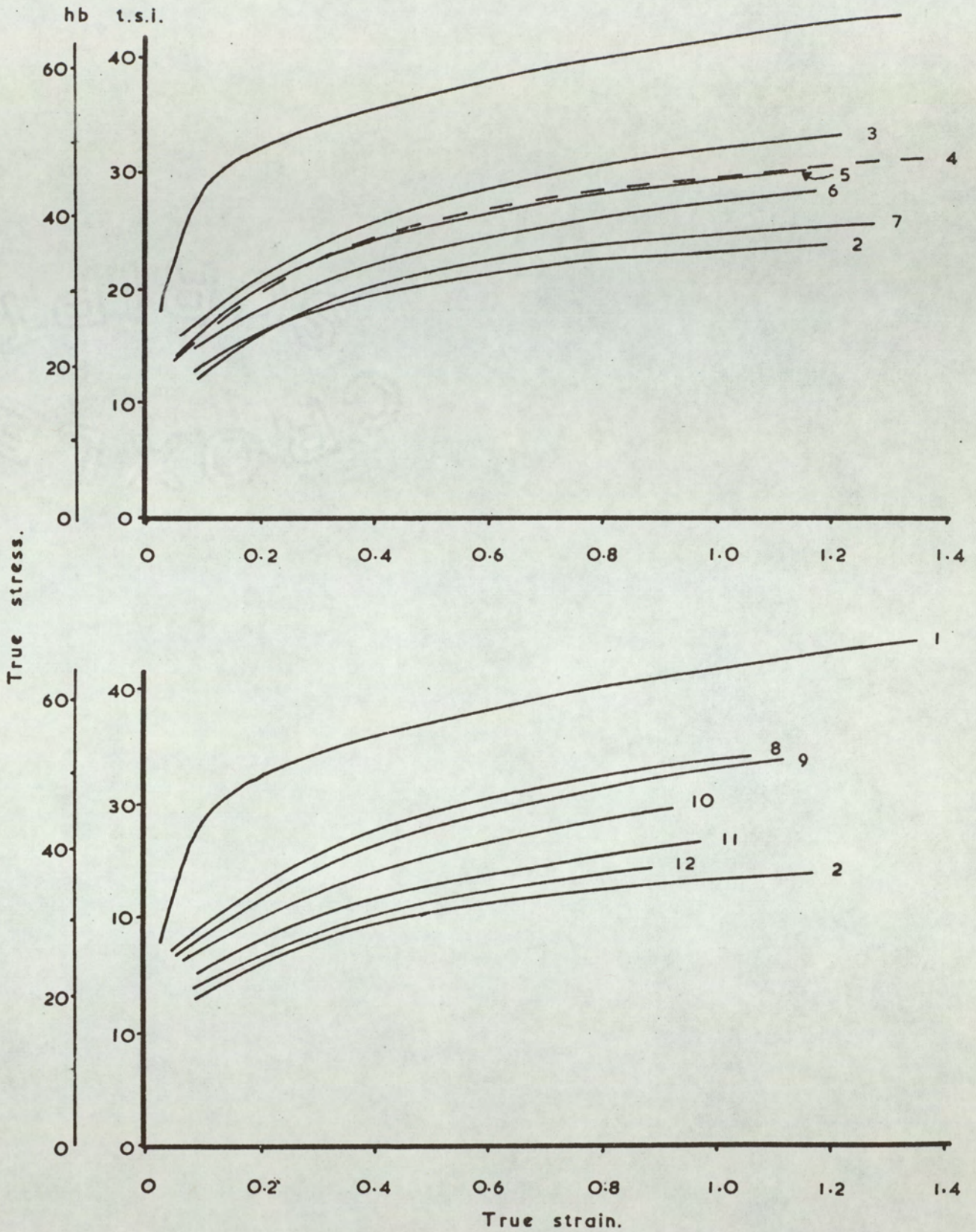


KEY:

	% Copper	% Steel		% Copper	% Steel
1.	0	100	7.	80	2 x 10
2.	100	0	8.	20	80
3.	34	2 x 33	9.	33	67
4.	50	2 x 25	10.	50	50
5.	2 x 25	50	11.	67	33
6.	2 x 33	34	12.	80	20

Figure 7.8 True stress - true strain curves for the roll bonded composites for the plane strain compression tests with  $dE_y = 0$ .





KEY: As for figure 7.8.

Figure 7.9 True stress - true strain curves for the roll bonded composites for the plane strain compression tests with  $dE_z = 0$ .



Table 7.13 The variation in normal anisotropy ( $\beta$ ) with true strain.

Composite		$\beta$ at a true strain of:					
% Copper	% Steel	0.1	0.2	0.4	0.6	0.8	1.0
-	100	0.95	0.95	0.97	0.97	0.97	0.97
100	-	0.99	0.98	1.00	0.99	0.98	1.00
20	80	0.97	1.01	1.00	1.00	0.98	-
33	67	1.00	1.03	1.02	1.01	0.99	0.99
50	50	0.96	1.00	1.01	0.98	0.95	-
67	33	0.93	0.97	1.01	1.01	0.98	-
80	20	0.91	0.98	1.00	0.99	0.98	-
34	2x33	1.06	1.07	1.07	1.05	1.04	1.04
50	2x25	1.03	1.05	1.07	1.05	1.06	1.04
80	2x10	0.99	0.99	1.01	1.01	1.00	1.00
2x25	50	1.00	1.01	1.02	1.02	1.00	1.00
2x33	34	0.95	1.00	1.01	1.00	0.99	0.97



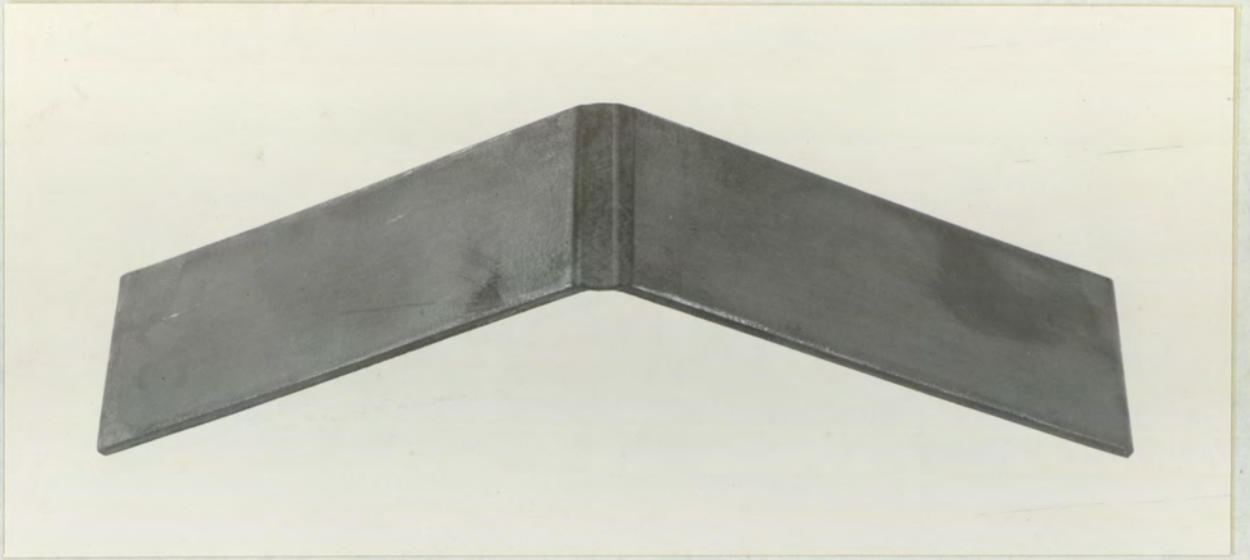


Figure 7.10 A specimen of a bilayer composite illustrating "bowing".

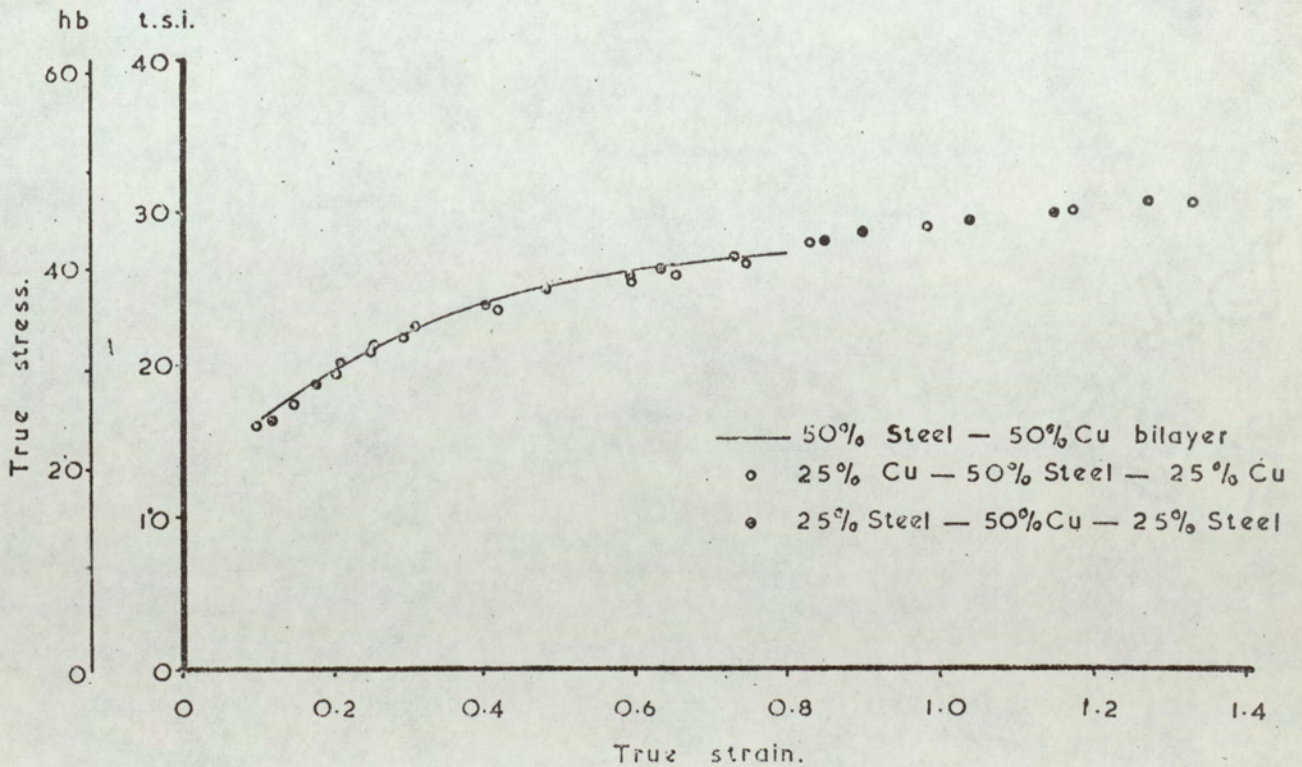


Figure 7.11 Plane strain compression curves for samples made from two bilayer composites.



It may be seen from figure 7.11 that there is little difference in the three curves thus illustrating that "bowing" of the bilayer composites did not significantly affect the experimental results. Figure 7.11 also illustrates that frictional conditions between the die and the steel components were similar to those between the die and the copper components.

## 7.6 TESTS ON THE STEEL AND COPPER COMPONENTS OF THE ROLL BONDED COMPOSITES

### 7.6.1 Tensile properties:

The results of the tensile tests on the steel and copper components of the composites are shown in tables 7.14 – 7.17.

Pitting of several of the steel samples was observed; on the majority of these the degree of pitting was slight but was probably sufficient to cause premature failure of some of the testpieces, particularly those marked with an asterisk in table 7.14. The steel component of the 10% steel/80% copper/ 10% steel composite was so severely pitted that reliable results were <sup>not</sup> obtained.

A linear relationship was obtained between true stress and true strain, the degree of correlation about this line being similar to that obtained for the composites. The true stress – true strain relationship for the steel and copper components, like the relationship for the composites, may be represented by equation 4.1 :

$$\sigma = k \epsilon^n$$

The values of the coefficients 'k' and 'n' are given in table 7.18

### 7.6.2 Deep drawing and stretch forming properties:

The results of the deep drawing and stretch forming tests are shown in tables 7.19 and 7.20. The techniques used to obtain samples of the steel and copper components were time consuming and, because of the large bulk of material required to determine drawability, the C.B.D's. of the components of only three of the composites were determined.



Table 7.14 Mechanical properties of the steel components of the roll bonded composites.

Steel from composites		0.5% P.S. (hb)			U.T.S. (hb)			% Elongation						n			R		
								Total			Uniform								
% Cu	% Steel	0	45	90	0	45	90	0	45	90	0	45	90	0	45	90			
20	80	23.2	26.4	26.0	32.1	33.9	32.7	29.1	24.8	34.5	19.6	18.6	26.4	0.238	0.158	0.237	0.61	0.72	1.32
33	67	30.6	31.9	29.8	33.3	35.1	33.2	31.6	28.2	38.8	25.1	20.9	29.4	0.198	0.188	0.195	1.30	0.66	1.66
50	50	20.8	23.8	22.8	30.9	31.6	31.4	28.3	27.7	31.9	22.3	22.3	23.3	0.205	0.188	0.189	0.81	0.87	1.37
67	33	29.7	29.6	28.0	32.8	33.4	31.9	31.0	17.5*	36.5	24.8	14.3*	26.7	0.207	0.190	0.220	1.27	0.53	1.85
80	20	29.7	28.2	26.8	31.5	30.6	29.0	28.4	16.8*	27.3	16.4	15.1*	20.8	0.198	0.171	0.191	0.96	0.45	1.29
34	2x33	29.6	31.3	28.9	31.5	33.0	31.2	29.1	21.3	29.8	23.9	16.3	21.3	0.201	0.195	0.203	0.96	0.57	1.75
50	2x25	29.9	32.0	33.3	31.7	32.8	32.0	25.6	18.3*	26.9	22.4	13.8*	13.7	0.210	0.191	0.208	1.16	0.44	1.10
80	2x10	NOT TESTED																	
2x25	50	30.3	33.0	30.2	33.4	34.5	32.9	39.6	30.1	38.6	30.2	21.0	29.3	0.198	0.178	0.195	1.55	0.73	1.81
2x33	34	27.2	27.8	28.5	30.2	31.9	30.3	36.5	29.2	43.0	30.4	25.8	32.0	0.238	0.236	0.253	0.84	0.43	2.06

cf 100% Steel      27.3   30.6   26.4      34.9   37.0   35.4      24.0   20.4   23.1      15.5   11.2   13.1      0.180   0.151   0.155      0.70   0.82   1.19

\* Premature failure due to pitting of samples



Table 7.15 Mechanical properties of the copper components of the roll bonded composites.

Cu from composites		0.5% P.S. (hb)			U.T.S. (hb)			% Elongation						n			R		
								Total			Uniform								
% Cu	% Steel	0	45	90	0	45	90	0	45	90	0	45	90	0	45	90	0	45	90
20	80	5.8	7.2	6.4	19.1	18.4	18.3	37.9	40.3	38.9	34.9	37.1	36.2	0.485	0.420	0.479	0.87	0.95	0.92
33	67	6.9	6.7	6.1	19.6	19.0	19.4	28.2*	39.8	46.9	30.0	38.2	43.7	0.419	0.514	0.496	0.76	1.11	0.89
50	50	6.1	6.1	5.7	20.0	19.4	19.8	43.7	42.4	47.3	40.0	41.8	42.3	0.473	0.499	0.491	0.83	1.01	0.93
67	33	6.3	6.3	6.0	20.6	19.5	19.6	40.4	50.2	51.1	38.5	42.5	47.8	0.462	0.470	0.493	0.77	1.13	0.93
80	20	5.5	5.7	5.7	20.0	19.5	19.9	39.8	49.0	52.3	35.6	43.4	48.5	0.490	0.485	0.488	0.76	1.11	0.94
34	2x33	5.3	5.7	5.7	20.0	18.5	19.4	28.5	40.9	40.0	27.6	37.6	38.4	0.506	0.492	0.521	0.73	1.24	0.82
50	2x25	5.8	5.7	5.5	20.5	19.1	19.3	33.5	47.1	42.0	30.9	41.8	39.0	0.501	0.491	0.505	0.74	1.16	0.86
80	2x10	5.2	5.2	5.4	19.9	19.5	19.5	43.7	45.1	51.7	38.3	39.5	44.8	0.526	0.532	0.527	0.75	0.96	0.93
2x25	50	0.2	6.4	5.9	19.9	18.9	19.2	30.0	41.3	39.3	29.7	38.5	37.6	0.487	0.455	0.492	0.78	1.12	0.88
2x33	34	7.2	6.6	6.5	21.4	18.1	19.1	32.2	35.8	46.1	30.9	30.8	43.8	0.454	0.455	0.488	0.74	1.65	0.55

cf 100% copper 6.8 6.5 7.0 22.7 21.8 22.2 49.7 49.9 47.9 44.6 42.1 40.5 0.445 0.443 0.444 0.86 1.11 0.97

\* test piece broke outside the gauge length so that this result is unreliable; the total elongation must be greater than the uniform elongation.



Table 7.16. Average mechanical properties of the steel components of the roll bonded composites.

Steel from Composites		0.5% P.S. (hb)	U.T.S. (hb)	% Elongation		n	R	$\Delta R$
% Cu.	% steel			Total	Uniform			
20	80	25.5	33.2	29.3	20.8	0.198	0.84	0.291
33	67	31.0	31.8	31.7	24.1	0.192	1.07	0.766
50	50	22.8	31.4	28.9	22.6	0.193	0.98	0.224
67	33	29.2	32.9	(25.6)	(20.0)	0.202	1.05	0.986
80	20	28.2	30.4	(22.3)	(16.9)	0.183	0.79	0.857
34	2x33	30.3	32.2	25.4	19.5	0.198	0.96	0.816
50	2x25	31.8	32.3	(22.3)	(15.9)	0.202	0.79	0.879
80	2x10	-----		NOT TESTED		-----		
2x25	50	32.1	33.8	34.6	25.4	0.187	1.21	0.788
2x33	34	27.8	31.1	34.5	28.5	0.241	0.94	1.085

cf 100% Steel 28.7 36.1 22.0 12.8 0.159 0.88 0.284



Table 7.17 Average mechanical properties of the copper components of the roll bonded composites.

Copper from Composites		0.5% P.S. (hb)	U.T.S. (hb)	% Elongation		n	R	$\Delta R$
% Cu	% Steel			Total	Uniform			
20	80	6.7	18.6	39.4	36.3	0.451	0.92	-0.060
33	67	6.6	19.3	-	37.5	0.495	0.97	-0.295
50	50	6.0	19.7	44.0	41.5	0.491	0.95	-0.138
67	33	6.2	19.8	48.0	42.8	0.473	0.99	-0.283
80	20	5.7	19.7	47.5	42.7	0.487	0.98	-0.265
34	2x33	5.6	19.1	37.6	35.3	0.503	1.01	-0.462
50	2x25	5.7	19.5	42.4	40.5	0.497	0.98	-0.367
80	2x10	5.3	19.6	46.4	40.5	0.529	0.90	-0.133
2x25	50	6.2	19.2	38.0	36.1	0.472	0.98	-0.297
2x33	34	6.7	19.1	37.5	34.1	0.463	1.15	-0.876

Cf 100% Copper 6.7      22.1      49.4      42.3      0.444      1.01      -0.193



Table 7.18 Co-efficients 'k' and 'n' for the copper and steel components of the roll bonded composites.

Composite		Copper component		Steel component	
% Copper	% Steel	k (hb)	n	k (hb)	n
20	80	43.7	0.451	52.5	0.198
33	67	50.2	0.495	56.7	0.192
50	50	49.3	0.491	52.4	0.193
67	33	48.3	0.473	55.7	0.202
80	20	49.3	0.487	49.9	0.183
34	2 x 33	48.9	0.503	53.9	0.198
50	2 x 25	49.7	0.497	54.5	0.202
80	2 x 10	52.9	0.529	—	—
2 x 25	50	47.4	0.472	55.8	0.187
2 x 33	34	45.9	0.463	55.6	0.241



Table 7.19 Deep drawing and stretch forming results for the copper and steel components of the roll bonded composites. (The stretch forming results are the mean of duplicate tests).

Composite		Copper Component				Steel Component			
% Copper	% Steel	Deep drawing		Stretch forming		Deep drawing		Stretch forming	
		C.B.D. (m.m.)	Maximum Punch Load (Kg)	Erichsen Value (m.m.)	Maximum Punch Load (Kg)	C.B.D. (m.m.)	Maximum Punch Load (Kg)	Erichsen Value (m.m.)	Maximum Punch Load (Kg)
20	80	—	—	10.90	200	—	—	11.51	2000
33	67	—	—	11.80	450	—	—	11.05	1450
50	50	69	1750	12.70	850	71	3150	10.51	1000
67	33	68	2450	13.70	1100	70	2200	9.95	650
80	20	68	2900	14.01	1450	68	1350	8.10*	350
34	2x33	—	—	10.95	400	—	—	9.55	(2x)750
50	2x25	—	—	12.75	800	—	—	8.95	(2x)500
80	2x10	—	—	14.30	1500	—	—	—	—
2x25	50	—	—	11.50	(2x)350	—	—	10.65	1200
2x33	34	—	—	11.65	(2x)500	—	—	10.95	800

\* premature failure of sample due to pitting.



Table 7.20. Earing of cups drawn from 65 m.m. diameter blanks of the copper and steel components of the roll bonded composites (Results are mean of two tests).

Composites		Copper Component				Steel Component			
% Copper	% Steel	Maximum Punch Load (kg)	Ear Height (m.m.)	% Earing	Mean Cup Height (m.m.)	Maximum Punch Load (kg)	Ear Height (m.m.)	% Earing	Mean Cup Height (m.m.)
20	80	750	1.09	-3.69	29.57	4,825	1.27	4.63	27.32
33	67	1,000	0.96	-3.66	26.17	3,700	1.99	7.78	25.61
50	50	1,600	0.46	-1.76	26.53	2,700	0.81	3.15	25.84
67	33	2,300	0.80	-2.95	26.99	1,850	2.56	10.31	24.83
80	20	2,800	0.67	-2.40	27.83	1,100	2.54	9.80	25.92
34	2 x 33	1,000	1.37	-5.24	26.27	(2x)1,800	3.06	12.37	24.74
50	2 x 25	1,550	1.23	-4.62	26.82	(2x)1,370	2.86	11.47	24.94
80	2 x 10	2,820	0.52	-1.90	27.52	NOT TESTED			
2 x 25	50	(2x)800	0.94	-3.48	27.00	2,650	2.30	9.02	25.44
2 x 33	34	(2x)1,050	2.53	-9.57	26.42	1,900	2.74	10.86	25.26



The drawing tests on the copper components showed that all the copper components exhibited 45° earing, as was predicted from the textures illustrated in figure 7.2. The steel components of the composites exhibited 90° earing.

### 7.7 DEEP DRAWING OF UNBONDED COPPER/STEEL COMPOSITES

Unbonded copper/steel composites were drawn with three different interfacial conditions:

1. degreased
2. polished and lubricated with polythene
3. etched and scored

Two composites, having copper : steel ratios of 33 : 67 and 50 : 50 were tested. The components of the former composite were separated from the roll bonded 33% copper / 67% steel composite, so that the results would be comparable with those of the roll bonded composite. The copper and steel components of the latter composite were separated from the 80 : 20 and 20 : 80 copper/steel composites respectively, the total thickness of the composite being 3.0 m.m. (0.12 ins.) [N.B. The steel component of the 20% copper/80% steel composite had a hardness of 125 D.P.N. so that the properties of this component were not comparable with those of the steel component of the 20% copper/80% steel composite given in tables 7.19].

The results of drawing cups from 65 m.m. diameter blanks of the composites are summarised in table 7.21, the cups being drawn with the copper component on the outer surface. The copper component of the 33% copper / 67% steel composite failed during drawing as shown in figure 7.12, although this was not accompanied by a fall in the drawing load. This failure was attributed to relative slip of the two components occurring during radial drawing-in of the flange such that one component, in this case the copper, was not restrained by the blank holder force and was thus free to wrinkle. Failure of the copper occurred when the wrinkled flange of the copper was drawn through the die throat.

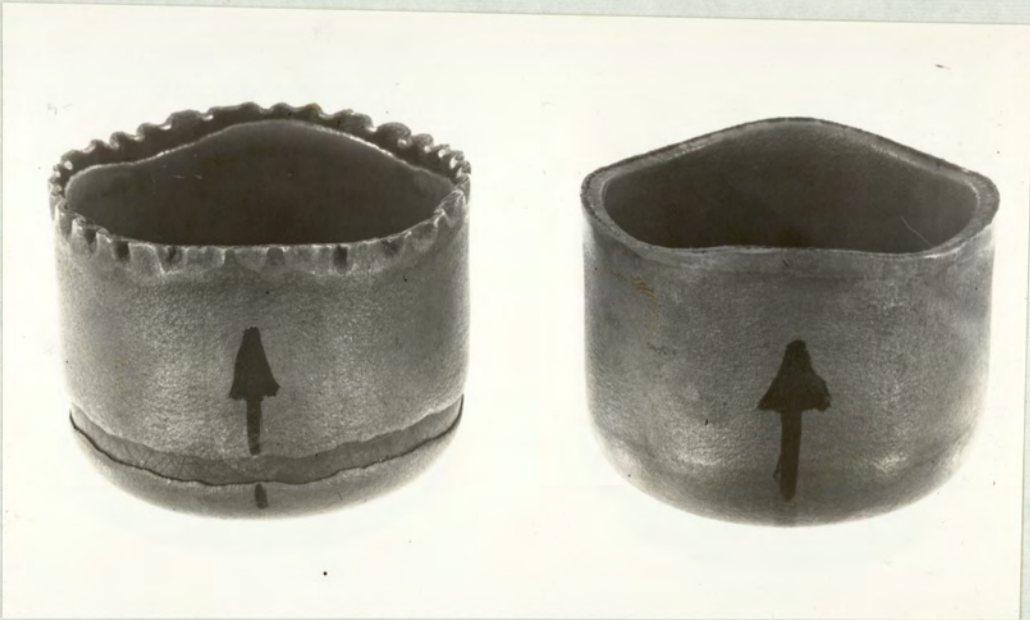
Relative movement of the components of the 50 : 50 composite also occurred but the components were sufficiently thick to withstand the tendency to wrinkle. The components of the composites had not been equally strained in the cup walls, the copper components of those composites with degreased or etched interfaces projecting approximately 1 m.m. and 0.5 m.m. respectively above the steel component, whereas with the lubricated interface, the steel component projected approximately 1 m.m. above the copper component.



Table 7.21 Deep drawing results for unbonded copper/steel composites having differing interfacial conditions.

Composite		Thickness (m.m.)		Interface Condition	Maximum Punch Load (Kg)	% Earing	Mean Cup Height (m.m.)
% Copper	% Steel	Copper	Steel				
33	67	0.61	1.22	Lubricated	4,800	Copper failed	
33	67	0.61	1.22	Degreased	4,900	" "	
33	67	0.61	1.22	Etched	4,900	" "	
33	67	0.61	1.22	Roll bonded	4,960	5.14	27.15
50	50	1.53	1.53	Lubricated	7,400	1.51	25.01
50	50	1.53	1.53	Degreased	7,450	1.85	25.49
50	50	1.53	1.53	Etched	7,400	0.95	25.33
100	—	1.53	—	—	2,800	— 2.40	27.83
—	100	—	1.53	—	5,000	2.42	25.39





*Figure 7.12 Illustration of the influence of interfacial friction in the drawing of cups from 65 m.m. diameter blanks for the 33% copper/67% steel composite.*

*Left: no bond*

*Right: roll bonded.*



The earing measurements shown in table 7.21 are, therefore, a measure of the earing behaviour of the copper components for those composites having degreased or etched interfaces, and of the steel component when the interface was lubricated, rather than of the copper/steel composites.



## 8.0 DISCUSSION

### 8.1 *Curling of test pieces in the tensile tests*

During the tensile tests on the composites, curling about the longitudinal tensile axis was observed, the degree of curling increasing with strain. Curling was observed with both the adhesive and the roll bonded composites but was only observed on the bilayer composites. Photo macrographs of typical transverse samples taken from strained test pieces are shown in figure 8.1 for the adhesive bonded 67.4% copper / 32.6% steel composite (i.e. 58% copper, 29% steel, 13% Redux).

Curling has previously been reported by Roberts<sup>(64)</sup> who observed this behaviour on a sample of tough pitch copper. Roberts related curling to through thickness textural variations which had been produced during rolling. In a similar way, curling of composites may be related to through thickness textural variations, the different textures being those of the composite components. Since texture and R values are closely related, it may be seen that through thickness variation in R would give rise to curling during the tensile test. For a given longitudinal strain the component having the lower R value will narrow down less in the width direction than the one having the higher R value.

The components of the composite were rigidly bonded so that relative movement of the components was prevented, as a result transverse stresses (tensile in the component having the high R value and compressive in that having the low R value) were produced in the components. This stress was reduced, or relieved, in the bilayer composites by curling about the longitudinal axis, the convex surface of the curled test piece being that having the lower R value as shown in figure 8.1. With the three layer composites the transverse stresses could not be relieved by curling and, as a result, the edges of the test pieces became convex or concave, as shown in figure 8.2, as each component attempted to deform as they would normally do, were it not for the restraint of the other components.

Qualitatively the tendency to curl decreased as the ratio of the R values of the components became unity, as may be seen in figure 8.1, the degree of curling, for a given ratio, increasing with strain. It is likely that the tendency to curl is also influenced by the relative thickness and/or strengths of the composite components, these two being taken as a measure of the inherent resistance of the composite to curling. Attempts to quantitatively determine the curling behaviour of composites from a combination of the R values, relative thicknesses and/or strengths of the composite components were not, however, successful.




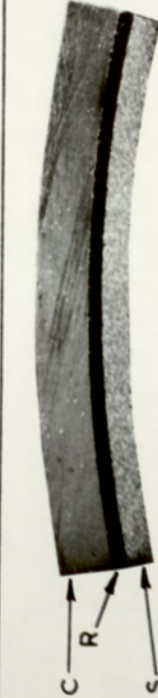

STEEL 291	COPPER 581	REDUX 131	ANGLE TO R.D.	R VALUE		UNIFORM ELONG. <sup>n</sup> %
				COPPER	STEEL	
			0°	0.89	0.78	40.9
			45°	0.47	0.92	52.8
			90°	0.96	2.00	37.4

Figure 8.1. Photomicrographs of transverse samples taken from strained testpieces of an adhesive bonded composite. (magnification x 8).



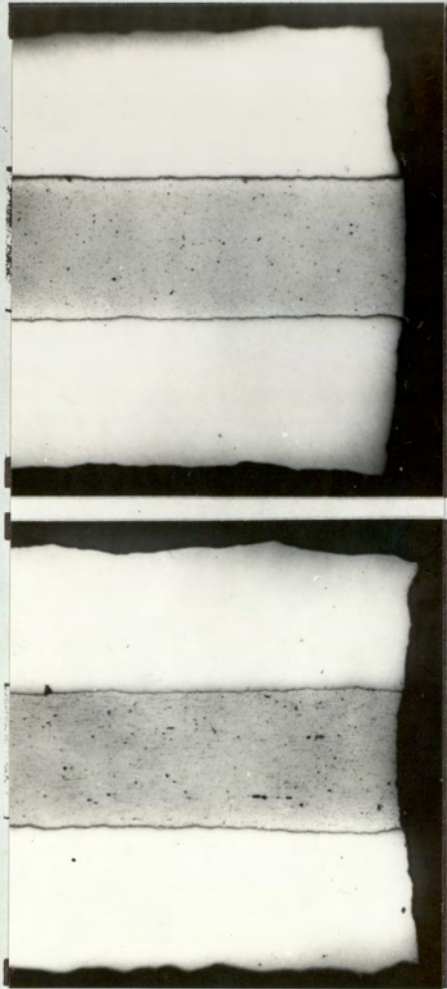


Figure 8.2. Photomicrographs of transverse samples taken from strained testpieces of the 33%Cu/34%steel/33%Cu roll bonded composite. (magnification  $\times 35$ ).

Upper:  $45^\circ$  to rolling direction ( $R_{Cu} > R_{steel}$ )

Lower:  $90^\circ$  to rolling direction ( $R_{Cu} < R_{steel}$ )



When the test pieces of the composites deformed as illustrated in figures 8.1 or 8.2, their R values could not be determined as accurately as could those of the individual components of the composites, because accurate measurement of the width of the test pieces was difficult. With the bilayer composites the maximum and minimum widths of the test pieces, corresponding approximately to the outer and inner edges of the curled test pieces, were measured. The mean of these two measurements was taken as the width of the composite this technique would, however, yield low R values since the chord length, rather than the actual length was measured. Similar measurements for the three layer composites were not possible, the width measured was, therefore, that of the component having the lower R value.

Although the degree of curling was generally small the influence on the R value determinations was demonstrated by straining a transverse sample of the 67% copper / 33% steel composite to 15% strain, measuring specimen width as already described and also measuring the maximum and minimum widths using a travelling microscope. From these measurements the R values for the composite, the outer component (steel) and the inner component (copper) were determined, these yielding values of 0.98, 1.41 and 0.87 respectively. The measurements of the maximum or minimum width of the test pieces gave R values which are comparable with those of the individual components of the composites, these being 1.80 and 0.93 respectively for the steel and copper components of this particular sample.

The implications of the uncertainty in determining the R value for the composites will be discussed in a later section.

## 8.2 *THE COMPARISON OF CALCULATED AND EXPERIMENTAL STRESS — STRAIN CURVES*

The calculation of some of the mechanical properties of composite materials was reviewed in section 2.2. All the analyses outlined in section 2.2 made the basic assumption that the composite components were equally strained, although several of the workers<sup>(12, 23, 24)</sup> reported differential straining of the composite components. The composites used to verify these analyses were unbonded, relative movement of the components being prevented merely by frictional restraint or, at best, by rivots along the length of the test pieces<sup>(24)</sup>, but despite this, the agreement between calculated and experimental results was sufficiently good, generally less than 10% difference, to justify using the rule of mixtures in this work.



In this section, the rule of mixtures, in the form of both the equal stress and equal strain hypothesis, was used to calculate the stress – strain behaviour of the composites from the behaviour of the composite components. The calculated and experimental stress – strain curves were compared, the results being discussed in the following sections :

### 8.2.1 *Application of the equal stress hypothesis*

In the equal stress hypothesis it is assumed that the stress on each component of the composite is equal, the strain on the composite being given by equation 2.2 Page 9. Length and width are the same for both components in composites of the type studied in this work, so that volume fraction may be replaced by thickness fraction and equation 2.2 rewritten as :

$$\varepsilon_{\text{comp}} = \varepsilon_{\text{Cu}} t_{\text{Cu}} + \varepsilon_{\text{S}} t_{\text{S}} \quad \dots\dots\dots 8.1$$

where  $\varepsilon$  = strain

$t$  = thickness fraction ( $t_{\text{Cu}} + t_{\text{S}} = 1$ )

Comp., Cu, S refer to the composite, copper and steel respectively.

The equal stress hypothesis assumes that there is no restraint to relative movement of the composite components, in other words the components are free to deform more or less independently.

### 8.2.2 *Application of the equal strain hypothesis*

In the equal strain hypothesis it is assumed that the strain on each component is equal, the formula used to calculate the stress,  $\sigma$ , on the composite (equation 2.1 Page 8) was rewritten in the form :

$$\sigma_{\text{comp}} = \sigma_{\text{Cu}} t_{\text{Cu}} + \sigma_{\text{S}} t_{\text{S}} \quad \dots\dots\dots 8.2$$

In the tensile tests on the composites there was a double restraint to independent deformation of the components, because they were restrained by the adhesive or roll bond and also by the fact that the components were rigidly clamped together at the test piece ends. Under these conditions the equal strain hypothesis was expected to be more applicable than was the equal stress hypothesis.



### 8.2.3 *Graphical interpretation of the equal stress and equal strain hypotheses*

Graphical representations of the equal stress and equal strain hypotheses, when applied to typical stress—strain curves obtained for steel and copper, are shown in figure 8.3 (a) and (b) respectively. Figure 8.3(a) shows that with the equal stress hypothesis the strain experienced by the copper is greater than that experienced by the steel, the differential extension being more marked at high strain levels. For the equal stress hypothesis to be valid, therefore, extensive differential extension of the composite components would have been observed, but this was not so. As a measure of differential extension the steel : copper thickness ratio of strained test pieces was measured and compared with the original ratio. In all cases, even when the measurements were made within the 'necked' region, the difference between the initial and final steel : copper thickness ratios was less than 5%, and was considered to be within the limits of experimental measurement. With the bilayer composites differential extension was also checked by elongation measurements on both components of the composite and in no case was this difference more than 5%.

The experimental results, therefore, indicate that there was little differential extension of the composite components, i.e. the components were not free to deform independently and hence the equal stress hypothesis was not applicable. The results, however, indicate that the composite components were equally strained, as represented in figure 8.3(b), and hence the properties of the composites may be calculated using equation 8.2. Comparison of results calculated using equation 8.2 with the experimental results will be discussed in section 8.3.

### 8.2.4 *Stress — strain analysis for roll bonded composites*

For accurate assessment of the validity of the equal strain hypothesis in predicting the stress — strain curves for the roll bonded composites, the stress — strain characteristics of the appropriate copper and steel components were used, the 100% copper and 100% steel samples having been processed differently (figure 6.2 Page 41 ).

Calculated and experimental stress — strain curves for longitudinal samples of a bilayer and of a trilayer composite are shown in figure 8.4. The maximum difference between the calculated and experimental curves for the bilayer composite was less than 2%, whereas that for the three layer composite was less than 4.5%. With none of the composites did the maximum difference between the calculated and experimental results exceed 6%. From this it may be deduced that the equal strain



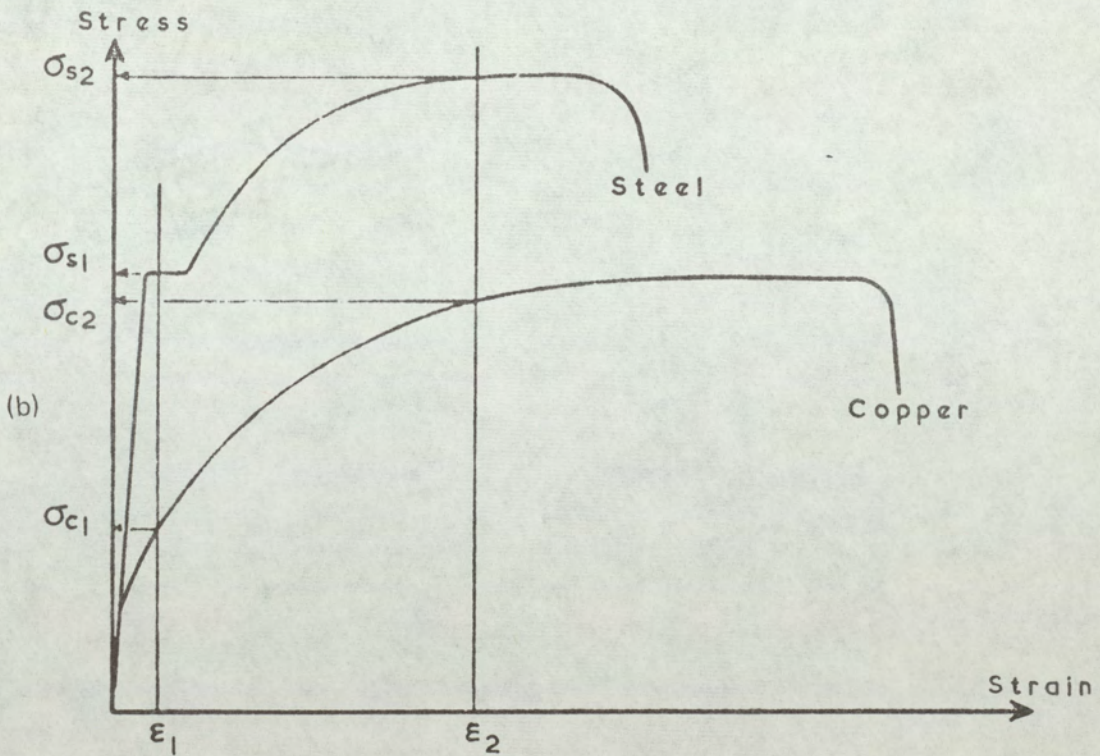
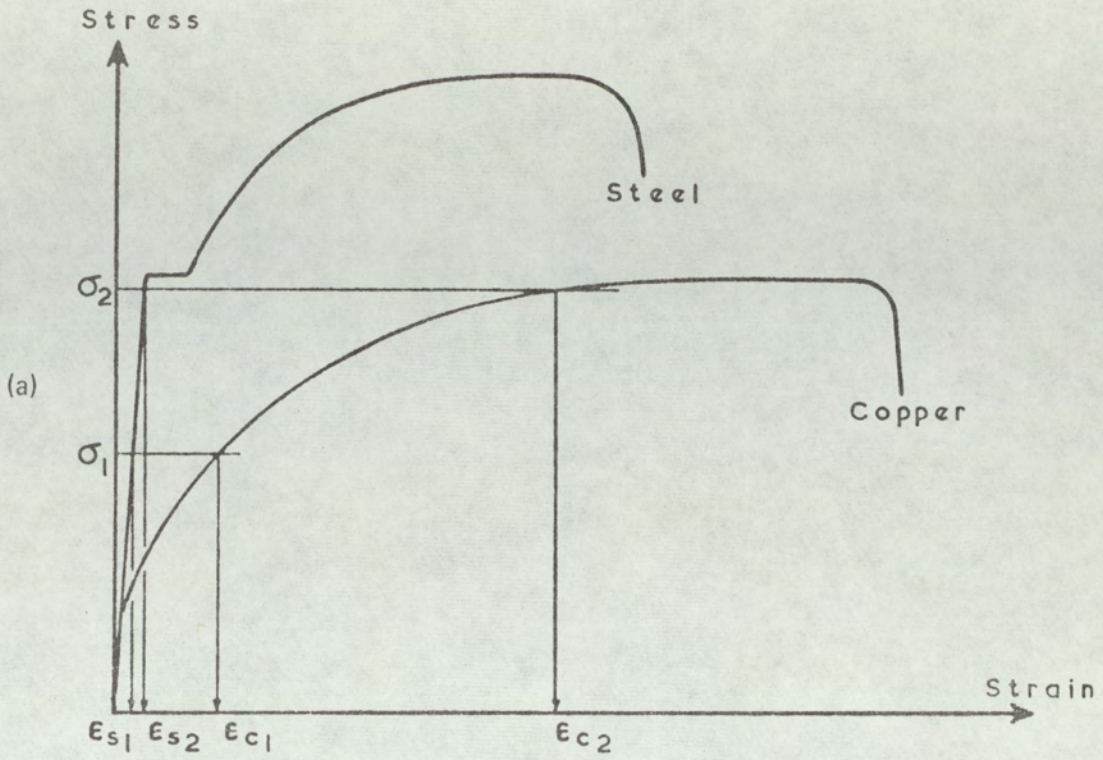


Figure 8.3 Analysis of typical stress/strain curves using (a) equal stress hypothesis, and (b) equal strain hypothesis.



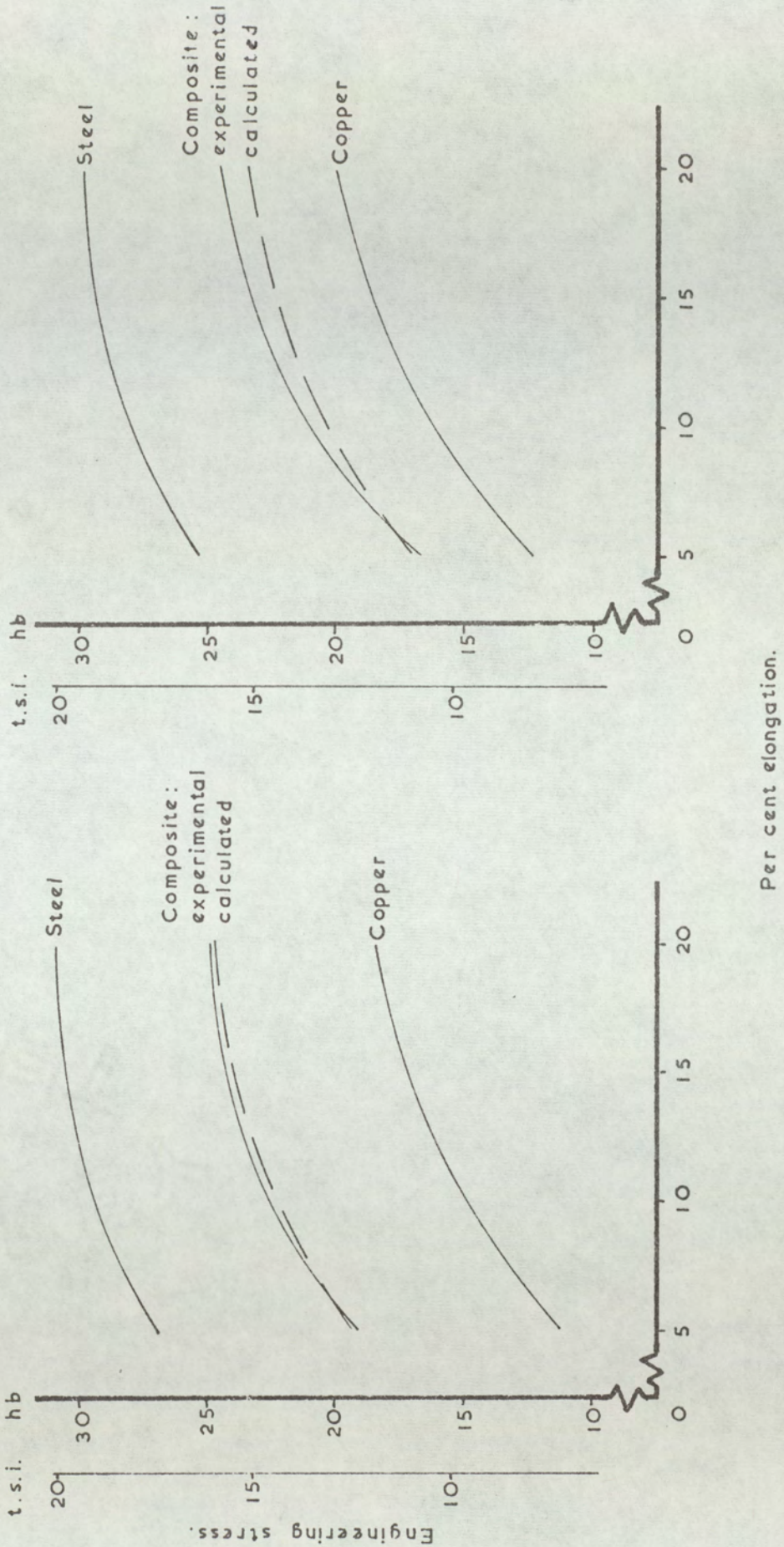


Figure 8.4 Comparison of the calculated and experimental stress-strain curves for longitudinal samples of the roll bonded composites:  
 left: 50% Copper/50% Steel bilayer  
 right: 33% Copper/34% Steel/33% Copper three layer composite.



hypothesis may be used to accurately predict the stress – strain characteristics of the composites from a knowledge of the relative thicknesses and the stress – strain characteristics of the composite components.

#### 8.2.5 *Stress–strain analysis for adhesive bonded composites*

The experimental values of stress for the adhesive bonded material, shown in tables 7.1 and 7.2 were calculated in two ways:

- (a) excluding the area of the Redux, i.e. assuming that the Redux did not contribute to the load bearing area of the composites
- (b) including the area of the Redux, i.e. assuming that the Redux contributed to the load bearing area of the composites.

When the latter assumption is made the composite is effectively a three-layer one consisting of steel, copper and Redux and so equation 8.2 should be modified to also include Redux:

$$\sigma_{\text{comp}} = \sigma_{\text{Cu}} t_{\text{Cu}} + \sigma_{\text{S}} t_{\text{S}} + \sigma_{\text{R}} t_{\text{R}} \quad \dots\dots\dots 8.3$$

where R refers to Redux.

The stress – strain behaviour of the Redux was, however, unknown so that, in order to apply equation 8.3 to the experimental results, the following assumptions were made:

- (a) That Redux behaves as a perfectly plastic material, i.e. it does not work harden,
- (b) That the maximum strength is reached at a strain level less than 5%.

The ultimate tensile strength of the Redux was determined from its shear strength, since, by the Tresca yield criterion, the yield strength in tension is twice that in shear. The shear strength of a Redux bond is dependent upon its thickness, as may be seen in figure 8.5. In the composites the thickness of the Redux was approximately 0.01", indicating a shear strength of 4500 p.s.i. from figure 8.5 and hence a tensile strength of 4 t.s.i., (6.18 hb.).



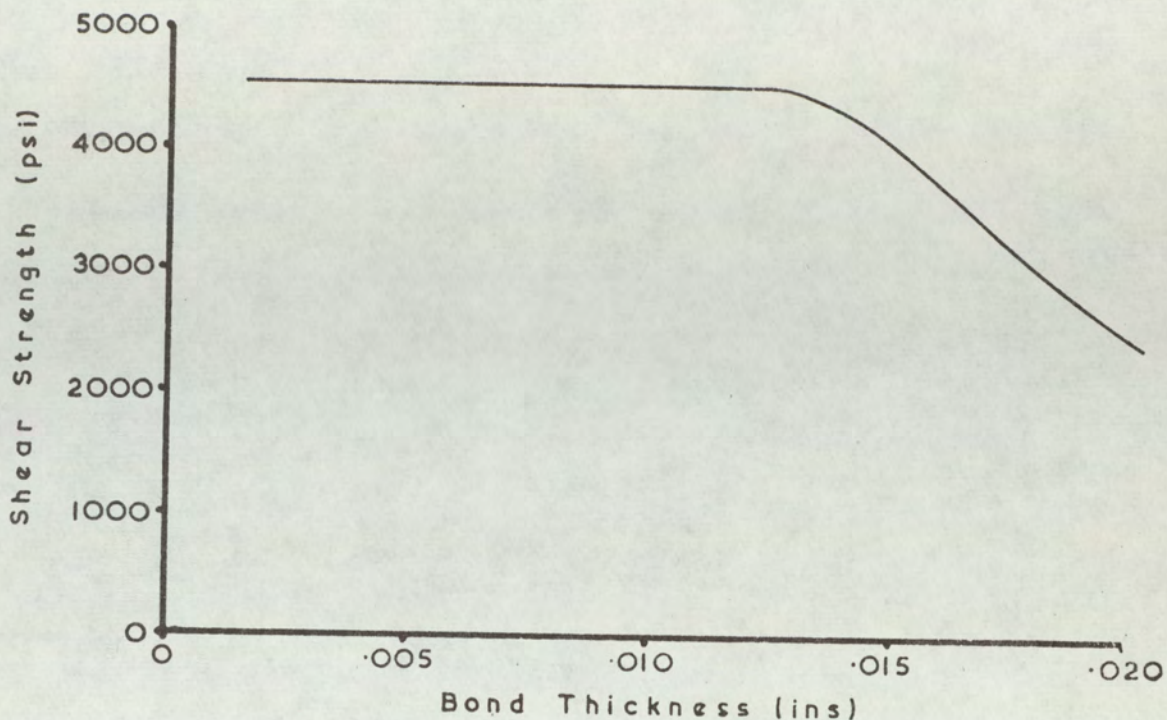


Figure 8.5 Variation of shear strength of Redux with bond thickness <sup>(65)</sup>

Using equations 8.2 and 8.3 the stress – strain curves for the composites were calculated from the stress – strain curves of the individual composite components. The results obtained were compared with the experimental curves, typical stress – strain curves obtained being shown in figure 8.6

From figure 8.6 it may be seen that the difference, between the experimental and calculated curves, varied with strain. At 5% elongation the maximum difference, expressed as a percentage of the experimental value, was – 9% for both composites, when the Redux was excluded, and – 4% when the Redux was included in the calculations. At 20% elongation the differences were – 1% and + 3% respectively.

At low strain levels, including Redux in the calculations gave smaller differences between the experimental and calculated values than when it was omitted; however, at higher strain levels this was reversed. When Redux was excluded from the calculations, the experimental values were higher than the calculated ones for all strain levels examined. With the calculations including Redux, the experimental values were higher than the calculated values at low strain levels but were lower than the calculated at higher strain levels. This indicates that, either the strength of the Redux was over-estimated in the calculations, or that the influence of the Redux decreased with increasing strain.



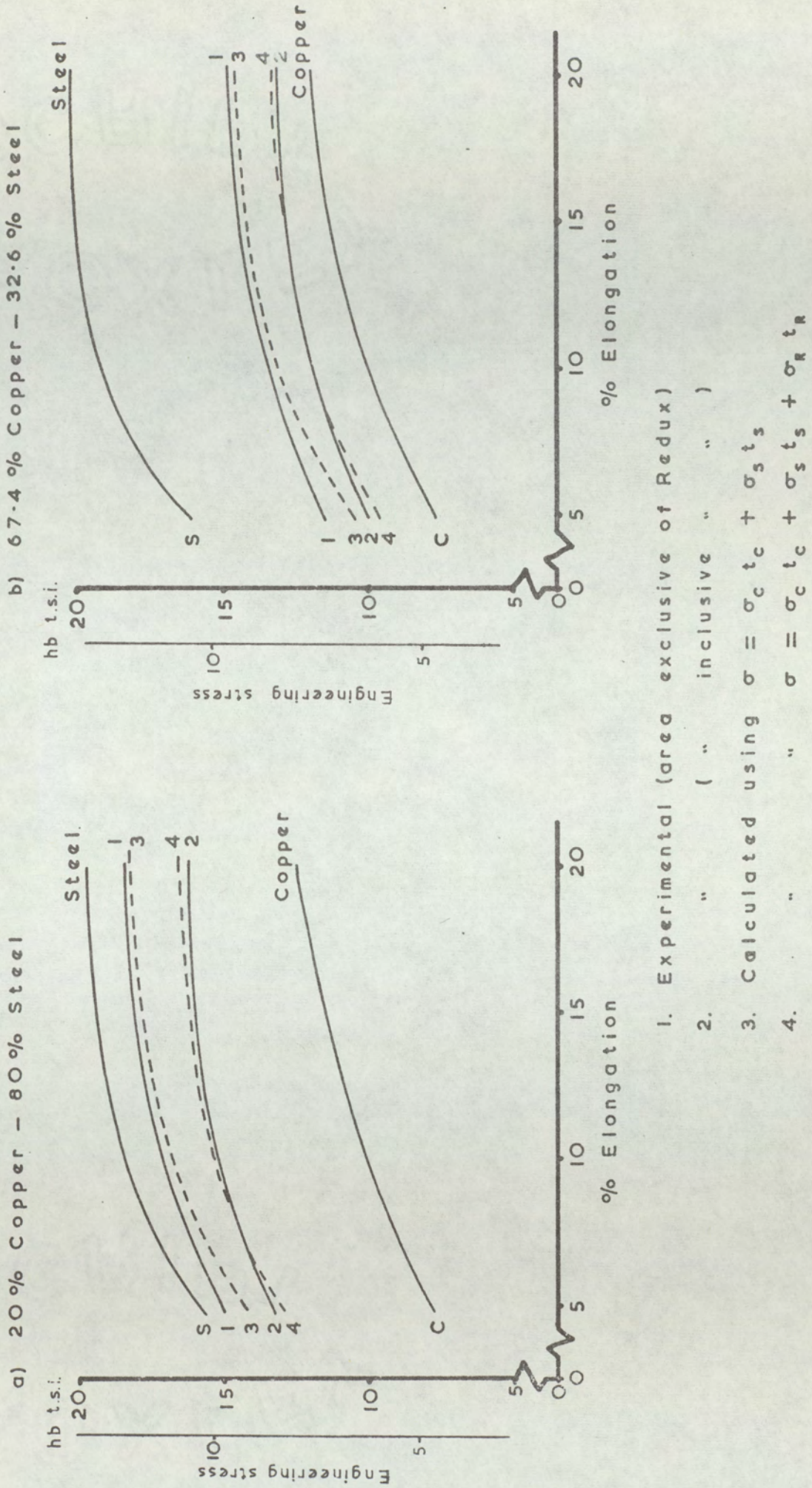


Figure 8.6. Comparison of the calculated and experimental weighted mean stress-strain curves for the adhesive bonded composites.



It was not possible to isolate experimentally the stress – strain characteristics of the Redux layer for the conditions existing when the Redux was deformed between the steel and copper. At this stage, therefore, it was not possible to comment on the validity of the estimate of the strength of the Redux.

The alternative possibility, which may be used to explain the differences between the experimental and calculated stress – strain curves, is that the influence of the Redux decreased with increasing strain, indicating that failure of the Redux occurred during the test. Failure of the Redux may occur either by the breakdown of adhesion to one or both of the components, or by local failure of the Redux so that, although it still acted as a bond between the steel and copper, it no longer contributed its full area to the load bearing capacity of the composite.

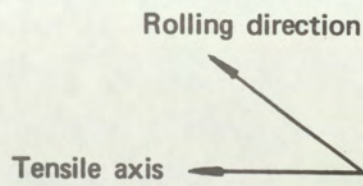
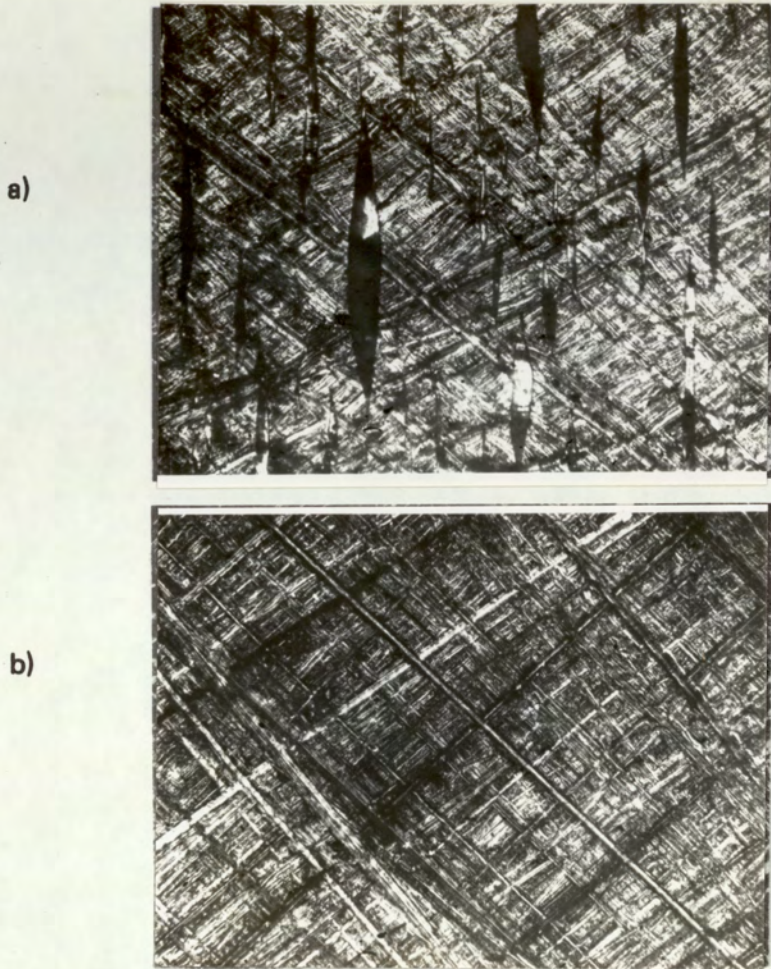
Complete breakdown in adhesion only became apparent in the latter stages of deformation when 'necking' of the test pieces had commenced. As soon as complete breakdown in adhesion occurs, failure of the copper component occurs rapidly because it can no longer withstand the applied tensile stress. Local failure of the adhesive may occur by internal shear or by the formation of transverse cracks in the bond. Transverse cracks were detected in the Redux film by peeling off the copper component from strained test pieces (Redux having a low strength under peel or cleavage loading). Photomicrographs of the Redux from a strained test piece are shown in figure 8.7. Figure 8.7a shows that, within the test piece gauge length there were numerous transverse cracks but, as may be seen in figure 8.7b none were evident in the "unstrained" regions i.e. the 'shoulders' of the test piece, this indicating that the cracks were not initiated in peeling off the copper component.

Transverse cracks were detected in the Redux after only 5% strain, the number of cracks increasing progressively with strain. This indicates that the effective load bearing area of the Redux decreased with strain and, hence, explains why the values of stress, calculated using equation 8.3, were higher than the experimental values at high strain levels.

### 8.3 *COMPARISON OF CALCULATED AND EXPERIMENTAL MECHANICAL PROPERTIES*

Using the average properties given in tables 7.1, 7.2, 7.4, 7.16 and 7.17, the equal strain hypothesis was used to predict yield strength, ultimate tensile strength, uniform elongation, 'n' and 'R' values for the composites from the properties of the components of each composite





**Figure 8.7**

*Photomicrographs of Redux from a strained test piece.*

- a) *from a strained region*      *i.e. within the gauge length*  
 b) *from an unstrained region*      *i.e. "shoulders" of the test piece.*

*(Magnification X50)*



For the roll bonded composites, two methods of calculation could be used. In the first, it was assumed that the properties of the 100% steel and of 100% copper might be representative of the properties of these metals in the composites although the production procedure was different for the latter. A better comparison was expected from the use of mechanical properties of the components stripped from composites.

Comparisons were made between calculated and experimental results on the adhesive bonded composites in two ways: by considering the cross sectional areas of the metals only and also by considering the cross section of the metals and of the Redux bond layer.

### 8.3.1 *Properties of the roll bonded composites*

The properties of the roll bonded composites were calculated using the mechanical properties of the appropriate steel and copper components, shown in tables 7.16 and 7.17. For comparison purposes the properties of the composites were also calculated using the properties of the 100% steel and 100% copper samples shown in table 7.4. The differences between the calculated and experimental values, expressed as a percentage of the experimental value are tabulated in table 8.1.

Considering first the 0.5% proof stress, the percentage differences between calculated and experimental results ranged from  $-11.9\%$  (i.e. the experimental results were higher than calculated) to  $+23.3\%$  when using the properties of the 100% steel and 100% copper (table 7.4) as the basis for calculation. When the appropriate properties of the steel and copper components were used in the calculations, the range of differences was  $-13.3$  to  $+1.4\%$ , although all but two of the results were within the range  $-6.0$  to  $+1.4\%$ . In general using the appropriate properties of the composite components yielded more accurate results than did using the properties of the 100% copper and 100% steel samples. With the exceptions of the 67% copper / 33% steel and the 33% copper / 34% steel / 33% copper composites, the differences between calculated and experimental values of proof stress were significantly less than the differences reported by Davies<sup>(12)</sup>.

With regard to the U.T.S. figures, the differences ranged from  $-9.1$  to  $+13.4\%$  when the calculations were based on the properties of the 100% steel and 100% copper samples and  $-5.5$  to  $+0.6\%$  when based on the properties of the appropriate copper and steel components. These latter results illustrate that there was a significant improvement in the calculated results when the real properties of the copper and steel components were used.



Table 8.1. The Percentage differences between calculated and experimental mechanical properties for the roll bonded composites.

COMPOSITE		Properties used in Calculations	0.5% Proof Stress	U.T.S.	Uniform Elong <sup>n</sup> .	n	R	△ R
% Copper	% Steel							
20	80	A	9.3	10.7	-33.9	0.5	-7.6	-38.4
		B	- 2.6	0.6	-15.5	10.0	-12.7	-27.8
33	67	A	- 5.6	-9.1	3.9	9.2	-5.6	-75.9
		B	- 4.0	-5.5	- 0.4	28.5	-0.4	-18.8
50	50	A	23.3	13.4	- 8.8	3.7	0.4	-60.7
		B	0.5	-0.5	6.6	17.7	2.7	-63.6
67	33	A	- 8.0	8.8	4.7	7.0	11.2	-116.2
		B	- 9.3	-1.5	13.4	16.3	16.1	-38.3
80	20	A	- 5.3	10.4	- 1.9	-3.7	14.4	-913.3
		B	- 2.9	-2.9	1.2	6.7	9.5	-438.3
34	2 x 33	A	- 5.3	8.0	-31.0	1.5	-6.6	-81.8
		B	- 0.02	-3.4	-25.8	17.3	-1.4	-39.2
50	2 x 25	A	- 6.9	7.7	-19.9	3.3	-8.3	-91.0
		B	1.4	-3.5	-19.5	17.7	-14.4	-44.4
80	2 x 10	A	15.5	11.9	- 3.4	-10.2	14.4	-1,726.7
		C	4.0	3.2	- 7.3	5.6	4.2	-926.7
2 x 25	50	A	-13.0	8.4	-22.2	13.6	-15.5	-88.4
		B	- 6.0	- 1.3	-13.8	25.4	- 2.4	-33.0
2 x 33	34	A	-11.9	11.5	-17.9	2.1	- 0.4	-199.4
		B	-13.3	- 3.5	-18.1	14.0	11.2	-775.0

A Calculated using the properties of the 100% steel and 100% copper (table 7.4)  
 B " " " " of the appropriate steel & copper components (tables 7.16 & 7.17)  
 C " " " " of the 100% steel sample (table 7.4) and the appropriate copper component from table 7.17.



The results for 0.5% proof stress and U.T.S. shown in table 8.3 indicate that, in the majority of cases, proof stress and U.T.S. may be calculated to the same degree of accuracy, there being no indication that the accuracy of prediction was *consistently* improved at high strain levels.

The calculated values of uniform elongation were not improved by the use of the elongations of the appropriate copper and steel components, there was, however, a trend for the differences to become more positive. The range of differences were  $-33.9$  to  $+4.7\%$  when the calculations were based on the properties of the 100% steel and 100% copper, and  $-25.8$  to  $+13.4\%$  when based on the properties of the copper and steel components. The large variation in the accuracies of the predicted uniform elongations probably results from inaccuracies in the experimental values, rather than showing that the equal strain hypothesis is not valid.

Uniform elongation is the most inaccurate of all the measurements made during the tensile tests because it is dependent upon factors such as accurate machining of the test pieces and surface finish of the material. Poor machining of test pieces or poor surface finish can lead to premature failure of the test pieces and hence give low values of elongation. Even with good test pieces false results may be obtained if the region of high local extension, i.e. the necked portion, is not totally eliminated in determining the uniform elongation, in which case, high uniform elongations are obtained.

The predicted R values, as with uniform elongation, were not improved when the properties of the steel and copper components were substituted in place of those of the 100% samples, although there was a tendency for the values to become more positive; the range of differences being  $-12.7$  to  $+16.1\%$  and  $-15.5$  to  $+14.4\%$  respectively. As with uniform elongation, inaccurate experimental R values was the probable cause of the wide variation in the accuracies of the predicted R values (50% of the results were, in fact, within the range  $-2.4$  to  $+4.2\%$ ). The sources of errors in measuring R values on the composites were discussed in detail in section 8.1 where it was shown that the technique used would tend to give low R values particularly when curling was severe, as with the 67% copper / 33% steel composite. The large differences between the predicted and experimental  $\Delta R$  values, which are orders of magnitude greater than the differences for other properties, probably result partly from inaccuracies in the R values and partly from expressing the differences as a percentage of the experimental values, these being very small.



Unlike the properties that have previously been discussed the n values predicted from the appropriate copper and steel components are significantly less accurate than those predicted from the 100% copper and 100% steel samples, the range of differences being +28.5 to +6.7% and -10.2 to +13.6% respectively. If it is assumed that the results based on the properties of the individual copper and steel components are more representative than those based on the 100% samples, it may be seen that for all the composites; the calculated n values are greater than the experimental values. In other words the composites work-hardened less rapidly than the equal strain hypothesis predicted. It is not, however, valid to predict n values by means of the equal strain hypothesis because n values are logarithmic ratios, as shown below, and, therefore, are not additive as are properties such as proof stress and U.T.S.

The n values for the composites may be derived in two ways

- a. predict the true stress — true strain curve for the composites, by means of the equal strain hypothesis, and from this data determine k and n in the normal manner
- or b. calculated using the formula derived below:

if  $\sigma = k\delta^n$

then  $\delta^n = \frac{\sigma}{k}$

and so  $n = \frac{\log \sigma - \log k}{\log \delta}$  ..... 8.4

But true stress for the composite may be determined using the equal strain hypothesis:

i.e.  $\sigma_{comp} = \sigma_{c^t_c} + \sigma_{s^t_s}$  ..... 8.5

and, as k is merely the true stress at a true strain of 1.0, it follows that:

$k_{comp} = k_{c^t_c} + k_{s^t_s}$  ..... 8.6



Substituting equation 8.5 and 8.6 in equation 8.4:

$$n_{\text{comp}} = \frac{\log(\sigma_c t_c + \sigma_s t_s) - \log(k_c t_c + k_s t_s)}{\log \delta} \quad \dots\dots\dots 8.7$$

The percentage differences between n values calculated by either of these techniques and the experimental values are shown in table 8.2.

The results show that n values, calculated by either of the two techniques outlined above, give good agreement with the experimental values, although those calculated using equation 8.7 were not as accurate as those determined by analysis of the calculated true stress – true strain curves. The accuracy of the results yielded by equation 8.7 is determined by the accuracies with which  $\sigma$  and k for the composite may be calculated using the equal strain hypothesis.

### 8.3.2 Properties of the Adhesive bonded composites

The differences between the experimental and calculated values, expressed as a percentage of the experimental value, are tabulated in table 8.3, negative differences indicating that the calculated values were lower than the experimental values.

*Table 8.3 The Percentage differences between the calculated and experimental mechanical properties for the Adhesive bonded composites.*

Composite		0.5% Proof Stress	U.T.S.	Uniform Elongation	R
%Copper	%Steel				
20	80	-3.4 -0*	-0.5* +2.4	+5.7	+22.7
67.4	32.6	-11.0 -5.6*	0 * +2.9	-17.8	+32.8

\* Redux included in the calculations



Table 8.2. The percentage difference between  $n$  values calculated either graphically or from equation 8.7 and the experimental values for the roll bonded composites.

Composite		Percent difference in		
% Copper	% Steel	$k$ (graphical)	$n$ (graphical)	$n$ (calculated)
20	80	-3.9	+5.1	+7.9
33	67	+1.7	+6.8	+13.5
50	50	-0.9	+0.7	-10.1
67	33	-0.6	+3.1	+8.3
80	20	-5.5	+3.2	+1.0
34	2 x 33	-3.7	+0.8	+6.7
50	2 x 25	-3.6	+0.7	+7.2
80	2 x 10	STEEL NOT TESTED		
2 x 25	50	+0.3	+3.0	+9.0
2 x 33	34	-2.6	+3.5	+7.1



The maximum differences between the calculated and experimental values of proof stress and U.T.S.,  $-11.0\%$  and  $+2.9\%$  respectively, are comparable with the results obtained on the roll bonded composites. The agreement between the calculated and experimental values of uniform elongation and R value;  $-17.8\%$  and  $+32.8\%$  respectively were, however, not as good.

The difficulties in measuring uniform elongation were discussed in detail in the preceding section. These sources of error also applied to the adhesive bonded results but, in addition, low elongations could also result from the breakdown of the Redux during the test, as was discussed in section 8.2.5.

The positive differences between the experimental and calculated R values indicate that the composite contracts less in the width direction than the calculated value predicts. However, in the calculations Redux was ignored because its stress/strain behaviour was unknown, but it was subsequently shown that the Redux influenced the rate of width thinning of test pieces. Attempts were made to bond "hard" copper to steel but, because of the poor adhesion between the copper and the bond, the copper component failed after less than 5% strain in the tensile tests. The tests were continued after the copper had failed, leaving the Redux bonded to one surface of the steel, and curling about the longitudinal axis then occurred. The Redux was on the outside of the curled test pieces indicating that it had a lower R value than the steel. Including the R value of the Redux in the equal strain hypothesis would, therefore, lower the calculated R value and hence reduce the difference between the calculated and experimental values.

Accurate R values for the composites were difficult to determine experimentally when curling occurred, because of the difficulties involved in accurately measuring the specimen width. The large differences between the calculated and experimental R values, therefore, probably result partly from the omission of Redux from the calculations and partly from inaccurate experimental values for the composites.

In the preceding section two techniques were outlined for the calculation of the n value for the composites and the results of using these two techniques to determine n for the adhesive bonded composites are shown in table 8.4 :



Table 8.4. The percentage difference between n values calculated either graphically or from equation 8.7 and the experimental values for the adhesive bonded composites.

Composite		% Difference in		
% Copper	% Steel	k (graphical)	n (graphical)	n (calculated)
20	80	+3.5	+10.9	+12.9
67.4	32.6	+9.0	+16.8	+18.8

From tables 8.4 and 8.2 it may be seen that the results for the adhesive bonded composites are not as accurate as those for the roll bonded composites this being the result of the progressive breakdown in the Redux during the tests.

If it is assumed that the equal strain hypothesis is applicable to the adhesive bonded composites, in the same way that it was for the roll bonded composites, and that the differences, shown in table 8.3, merely result from the omission of Redux from the calculations it is possible to derive the properties of the Redux using equation 8.1 rewritten in the form:-

$$P_R t_R = P_{comp} - (P_{Cu} t_{Cu} + P_{SS} t_{SS}) \dots\dots\dots 8.8$$

where P = Property under consideration  
t = thickness fraction

The results tabulated in tables 7.1A/7.1B and 7.2A/7.2B were substituted in equation 8.8 and the corresponding properties for Redux were derived, these being tabulated in table 8.5:



Table 8.5. Properties of Redux derived from the results shown in Tables 7.1A/7.1B and 7.2A/7.2B using the equal strain hypothesis.

Composite		0.5% Proof Stress		U.T.S.		Uniform Elongation %	R
% Copper	% Steel	hb	t.s.i.	hb	t.s.i.		
20	80	7.0	4.5	0.3	0.2	-4.5	-0.70
67.4	32.6	7.9	5.1	-3.2	-2.1	34.8	-0.62

The proof stresses for Redux of 7.0 and 7.9hb (4.5 and 5.1 t.s.i.) are equivalent to shear strengths of 5040 and 5712 p.s.i. respectively, these being 12 and 27% higher than the value indicated by figure 8.5. It must be remembered, however, that the derivation of properties, using equation 8.8 accumulates all the experimental errors in the final results, so that the results shown in table 8.5 do not necessarily represent the properties of the Redux in absolute terms. However, the predicted yield strength appears to be reasonable.

U.T.S. for the composites was measured at strain levels greater than 25% but at such strain levels there were numerous cracks in the Redux film, as shown in figure 8.7. Experimentally it was found that cracks had formed in the Redux after only 5% elongation and that the number of cracks increased rapidly with additional strain. The effective load bearing area of the Redux at the strain levels used in measuring U.T.S., was, therefore, negligible and the U.T.S. values quoted in table 8.5 are artificial.

Since the Redux was not continuous when failure of the composite occurred, the elongation figures shown in table 8.5 are meaningless. In the calculation of R value it is assumed that there is constancy of volume, but since voids are produced in the Redux this assumption is not valid and hence the calculations are also not valid.

### 8.3.3. Summary of the comparisons of calculated and experimental mechanical properties.

The results of the comparisons of the calculated and experimental mechanical properties have shown that the equal strain hypothesis may be used to predict proof stress, U.T.S., uniform elongation and R value but may not be used to predict the n values. The agreement between calculated and experimental values of the proof stress and U.T.S. were generally less than -5%, although differences of -9.3 and -13.3%



were obtained in the calculation of proof stress for two of the roll bonded composites. The agreement between calculated and experimental values of uniform elongation, and of R value, were not as good as for proof stress or U.T.S. probably because of inaccuracies in the experimental results.

For the roll bonded composites it was found that the accuracy of the predicted results was improved for proof stress, U.T.S. and uniform elongation, when the properties of the appropriate copper and steel components were used in the calculations in place of the properties of the 100% samples. With the R values, the accuracy of the predictions were not improved by use of these properties.

For those properties for which the equal strain hypothesis was found to be valid, it follows that there should be a linear relationship between the properties and per cent clad. The relationships for proof stress, U.T.S. and uniform elongation with per cent copper are shown in figures 8.8 and 8.9 for the roll bonded bilayer composites. The properties of the steel and copper components for each composite differed so, for clarity, mean values for the steel and copper have been used in figures 8.8 and 8.9. Some of the spread about the lines, therefore, represents the deviation of the properties of the composite components from the mean. The spread about the mean values was so great for R values that the relationship between  $\bar{R}$  and per cent copper could not be represented in this way.

The relationship between  $\bar{n}$  and per cent copper for the roll bonded bilayer composites is shown in figure 8.10. From figure 8.10 it may be seen that  $n$ , which could not be determined by the equal strain hypothesis produced a catenary with per cent copper.

The results show that for all practicable purposes the properties of the composites, with the exception of 'n', may be determined by the equal strain hypothesis. The properties of the composites may be determined graphically as there is a linear relationship between the properties and per cent clad.

The equal strain hypothesis does, however, assume that there is no transverse interaction of the composite components. Interaction of the components was experimentally observed in the form of curling (section 8.1) but the degree of agreement between the calculated and experimental results suggests that the transverse stresses are negligible in comparison to the longitudinal stresses. Ebert et al<sup>(66)</sup> have made a more accurate analysis for the stress - strain behaviour of concentric composite cylinders which made allowance for the transverse stresses. Although this analysis was more accurate than the equal strain hypothesis it was so complex that its practical usefulness is questionable.



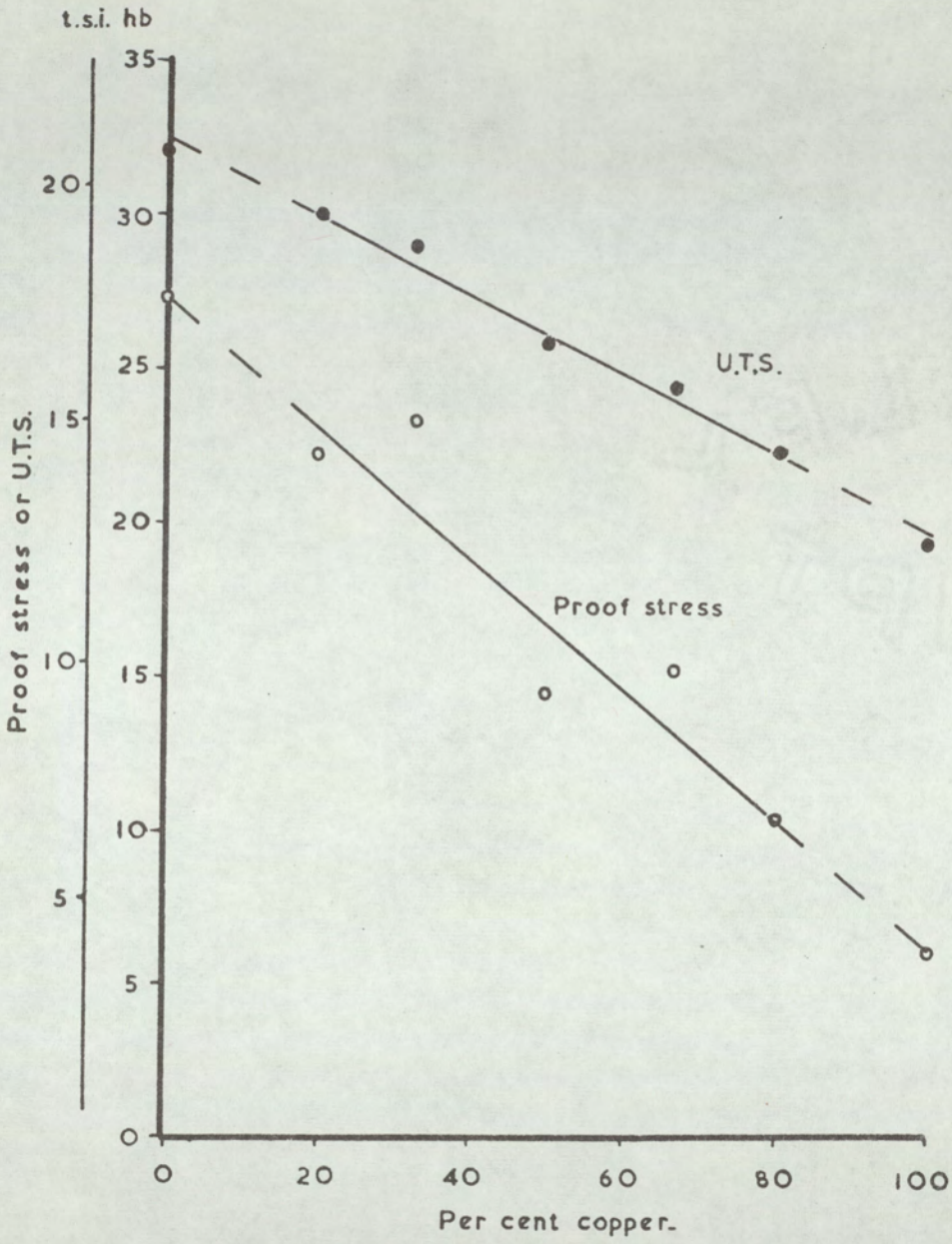


Figure 8.8 Variation of proof stress and U.T.S. with per cent copper for the bilayer roll bonded composites.



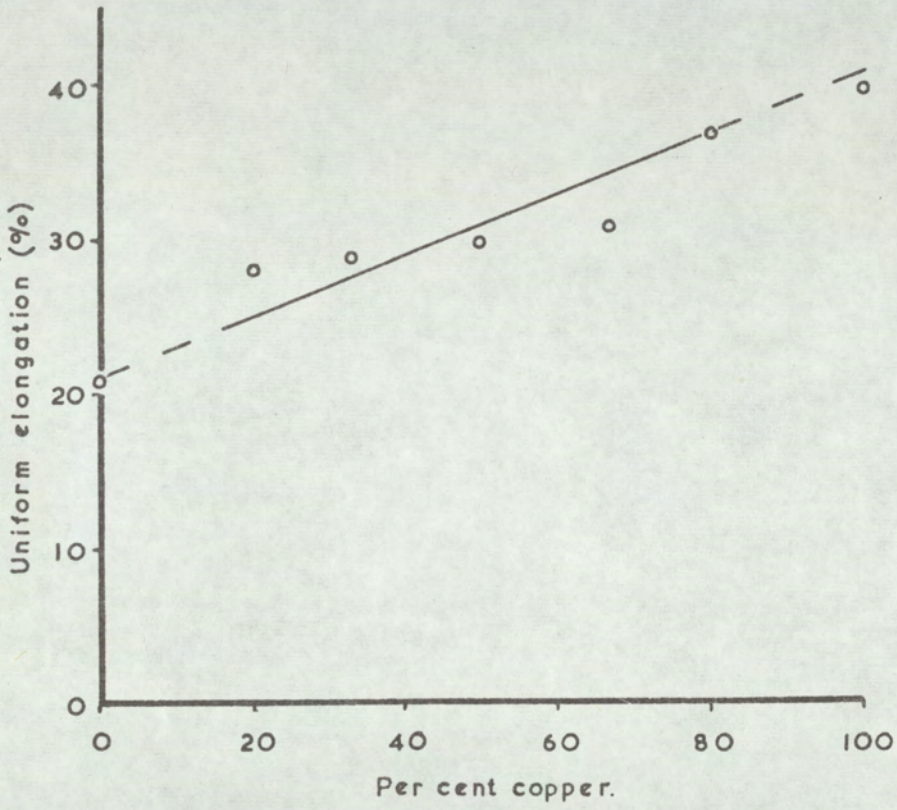


Figure 8.9 Variation of uniform elongation with per cent copper for the bilayer roll bonded composites.



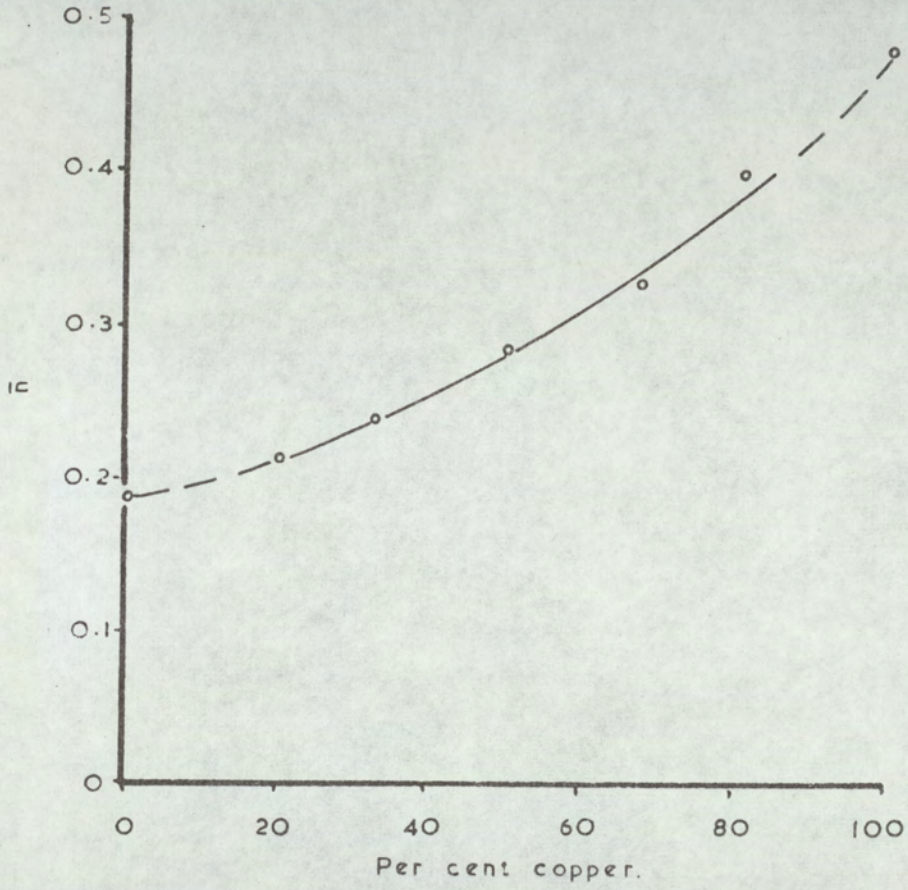


Figure 8.10 Variation of work hardening index with per cent copper for the roll bonded composites.



## 8.4 GENERAL DISCUSSION OF THE DEEP DRAWING AND STRETCH FORMING RESULTS.

### 8.4.1. *LIMITING DRAW RATIOS:*

From tables 7.7 and 7.10 it may be seen that the drawabilities of both the adhesive bonded and the roll bonded composites show little variation, all the L.D.R.'s being in the range 1.97 – 2.03. Such small differences in drawabilities are hardly significant for the number of tests made on each composite; much larger numbers would be required to increase the significance of these results.

Tests were made on the individual components of only three of the roll bonded composites (table 7.19) but it is interesting to note that the drawabilities of these three composites; (i.e. the 50:50; 67:33 and 80:20 copper : steel composites), were lower than those of the two components making up the composites. One of the adhesive bonded composites (67.4% copper/32.6% steel) also showed this effect, although this could have been caused by the influence of the Redux.

These results suggest that drawability is reduced by cladding, but it must be stressed that for these composites the differences were small, the critical blank diameters, of the composite and the component having the lower drawability, differing by only 2mm. Differences of this magnitude could result from variations in test parameters, particularly differences in the ratios of die profile radius to sheet thickness or punch profile radius to sheet thickness.

The profile radii of both the die and punch were constant for all thicknesses of sheet tested, these being 3mm and 4.5 mm respectively, whereas sheet thickness varied from 1.83mm (for the composites) to 0.37mm (for the thinnest component). The ratios of die or punch profile radii to sheet thickness varied from 1.6 to 8.1 and from 32.5 to 12.2 respectively, these large differences have a pronounced effect during drawing. During drawing localised thinning occurs when the material is bent and unbent over the die and punch profile radii whilst under a tensile stress in the radial direction, the severity of thinning increasing as the ratio of profile radius to sheet thickness decreases. These locally thinned regions also work harden, but the increase in load bearing capacity, brought about by work hardening does not compensate for the reduction in wall thickness, this region having to withstand



the stress necessary to draw in the work hardened flange.

It may be seen from this that the composite components, having higher ratios of profile radii to sheet thickness than have the composites, have a greater resistance to thinning and, hence, give higher drawabilities, but it does not follow that the drawability of either the steel or the copper components decrease as their thickness increases. The drawability of the different thicknesses is dependent upon their mechanical properties e.g. drawability increasing with  $\bar{R}$  <sup>(54)</sup> (figure 4.3 page 33).

From the limited results obtained it is not possible to determine the influence of cladding on drawability, the observed differences could have arisen from differences in tool geometry, particularly from the different ratios of profile radii to sheet thickness used for the composites and the components.

#### 8.4.2. *EARING:*

Earing tests on the steel, copper and the composites were made on cups drawn from 65 mm diameter blanks, the results for the adhesive bonded composites are shown in table 7.8; those for the roll bonded composites in table 7.11 and those for the components of the roll bonded composites are shown in table 7.20.

Both components of the adhesive bonded composites exhibited 0–90° earing, as did the composites having the rolling direction of the components matched. When the rolling directions of the components were mismatched by 45° the overall earing behaviour was that of the steel component for the 20% copper/80% steel sample but that of the copper component for the 67.4% copper/ 32.6% steel composite. The steel components of the roll bonded composites exhibited 0–90° earing, whereas the copper component exhibited 45° earing. With the adhesive bonded 67.4/32.6 copper/steel composite the copper component had a greater earing potential than had the steel component, whereas with the roll bonded composites the steel component exhibited the greater earing potential.

With the adhesive bonded composite greater per cent earing was obtained when the steel component was on the outer surface, whereas the roll bonded composites greater earing was obtained when the copper was the outer component.



For both types of composite, it may be seen that greater earing was obtained when the inner component of the composites had the greater earing potential. Tables 7.8 and 7.11 also show that the variation in earing was accompanied by a variation in mean cup height, mean cup height decreasing with earing for the adhesive bonded composites but increasing for the roll bonded composites.

Considering first the variation in mean cup height; mean cup height may be increased if more material is drawn off the punch i.e. when friction over the punch nose is low. This may explain the difference in the observed mean cup heights, shown in tables 7.8 and 7.11, only if, with polythene and graphite grease lubrication, friction between steel and steel is lower than that between copper and steel. If friction is similar, the observed difference in mean cup heights may be the result of the restraining influence of the outer component. The greater the restraint offered by the outer component, the greater will be the normal force acting on the inner component and the greater will be the resistance to drawing off the punch nose. It is likely that the stronger component will restrain the weaker more than the weaker component will restrain the stronger and lower mean cup heights would be expected when the stronger component was the outer one, as was observed for both the adhesive and the roll bonded composites.

Alternatively the difference in mean cup heights may be the result of different bending and unbending characteristics of the composite components when in the different positions on the punch and die radii. Differences in bending and unbending characteristics would be expected to produce differing drawing loads, but the observed differences (up to 75 Kg) were considered to be within the limits of experimental accuracy and it is possible that the equipment was not sufficiently sensitive to detect small changes in the drawing load.

The observed difference in mean cup height was only 0.3 to 0.5 mm, and although any differences resulting from the influence of the three factors discussed would be likely to be small, it is possible that one or more of these would account for the observed differences. However, thickness strain surveys on drawn cups have revealed that the amount of thinning over the punch nose is greater when the outer component is copper and that the degree of thinning increases with per cent copper. These results were summarized in figure 7.7 (page 80 ). This evidence therefore, supports the assumption that the differences



in mean cup height may be attributed to the normal restraint offered by the outer component.

The variation in mean cup height influences the per cent earing values because these were calculated by dividing the ear height by the mean cup height. For a material of constant earing potential, the apparent per cent earing will decrease as mean cup height increases. Comparisons of the earing values of the copper/steel composites having the steel component outermost, with those having the copper outermost, are not valid unless the mean cup heights are similar.

Mean cup height may be artificially increased by increasing the blank diameter, provided that the area of the 'dead' metal, i.e. the area over the punch nose remains constant and hence a calibration curve of per cent earing against mean cup height may be derived. Calibration curves for the composites were derived, a typical curve being shown in figure 8.11 which shows that per cent earing was unaffected by increasing cup height. This was probably due to a balance of two effects:

- (a) increasing the blank diameter increases the flange area so that, because ears are developed during drawing in of the flange the ear height will increase with increasing flange area. This is illustrated in figure 8.12 where ear height is plotted against blank diameter.
- (b) as the blank diameter increases the maximum punch load necessary to draw in the larger flange will also increase. With higher punch loads more material may be drawn off the punch nose thereby further increasing the mean cup height, but, because this material is not radially drawn in, the ear height remains the same and hence the apparent per cent earing will decrease.

Since it was not possible to correct the earing values for the influence of mean cup height, ear height was considered a better measure of anisotropy than per cent earing. In figure 8.13 ear height is plotted against per cent copper for the roll bonded bilayer composites. Greater ear heights may be seen to be obtained when the composites were deformed with the copper on the outer surface. The difference between the two curves, although only approximately 0.2mm., was greater than the scatter in the results except for the 67% copper/33% steel composite. For the adhesive bonded composite greater ear heights were obtained when the composites were deformed with the steel on the outer surface.



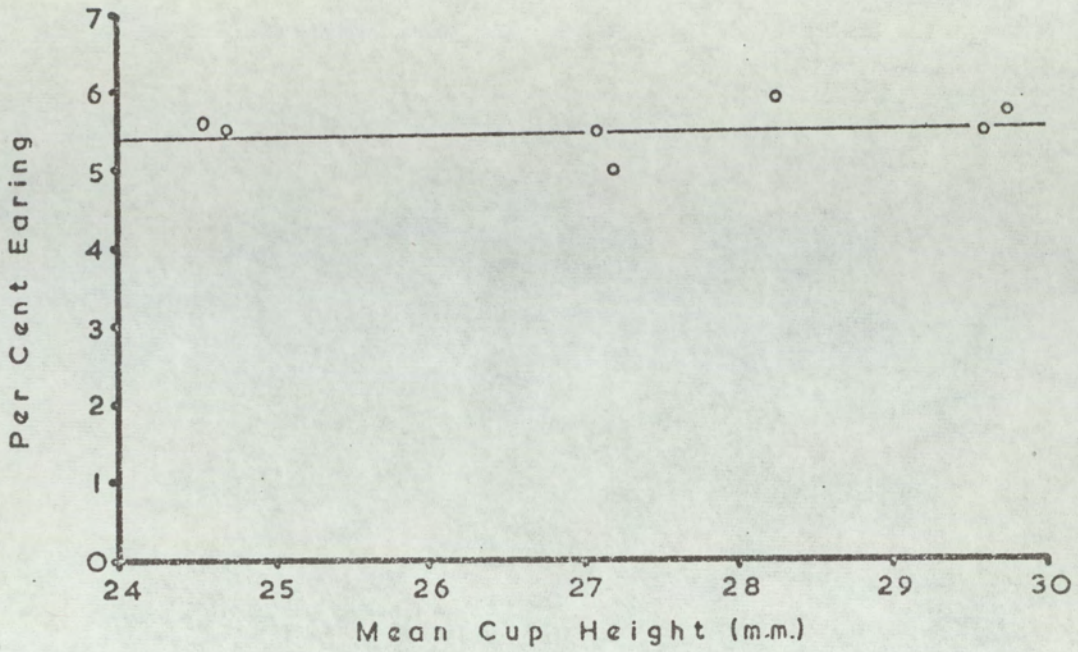


Figure 8.11. Variation of percent earing with mean cup height for the 67% Cu/33% Steel roll bonded bilayer composite.

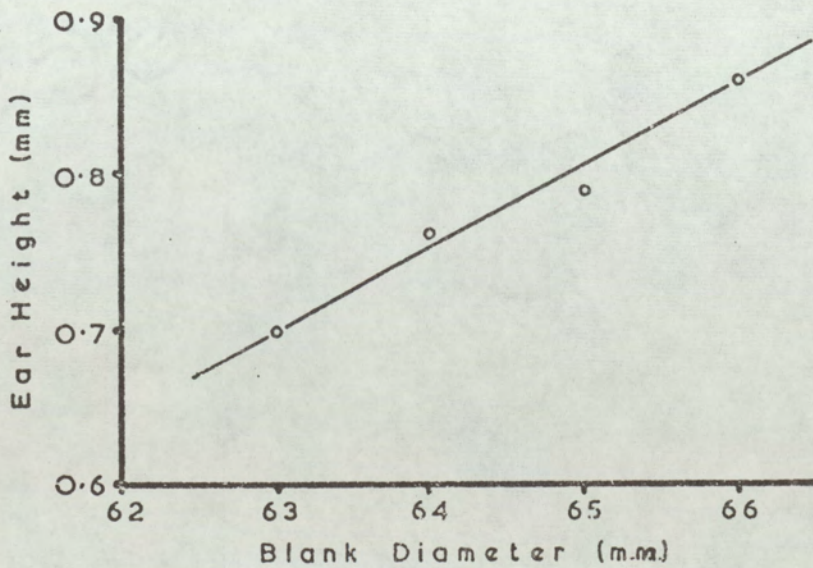


Figure 8.12 Variation of ear height with blank diameter for the 67% Cu/33% Steel roll bonded bilayer composite.



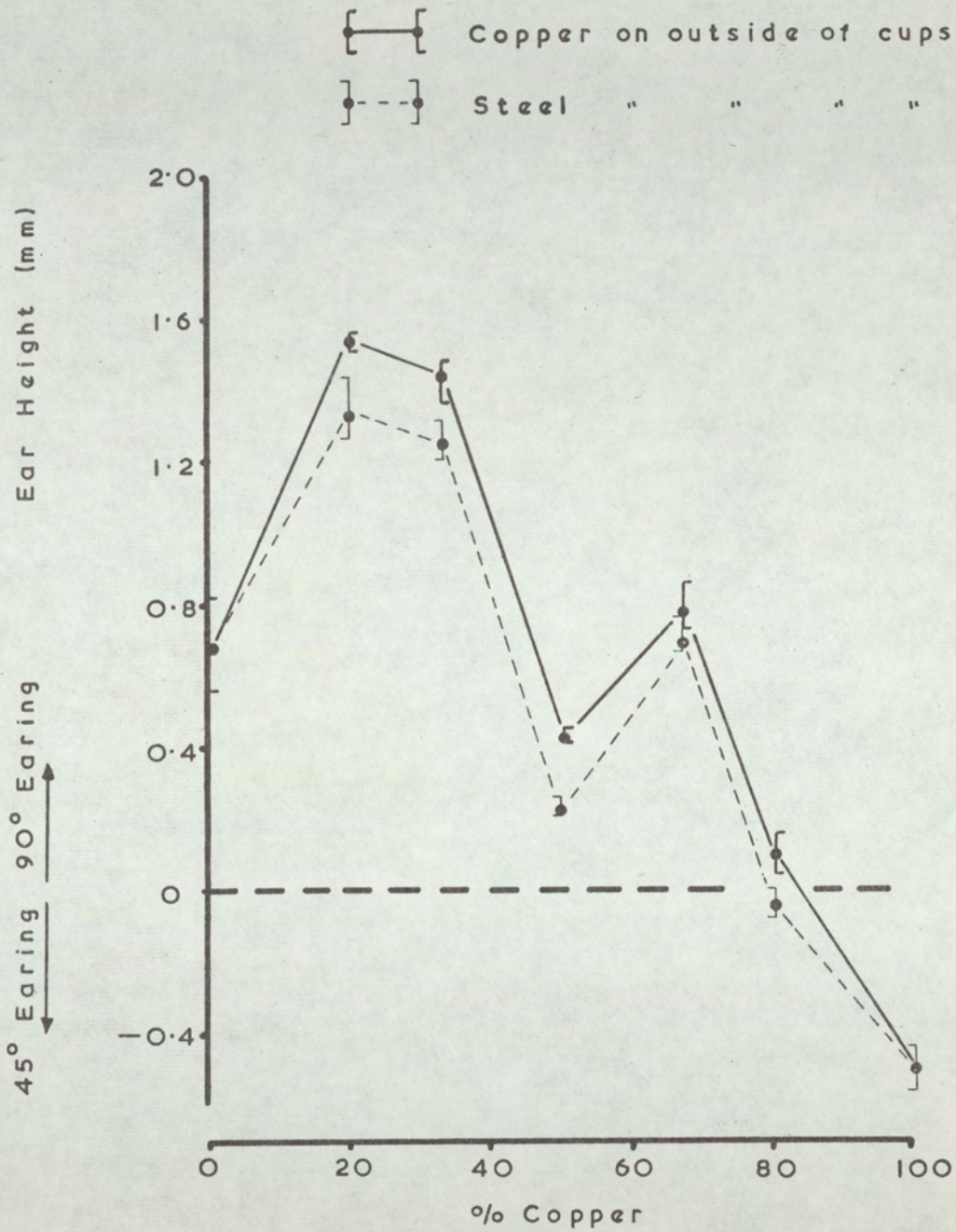


Figure 8.13

The variation of ear height with per cent copper for the roll bonded bilayer composites.



The component forming the inner surface of the cups, i.e. the one on the outer surface over the die radius, is radially drawn in more than the outer surface of the cups, and, because ears are generated by the process of radial shrinking of the flange, there will be a greater tendency for this component to produce ears. For the adhesive bonded composite  $90^\circ$  earing would be expected regardless of which component formed the inner surface. However, for roll bonded composites,  $90^\circ$  earing would be favoured when the inner component of the cups was steel and  $45^\circ$  earing when the copper was the inner component. A similar behaviour would be expected with the adhesive bonded composite in which the two components had their rolling directions mismatched by  $45^\circ$ , with the steel forming the inner component  $45^\circ$  earing (*with respect to the rolling direction of the copper*) would be favoured and  $90^\circ$  earing when copper was the inner component.

With the roll bonded composites the steel components had greater earing potentials than had the copper components (table 7.11), so that, with copper as the inner component of the cups,  $45^\circ$  earing would not be obtained unless the increase in  $45^\circ$  earing was greater than the "residual"  $90^\circ$  earing, but the degree of  $0-90^\circ$  earing would be decreased.

As may be seen from figure 8.13, when the copper was on the inside of the cups the magnitude of the  $90^\circ$  earing was reduced and for the 80/20 copper/steel composite this reduction was sufficient to change the overall earing direction of the composite. The adhesive bonded composite, with the rolling directions of its components mismatched by  $45^\circ$ , behaved in a similar manner, the results illustrating that earing may be reduced by cross-matching materials of differing planar anisotropies.

The results, for both the adhesive and the roll bonded composites, show that the earing characteristics of the composites are determined by the inner component unless the second component predominates in volume fraction and/or in earing potential. This mechanism may also explain some of the variation in the mean cup heights which has already been discussed.

With respect to the results for the roll bonded three layer composites it may be seen from table 7.11 that  $0-90^\circ$  earing increases and mean cup height decreases as the steel : copper ratio increases. These results can be explained in the same way as the results obtained on the bilayer composites.



### 8.4.3 DRAWING OF UNBONDED COMPOSITES

In the rolling of thin sheets of hard metals, sandwich pack rolling is often used to reduce the rolling load on the mill and hence reduce roll deflection. In this technique the hard metal, e.g. titanium, is 'sandwiched' between two layers of a softer, more ductile metal such as copper or brass. The softer metal is not bonded to the harder metal, although a high degree of friction is required at the interfaces to prevent relative slip and, hence, differential reduction taking place. <sup>(23)</sup>

It was thought that this technique may be utilised in deep drawing of hard metals to either reduce the drawing load or to obtain greater draw ratios. Another possible use of loose pack drawing would be to balance the earing potential of a given metal by the use of a suitable cladding metal. The cladding metal used need not necessarily produce ears at a different position from the base metal, but, provided the earing directions were known, the clad and base metal could be so arranged that the earing directions were mismatched.

The results of drawing unbonded composites were shown in table 7.21 and figure 7.12, from which it may be seen that relative movement of the composite components occurred. When relative movement of the composite components occurs, one of the components, in this case copper, is no longer restrained by the blank holder load and is free to wrinkle. If the component is not sufficiently thick to withstand the hoop compressional stress and wrinkles failure of this component can occur (figure 7.12) as the wrinkled flange is drawn through the die throat.

With the 50/50 copper/steel composite the individual components of the composites were sufficiently thick to withstand wrinkling and cups were successfully drawn. As was discussed in section 7.7 the earing values quoted in table 7.21 represent the earing of the component which elongated more in the cup wall. For the composites with degreased or etched interfaces, it may be seen that the presence of the steel (0–90° earing) altered the degree of earing of the copper component (45° earing) from – 2.4% to + 1.85% and + 0.95% respectively.

The high 0–90° earing, obtained when the interface was degreased, probably results from the steel "biting" into the surface of the copper after relative movement had occurred. The steel would tend to "bite" into the copper as the two components



thickened during flange shrinking and this would mean that the steel component would push out an annulus of copper, (the steel component being on the inner surface of the cups would be subjected to higher strains than the copper). When this occurred, the restraining influence of the copper would be reduced and earing is higher than would have been the case had there been no relative slip. With the composite having an etched interface, the degree of relative movement was less and, hence, the annulus of copper was smaller, the contribution from the copper greater and lower 0–90° earing was obtained.

With the composite having the lubricated interface the steel elongated more than did the copper and the presence of the copper reduced the earing of the steel from + 2.42 to + 1.51%.

The results show that if loose pack drawing is to be practicable, relative slip must be prevented e.g. by adhesive bonding, or alternatively the components should be of a thickness where wrinkling is not likely to be a problem. The use of adhesive bonding has already been successfully demonstrated in previous sections, although failure to draw the 20% copper/80% steel composite with the copper component on the outer surface of the cup was attributed to failure in adhesion. Copper is, however, a difficult material with which to achieve good adhesion and the use of a primer is recommended.<sup>(63)</sup> In the production of the adhesive bonded composites, C.I.B.A. did not use a primer on the copper components and, as a result, the adhesion was poor, particularly when subjected to peel or cleavage loading. A further practical difficulty to loose pack drawing would be the removal of the clad from the drawn components.

#### 8.4.4. *STRETCH FORMING*

From the tables of stretch forming results (tables 7.9 and 7.12) it may be seen that, with the exception of the 20/80 copper/steel composite, deeper penetrations were obtained when the bilayer composites were deformed with the copper component on the outer surface. With the 20/80 adhesive bonded copper/steel composite, the adhesion to the copper component was poor and this was probably the cause of the low Erichsen value, obtained when the composite was deformed with the copper component uppermost. Deep drawability of this composite was also influenced by adhesive break-down, as was discussed in section 7.4.



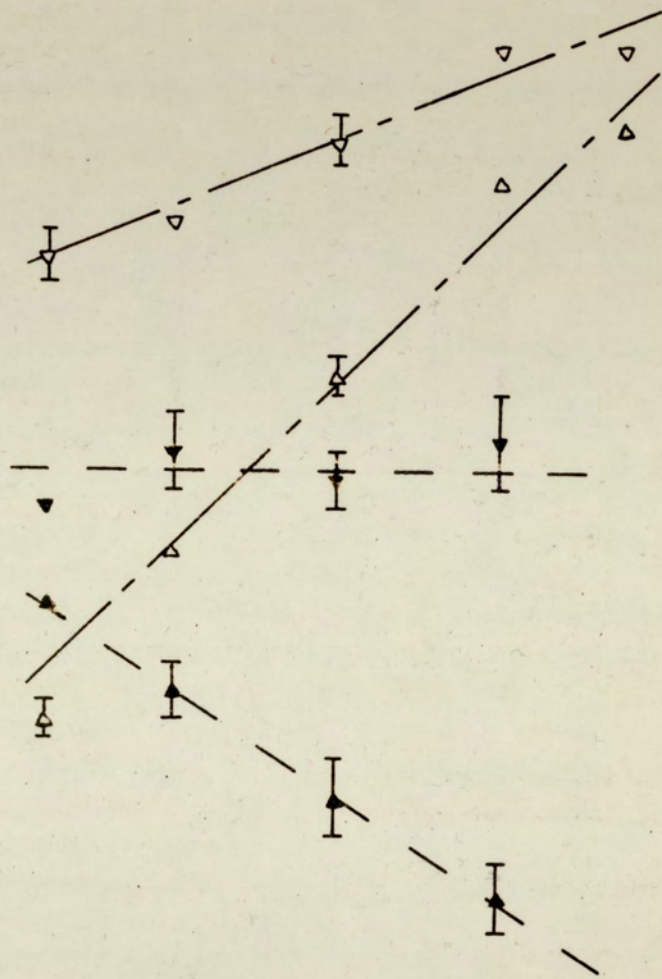
The Erichsen values of the roll bonded bilayer composites were independent of the copper: steel thickness ratio, an approximately constant value of 13.1 mm was obtained when the copper component was outermost and 12.4 mm when the steel component was outermost. These results, therefore, suggest that stretch formability of the composites was determined by the component on the outer surface and, as Erichsen value increases with uniform elongation, that the ductility of the individual components were similar for all the composites; the copper components having greater ductilities than the steel components. The ductilities of the copper components were greater than those of the steel components, tables 7.16 and 7.17, but, although the variation in ductilities of either component was small, there was a large variation in their stretch formabilities, table 7.19. The stretch formability of both the steel and of the copper components increased with thickness as shown in figure 8.14.

It is, however, a feature of the Erichsen test that the Erichsen value increases with increasing sheet thickness and calibration curves are published to compensate for this. In order that the Erichsen values of the steel and copper components may be compared with those of the composites, the experimental values must be corrected to a common sheet thickness of 1.83 mm. (0.072"). The calibration curves for steel, and for copper, issued by Erichsen are not necessarily representative of those for the steel or copper components of the composites, but may be used to illustrate the influence thickness could have on the test results.

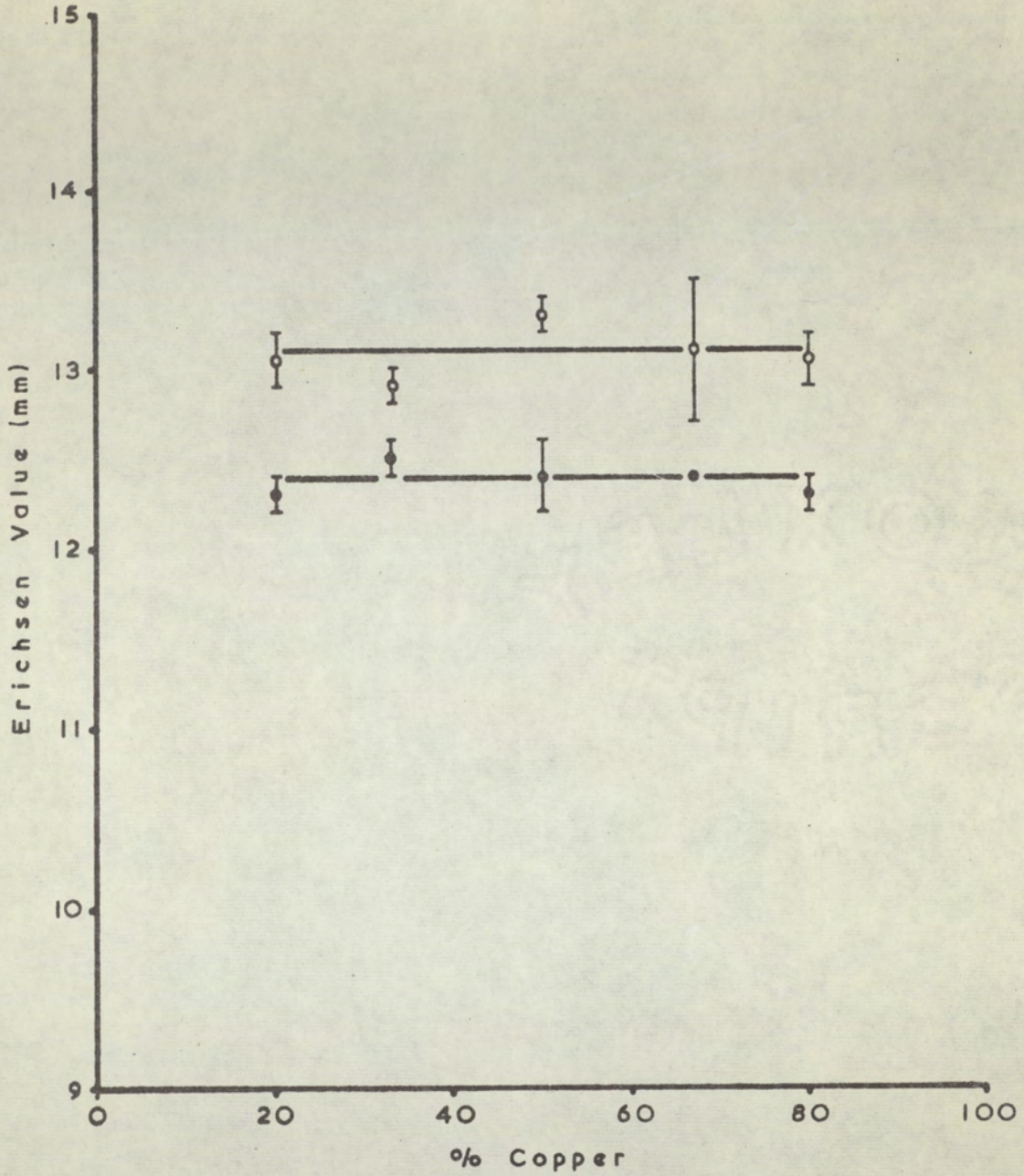
The experimental results, corrected to a thickness of 1.83 mm. are shown superimposed on figure 8.14. The corrected results for the steel give an approximately constant penetration of 12.2 mm, whereas the results on the copper vary from 13.3 to 14.4 mm. These results show that the Erichsen values, obtained on the composites, could represent the stretch formability of the individual components, the stretch formability of the composites being determined by the ductility of their outermost fibres. The ductility of these fibres is dependent upon the ductility of the outer component not that of the composite and, hence, the stretch formability of the composites does not increase with the ductility of the composites.

It has been reported by Rathbone<sup>(59)</sup> that, with bilayer composites of stainless steel/mild steel, greater penetrations were obtained when the thicker component, mild steel, was the outer one. Rathbone did not, however, indicate whether or not the deeper penetrations were obtained because the outer component was the thicker one or because it was mild steel rather than stainless steel. In the trade literature of Metals and Controls for copper/aluminium<sup>(67)</sup> and for stainless steel/aluminium<sup>(68)</sup>









- Copper on outside.
- Steel on outside.
- △ △ Results on copper or steel components respectively.
- ▽ ▽ Results corrected to 1.83 m.m's (0.072 ins.)

Figure 8.14

Variation of Erichsen value with per cent copper and sheet thickness for the roll bonded bilayer composites.



greater penetrations are quoted when the thinner component is the outer one and in the work now reported greater penetrations were obtained when the copper, irrespective of its thickness, was the outer component.

Strength, ductility and resistance to thinning are factors that are likely to influence stretch formability and the influences of these factors on the stretch formability of a range of bilayer composites are shown in table 8.6. In the table, strength has been represented by yield or proof stress, ultimate tensile strength or as the ratio of yield or proof stress to ultimate tensile strength, resistance to thinning being represented by the R values.

From table 8.6 it may be seen that, for all but the type 301 stainless steel/mild steel composite, greater penetrations were obtained when the outer component had the greater ductility. In drawing up table 8.6, it was assumed that the type 301 stainless steel had a greater ductility than had the mild steel component of the composite, this estimation being based upon the specification for type 301 stainless steel. The tensile strength of the stainless steel was, however, some 20% lower than that of the specification and so it is possible that the stainless steel was of poor quality and had a lower ductility than was estimated. If this was so, then for all the composites quoted in table 8.6, greater penetrations were obtained when the outer component had the greater ductility, for all the other factors considered, there were reliable examples that did not give the greater penetrations.

#### 8.5 *APPLICATION OF THE EQUAL STRAIN HYPOTHESIS TO THE DEEP DRAWING AND STRETCH FORMING PROPERTIES.*

The stretch formability of the composites has been shown to be dependent upon the ductility of the outermost component, rather than that of the composite, and so the equal strain hypothesis will not predict stretch formability. With respect to deep drawability, the dependence of the experimental results on tool geometry, which was discussed in section 8.4.1, would tend to obscure the accuracy of any results predicted from the equal strain hypothesis. For these reasons, the equal strain hypothesis was only used to predict punch loads, for both deep drawing and stretch forming, and earing properties of the composites, the results being discussed in the following sections:



TABLE 8.6. QUALITATIVE ASSESSMENT OF THE INFLUENCE OF VARIOUS FACTORS ON THE STRETCH FORMABILITY OF BILAYER COMPOSITES

Composite	Per Cent Clad	Ref: No.	Greater Penetrations obtained when the outer component of the composite has the:					
			Greater thick-ness	Lower P.S. or Y.S.	Higher U.T.S.	Higher P.S. or Y.S. U.T.S.	Greater Ductility	Higher R Value
Copper-Steel	20 - 80% Cu.	This work	< 50%Cu. x > 50%Cu. J	J	x	x	J	x
Copper-Aluminium	10 - 30% Cu.	67	x	x	J	x	J	J
Stainless Steel-Aluminium								
T 434 - 3003	17 - 20% S.Steel	68	*	*	*	*	*	*
T 434 - 5052	"	"	x	J	J	J	J	J
T 201 - 3003	"	"	*	*	*	*	*	*
T 201 - 5052	"	"	x	J	J	J	J	J
S. Steel - Mild Steel								
T 301 - .06% C	16 - 50% S.Steel	59	J	J	x	J	x <sup>†</sup>	J
T 430 - .06% C	"	"	J	J	x	x	J <sup>†</sup>	J

\* Equal penetrations obtained when outer component is either the stainless steel or the aluminium.

† Ductilities of the stainless steel estimated from the appropriate specification.



### 8.5.1. *Calculation of the punch loads for the composites.*

The punch load for deep drawing or stretch forming could be determined by simple addition of those for the individual components or by using the equal strain hypothesis to predict the punch load from those of samples of 100% copper and 100% steel. The punch loads for the 100% copper and 100% steel were determined from those of the various thicknesses of the copper and steel components, as shown in figure 8.15. The deep drawing punch loads represent the maximum punch load for drawing 65 mm. diameter blanks, whereas the stretch forming punch loads are those for a punch penetration of 7 mm. The punch loads determined from figure 8.15 were used to calculate the punch loads for the composites using the equal strain hypothesis, these results being compared with the experimental values and those determined by addition of the individual punch loads. The results are shown graphically in figure 8.16.

Figure 8.16 illustrates that the punch loads for deep drawing or stretch forming the composites may be accurately predicted by either method of calculation. The results determined using the equal strain hypothesis are generally more accurate than those determined by simple addition of the individual punch loads; the maximum differences between calculated and experimental values being  $-5.2\%$  and  $-10.1\%$  respectively for deep drawing and  $-8.5\%$  and  $-15.2\%$  respectively for stretch forming. This increase in accuracy is due to the experimental errors in the individual punch loads being "averaged" out when the punch loads for 100% samples of copper and steel were derived, by extrapolation, from figure 8.15.

The experimental punch loads for the roll bonded composites are shown in figure 8.17 plotted against per cent copper, illustrating that punch load, like proof stress and U.T.S., decreased linearly with per cent copper.

### 8.5.2. *Calculation of the earing properties of the composites.*

The equal strain hypothesis was used to predict the mean cup heights, ear heights and per cent earing of the composites from those properties of the appropriate components (shown in table 7.20), the calculated and experimental values being compared in table 8.7.

The results, shown in table 8.7, illustrate that only mean cup heights may be predicted to the same degree of accuracy as was obtained with properties such as proof stress, U.T.S. and punch load. The calculated results, shown in table 8.7, are



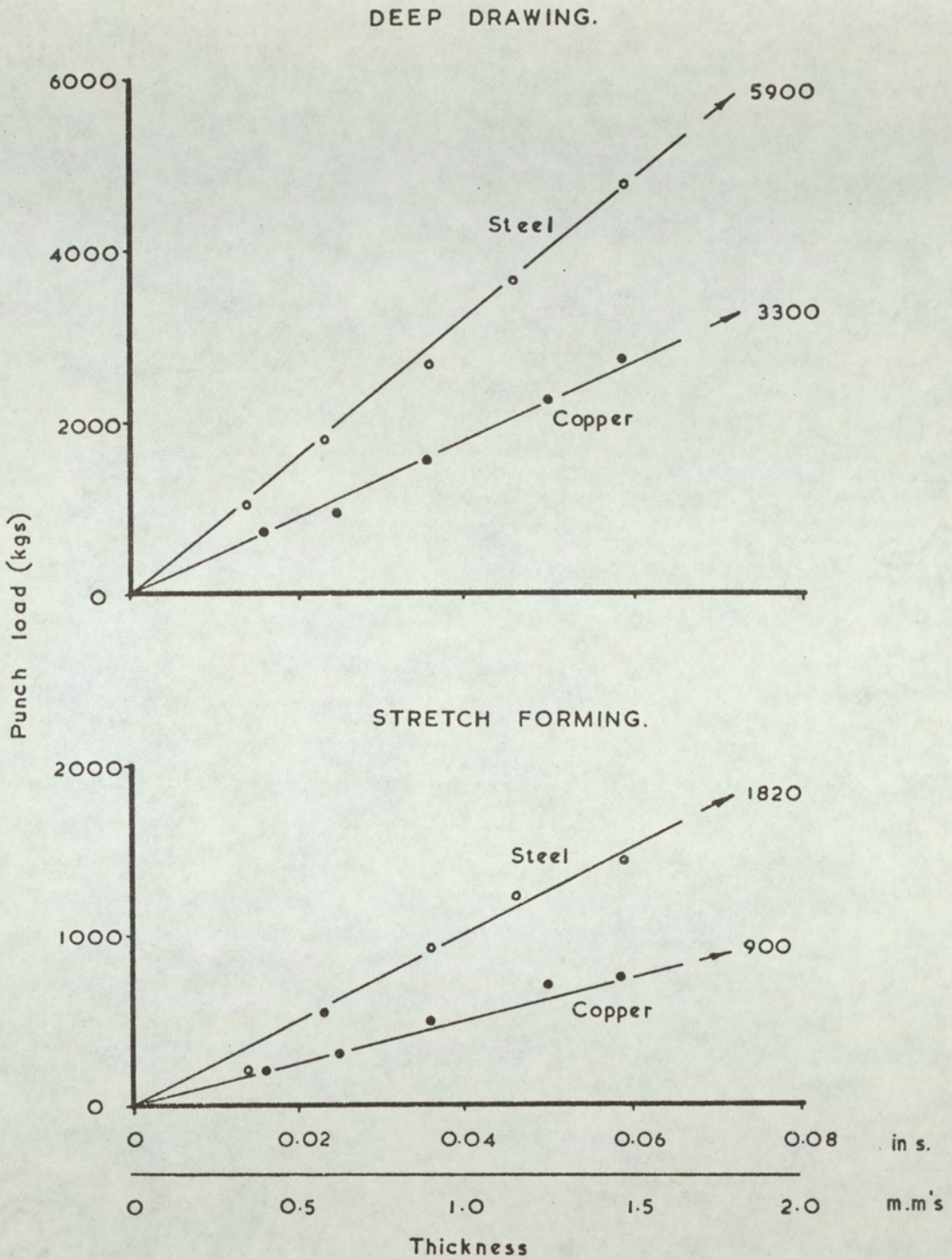
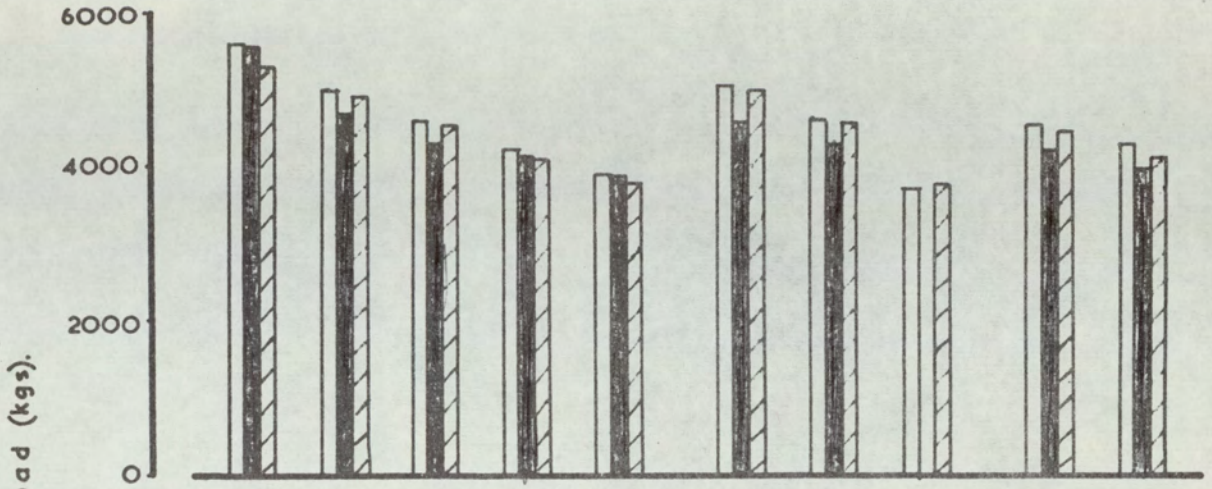


Figure 8.15

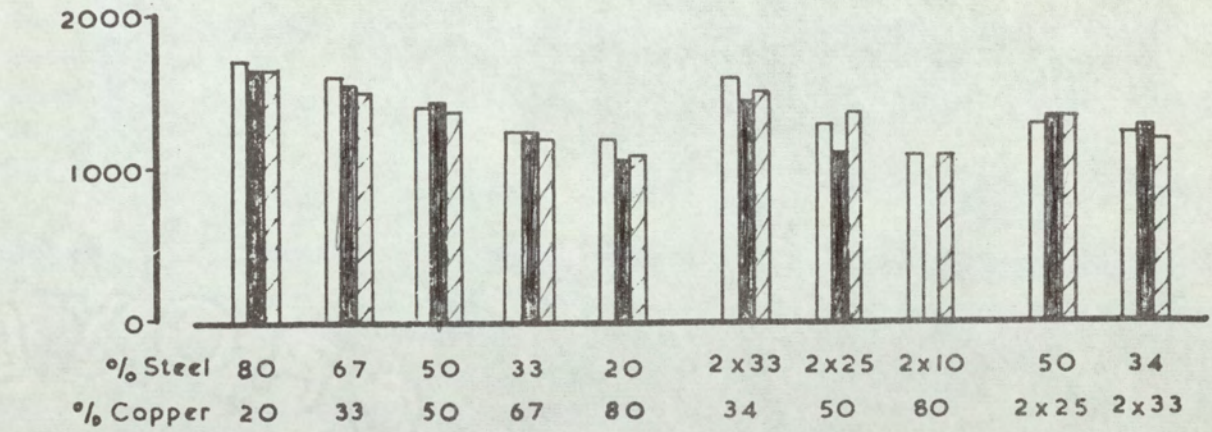
The variation of punch load with sheet thickness for the copper and steel components of the bilayer composites.



DEEP DRAWING.



STRETCH FORMING.



Experimental  
 Calculated - addition.  
 " - equal strain.

Figure 8.16 A comparison of the calculated and experimental punch loads for the roll bonded composites.



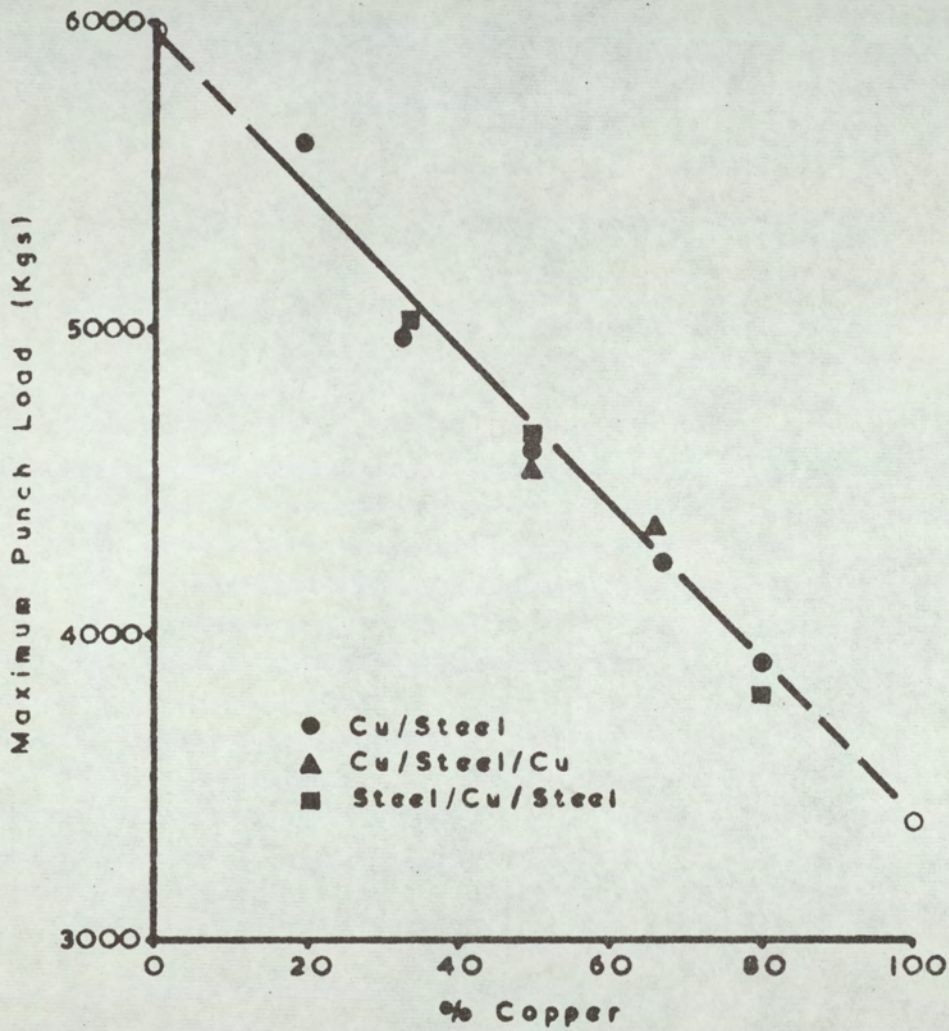


Figure 8.17 Variation of maximum punch load (for drawing cups from 65 mm diameter blanks) with per cent copper for the roll bonded composites.



generally significantly lower than the experimental results, indicating that the equal strain hypothesis underestimates the influence of the steel and/or overestimates the influence of the copper.

Table 8.7 The percentage difference between the calculated and experimental earing properties of the roll bonded composites.

Material		Steel or Copper Uppermost	PER CENT DIFFERENCE IN:		
% Copper	% Steel		Ear Height	% Earing	Mean Cup Height
20	80	Copper	- 46.5	- 47.5	+ 1.5
		Steel	- 39.0	- 40.7	+ 2.8
33	67	Copper	- 33.0	- 26.5	- 5.0
		Steel	- 23.4	- 20.0	- 2.8
50	50	Copper	- 57.3	- 60.8	- 5.6
		Steel	- 20.8	- 14.5	- 4.4
67	33	Copper	- 60.3	- 49.4	- 5.0
		Steel	- 55.9	- 45.2	- 3.2
80	20	Copper	- 127.7	- 85.2	- 2.7
		Steel	- 15.2	- 133.3	- 0.9
34	2 x 33	-	- 6.7	+ 4.7	- 7.9
50	2 x 25	-	- 22.7	- 10.6	- 6.1
80	2 x 10	-	STEEL COMPONENT NOT TESTED		
2 x 25	50	-	- 46.0	- 41.2	- 1.5
2 x 33	34	-	+ 720.2	+ 671.7	- 5.8



Ear height was shown in section 8.4.2 to be a better measure of anisotropy for the composites than was per cent earing and, for this reason, the discussion of the results, shown in table 8.7, will be concentrated on those for ear height. The difference between the calculated and experimental ear heights is shown graphically in figure 8.18. in which the calculated or experimental values of ear height are plotted against the calculated or experimental  $\Delta R$  values respectively. From figure 8.18b, where the calculated results are superimposed on the experimental values, it may be seen that the calculated results need to be moved in the general direction of the arrows to become coincident with the experimental results i.e. the calculated results need to be weighted in favour of the steel (more positive ear heights and  $\Delta R$  values).

The steel components may determine the overall earing patterns of the composites because they are the stronger and/or have the greater earing potentials. The equal strain hypothesis only considers the variation in the earing potentials and so predicts that the component having the greater earing potential, after weighting for thickness, determines the overall earing behaviour of the composite. This is not necessarily the case because, assuming there is no relative movement of the composite components, the initial earing behaviour of the composite will be determined by the component having the higher yield stress in compression, ears not being formed until this component yields. Ears are not formed until the steel component yields and, because the steel will yield preferentially in the directions having the lower yield stress i.e. either parallel or at right angles to the rolling direction, 0–90° earing is favoured. Once ears are produced the earing behaviour of the material is, to a certain extent, fixed because it requires less energy for the ears, initially formed, to continue growing than it takes for the reversal of this earing pattern.

The situation is not, however, so simple because the yield behaviour of the steel is modified by that of the copper and, in addition, the two components are radially drawn in differentially; this having been discussed in section 8.4.2. The results suggest though that for calculation of ear height, or per cent earing, a "strength factor" should be incorporated in the equal strain hypothesis in order to preferentially weight the component having the greater yield strength. This factor may be determined by a statistical analysis of the calculated and experimental results but such an analysis was not made because the number of results were not sufficient to give statistically significant results.



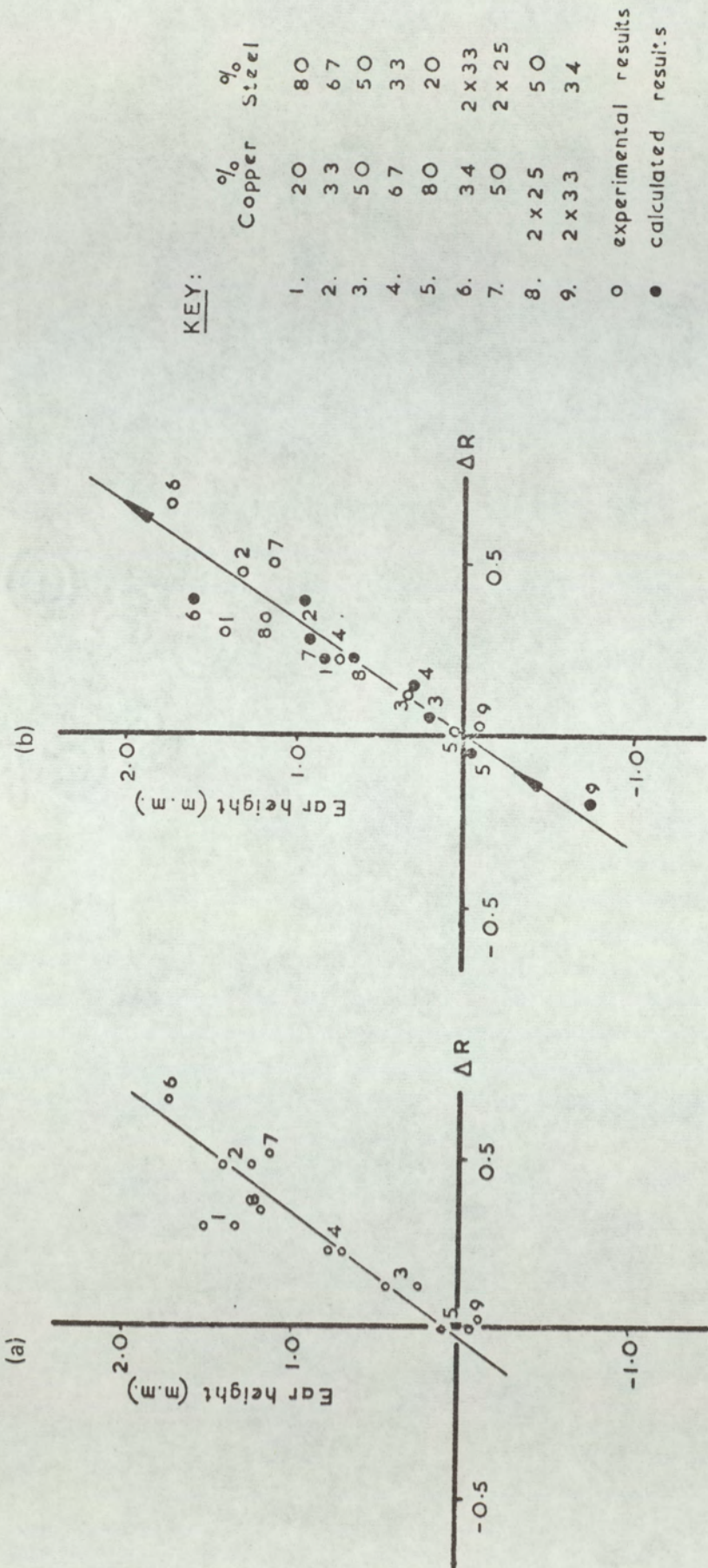


Figure 8.18 The relationship between ear height and  $\Delta R$ :  
 (a) experimental results.  
 (b) experimental and calculated results.



8.6 THE THEORETICAL CALCULATION OF MAXIMUM DRAW STRESS

The draw stress for the steel, copper and the roll bonded copper/steel composites were calculated using the analysis outlined in Appendix 1, a typical calculation being shown in Appendix 3 for the 100% steel sample. In the calculation of the stresses corresponding to the radial strains of the rim and of the element at the mean cup wall radius, the appropriate values of 'k' and 'n' were obtained from tables 7.6 and 7.18. For the composites these stresses were determined using the experimental 'k' and 'n' values for the composites and also by using the 'k' and 'n' values for the appropriate steel and copper components. With this latter technique the value of  $\bar{\sigma}$  for substitution in equation A.12 was determined by the equal strain hypothesis:

$$\bar{\sigma}_{comp} = \bar{\sigma}_{Cu} t_{Cu} + \bar{\sigma}_s t_s \dots\dots\dots 8.9$$

and equation A.16 was rewritten as:

$$\begin{aligned} \sigma_{Tr} = e^{\mu \pi/2} & \left[ m ( \bar{\sigma}_{Cu} t_{Cu} + \bar{\sigma}_s t_s ) \ln \frac{R}{r_p} + \frac{\mu H}{\pi r_p t_p} \right] \\ + & \left[ \frac{m ( \sigma'_{Cu} t_{Cu} + \sigma'_s t_s ) t ( e^{\mu \pi/2} + 1 )}{4 R_D} \right] \dots\dots\dots 8.10 \end{aligned}$$

where  $\sigma'$  = flow stress for the material at the mean cup wall radius.  
 $t_{Cu}, t_s$  = thickness fraction of copper and steel respectively.

The calculated and experimental maximum draw stresses are shown in figure 8.19. The maximum difference between the calculated and experimental draw stresses for the composites was + 4.7% and + 7.0% when the calculations incorporated the equal strain hypothesis.



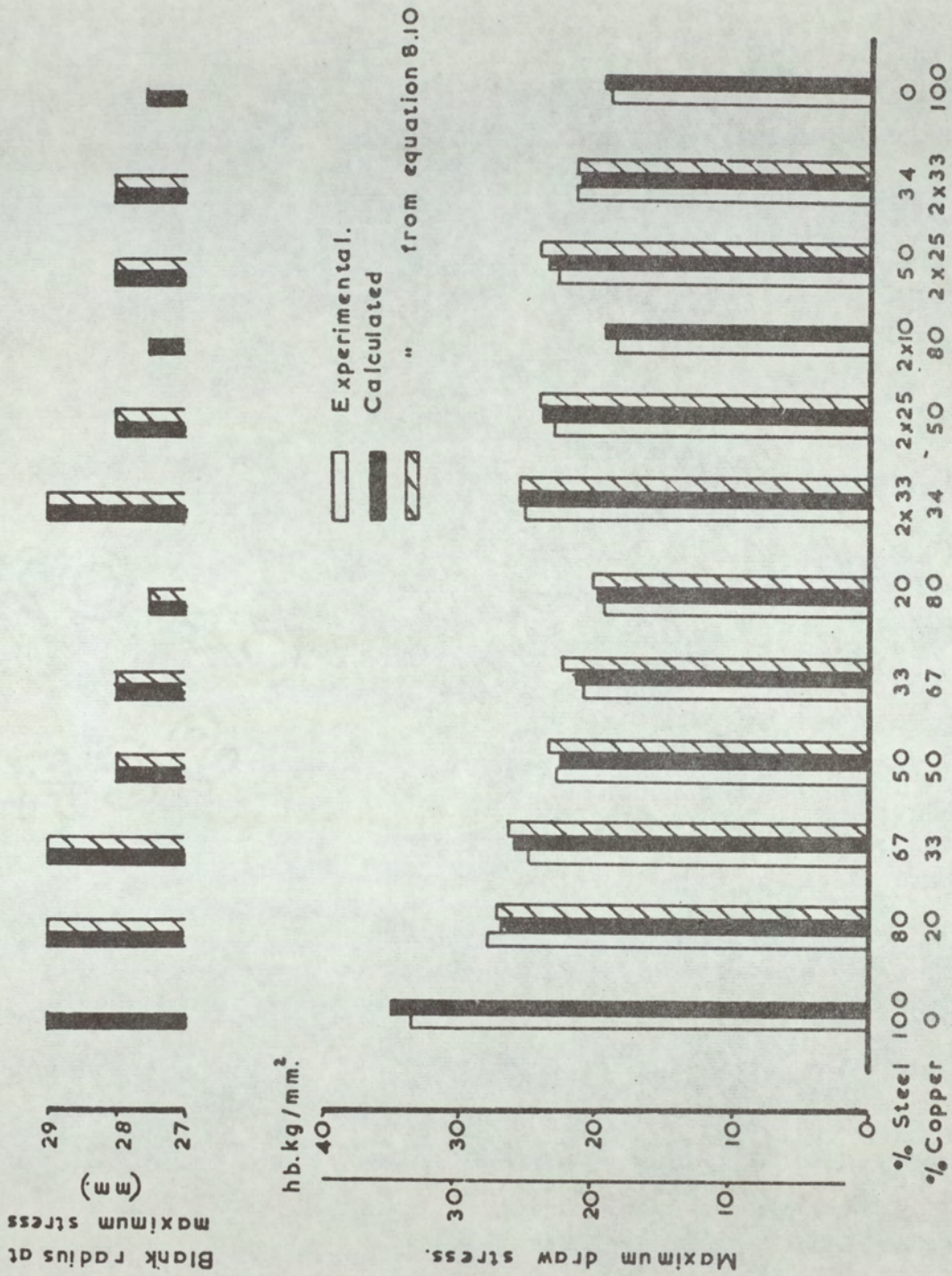


Figure 8.19 A comparison of the experimental and theoretically calculated draw stress for the roll bonded composites.



Also included in figure 8.19 is the diameter of the rim at which the calculated draw stress was a maximum. The calculated maximum draw stress was found to occur later in the draw as the proportion of copper in the composite increased, these results were not compared with the experimental results because of the practical difficulties involved in stopping the draw at the instant when the draw load was a maximum. The experimental values may, however, be assumed to follow a similar pattern as the calculated values; the degree of drawing off the punch nose increasing with per cent copper (figure 7.7 page 79) so that the maximum draw stress would occur later in the draw as the proportion of copper increased.

The agreement between calculated and experimental results is particularly good considering the large number of approximations used in the calculations and illustrates that the errors arising from these approximations are either small or that they cancel during the analysis. The results show that the maximum draw stress for the composites may be theoretically calculated, by use of equation 8.10, from a knowledge of the properties and relative thicknesses of the composite components, to approximately the same degree of accuracy as can those of single metals. In the theoretical calculation of the draw stress for the composite from the properties of its components, no additional assumptions to those made in the analysis for single metals are necessary, other than assuming that the stress on the composite may be determined by the equal strain hypothesis. The validity of this assumption has already been verified in preceding sections.

The analysis, outlined in Appendix 1, would not be expected to accurately predict the punch load – punch travel diagram, for either the single metals or the composites, because appreciable thinning over the punch nose was observed for all the materials (figure 7.7) thus invalidating one of the basic assumptions of the analysis.

## 8.7 *THE PLANE STRAIN COMPRESSION PROPERTIES OF THE ROLL BONDED COMPOSITES.*

### 8.7.1 *The relationship between true stress and true strain.*

The true stress – true strain curves for the roll bonded composites (figures 7.8 and 7.9) were all of the same general form with true stress increasing continuously with true strain. Davies <sup>(12)</sup>, however, found that in plane strain compression tests on adhesive bonded aluminium/copper/aluminium composites, failure of the core (copper)



occurred, the true stress – true strain curves for the composites passing through a maximum, as was shown in figure 2.5. The explanation proposed by Davies was that the horizontal tensile stress, induced on the copper at the interface with the aluminium, eventually reached a value where the overall stress deviator on the copper was tensile. Localised thinning, and eventual failure of the core, then occurred.

Walker <sup>(27)</sup> using copper/steel composites, having different hardness ratios to those used in the work now reported, produced sufficient evidence to show that fracture of the core, observed by Davies, could have been a consequence of using b/t ratios of 0.4 – 0.8; the recommended ratios for plane strain conditions being 2 – 4. Walker observed experimentally that necking of the core occurred although the core did not fracture. The number of necks observed appeared to depend upon the number, and the size of the dies used; each die producing two necks with the exception of the narrowest which produced a single neck.

Typical examples of the development of necking of the core observed by Walker are shown in figure 8.20. As may be seen from figure 8.20 necking of the core was observed regardless of whether the core was steel or copper. Similar results to those shown in figure 8.20 were also obtained in this work.

The explanation proposed by Davies to explain necking, and eventual failure of the core, predicts necking only when the core is the "hard" component of the composite and, therefore, cannot be used to explain the necking observed with the steel/copper/steel composites. Furthermore necking of the core was only observed in this work on those test pieces for which  $dE_y = 0$ .

In order to deform composites using b/t ratios comparable to those used by Davies, three layer composites were produced by bolting together two samples of the bilayer composites such that steel/copper/steel or copper/steel/copper composites were produced. Samples of these composites were deformed with an initial b/t ratio of 0.48, a single die being used to derive the complete true stress – true strain curves. For comparison purposes, samples were also deformed such that b/t was maintained throughout the test between 2 and 4.



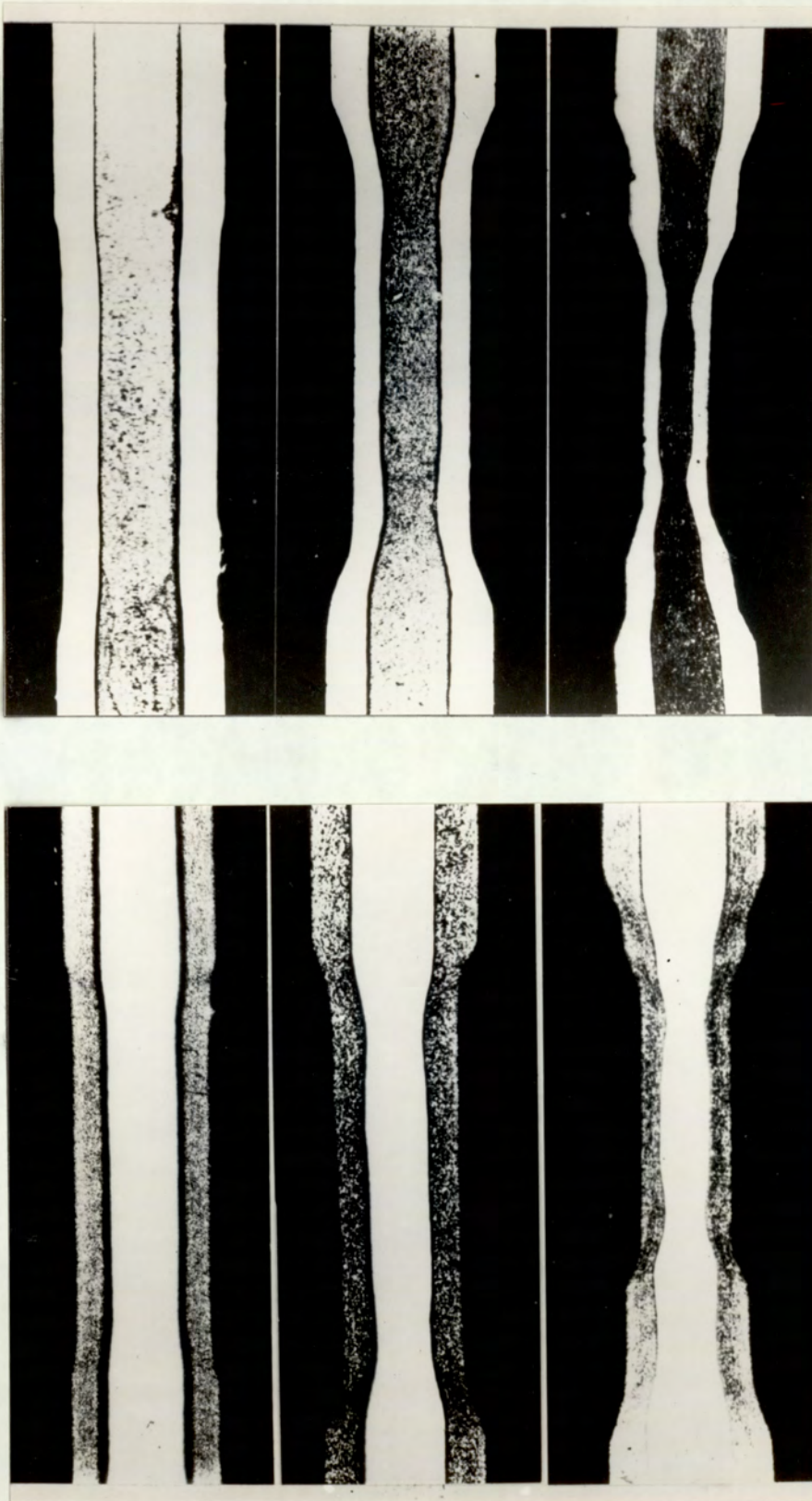


Figure 8.20 The development of necking in the plane strain compression tests on 25% steel/50% copper/25% steel (left) and 25% copper/50% steel/25% copper (right). (27)

top	—	10% reduction
centre	—	30% reduction
bottom	—	50% reduction

[Magnification x 10]



Examples of the true stress – true strain curves for these composites are shown in figure 8.21 for the 25% Copper/50% Steel/25% Copper composite. Fracture of the core (figure 8.22) was observed for those samples deformed with an initial  $b/t$  ratio of 0.48, fracture being observed for both the copper/steel/copper and the steel/copper/steel composites. The composites deformed using the correct  $b/t$  ratios gave deformation patterns similar to those previously discussed. Necking, and eventual fracture, of the core was again only observed on test pieces for which  $dE_y = 0$ , the test pieces having  $dE_z = 0$ . showed no traces of necking even when deformed with  $b/t$  ratios of 0.4.

The results show that fracture of the core of three layer composites does not result from the stresses induced at the interfaces between the clad and core, but result from the use of incorrect tooling.

The influence of tooling on the deformation patterns may be obtained from slip–line field theory. At the instant when  $b/t$  is an integral number, the slip–line field solution for frictionless plane strain compression is a simple pattern of  $45^\circ$  crosses, these representing bands of intense shear. The slip line field solution for integral values of  $b/t$  and zero friction are shown in figure 8.23.



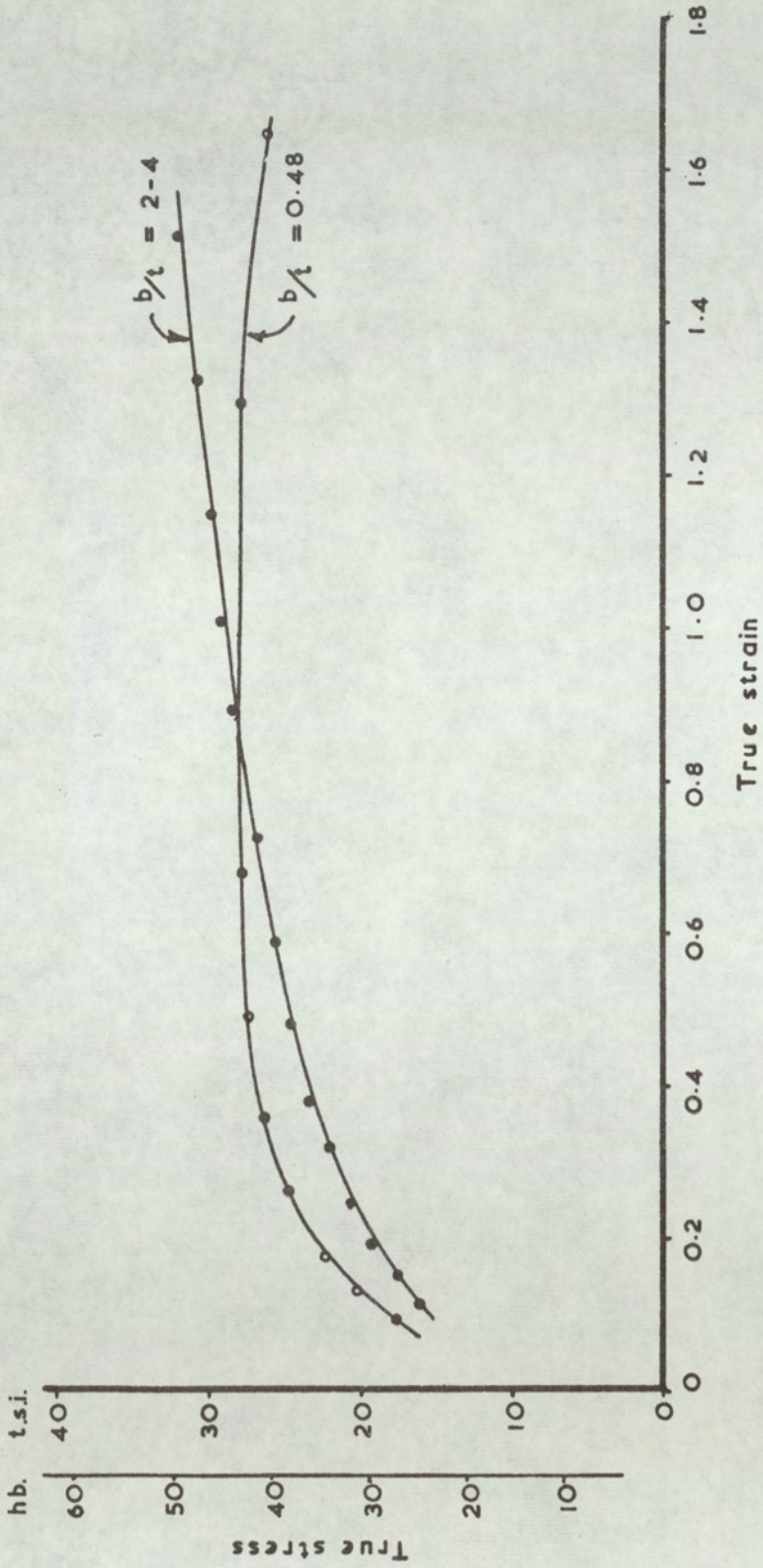


Figure 8.21 True stress - true strain compression curves with  $b/t$  ratios of 0.48 and 2 - 4.



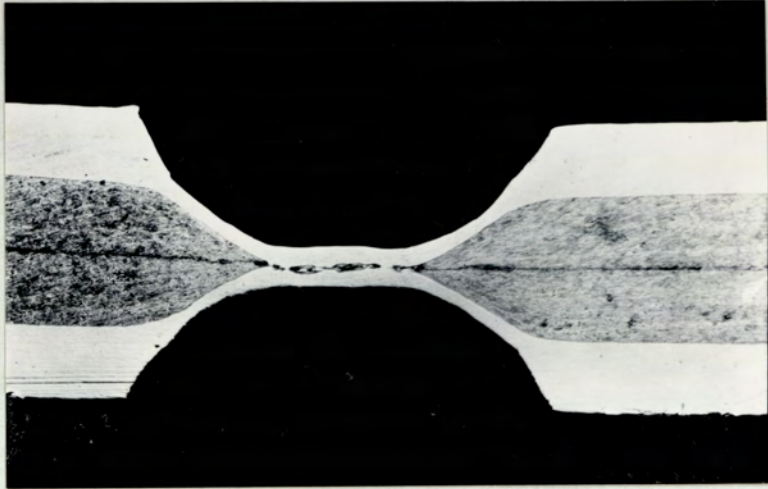


Figure 8.22 Fracture of the core of a copper/steel/copper composite deformed with  $b/t = 0.48$   
[Magnification  $\times 10$ ]



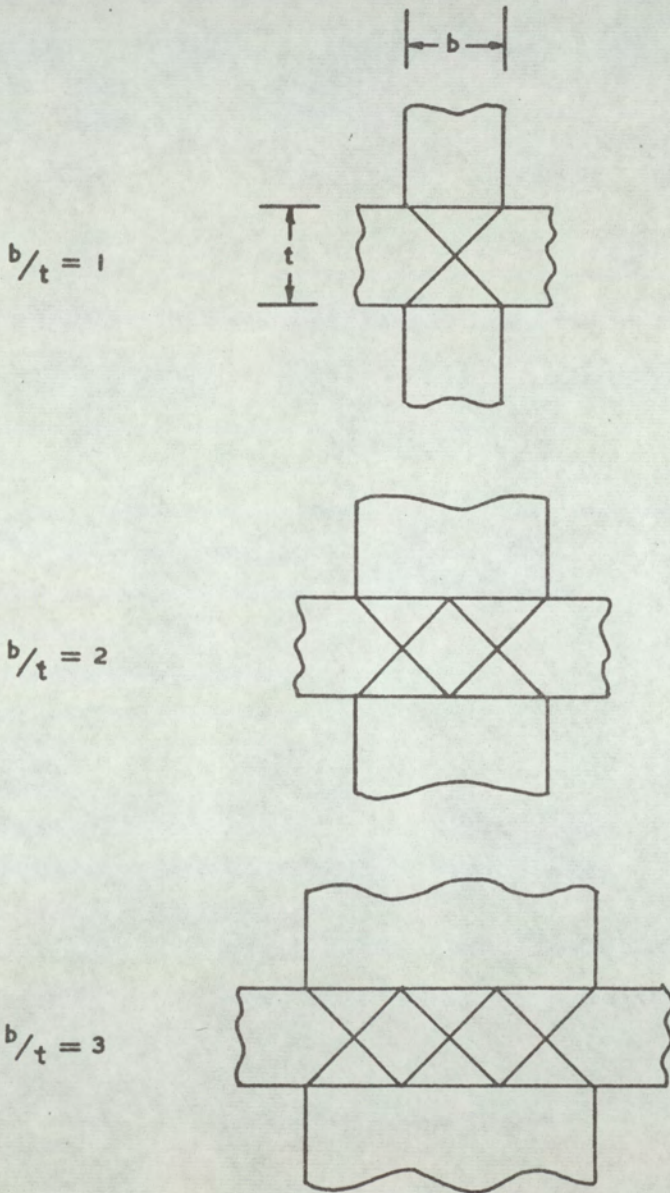


Figure 8.23 Slip line field solution for integral  $b/t$  ratios of 1, 2 and 3.



The patterns illustrated in figure 8.23, although representing those for the greatly simplified case of integral  $b/t$  ratios and frictionless compression, may be seen to closely resemble the deformation patterns obtained with the composites (figure 8.20), necks forming at the intersection of the bands of intense shear.

Necking, and fracture of the core of the composites was shown to be completely independent of any stresses set up at the interfaces between the clad and core, by making up a "composite" specimen consisting of three similar layers of mild steel. The specimen was deformed with an initial  $b/t$  ratio of 0.48. Necking of the central layer, as shown in figure 8.24, was observed thus illustrating that necking of the core of the composites results from stress concentrations determined by tool geometry rather than by stresses induced at the interfaces between clad and core.

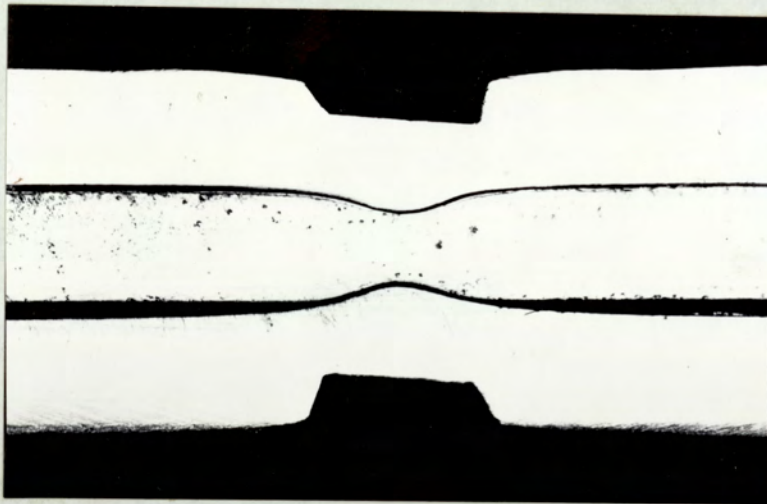


Figure 8.24

*Necking of the centre layer of a sample, consisting of three layers of steel, deformed with  $b/t = 0.48$ .*

[ Magnification  $\times 10$  ]



8.7.2. *Anisotropy in plane strain compression.*

Anisotropy in plane strain compression was assessed by measuring the  $\beta$  ratio suggested by Holcomb and Backofen<sup>(55)</sup>. The results, tabulated in table 7.13 illustrate that  $\beta$  did not vary markedly with strain.

The inter-relationship of  $\beta$  and R was discussed in section 4.2.3 (page 35) and for the special case of planar isotropy the relationship was given by equation 4.7<sup>(56)</sup> : i.e.  $\beta = \sqrt{\frac{R + 1}{2}}$  when the material exhibits planar anisotropy

the relationship may be modified, as was shown in equation 4.8<sup>(55)</sup> :

i.e.  $\beta = \sqrt{\frac{R_{rd} (R_{td} + 1)}{R_{rd} + R_{td}}}$

(where rd and td refer to the rolling and transverse directions respectively)

Equation 4.8 does not allow for anisotropy in directions other than the rolling and transverse directions although it is possible that a material may exhibit planar anisotropy and yet have  $R_{rd} \neq R_{td}$ , in which case equations 4.7 and 4.8 are equivalent. A better modification would be expected by the use of the mean R value ( $\bar{R}$ ), equation 4.7 being rewritten:

$$\beta = \sqrt{\frac{\bar{R} + 1}{2}} \dots\dots\dots 8.11$$

Using equations 4.8 and 8.11  $\beta$  was calculated from the R values determined in the tensile tests. The experimental and calculated  $\beta$  values, at a true strain of 0.2, are shown in table 8.8. The results show that for the case of planar anisotropy the relationship between  $\beta$  and R is more accurately represented by equation 8.11 than by equation 4.8, the maximum differences between the calculated and experimental  $\beta$  values being -6.9 and -15.2% respectively. The compression and tensile data for the composites yield similar anisotropies and illustrate that, for cases where the anisotropy does not markedly vary with strain, there is little to be gained by deriving  $\beta$  data; the measurements being time consuming and difficult to make.



Table 8.8. A comparison of  $\beta$  values determined experimentally with those calculated from the  $R$  values using equations 4.8 and 8.11.

COMPOSITE		$\beta$ at 0.2 true strain:		
% Copper	% Steel	Experimental	Calculated using eq <sup>n</sup> . 4.8	Calculated using eq <sup>n</sup> . 8.11
0	100	0.95	0.90	0.97
100	0	0.98	0.96	1.00
20	80	1.01	0.86	1.00
33	67	1.03	1.02	1.00
50	50	1.00	0.94	0.99
67	33	0.97	0.97	0.97
80	20	0.99	0.94	0.96
34	2 x 33	1.07	1.03	1.00
50	2 x 25	1.05	1.03	1.01
80	2 x 10	0.99	0.95	0.96
2 x 25	50	1.01	1.04	1.03
2 x 33	34	1.00	0.97	0.99



### 8.7.3. *Optimum clad ratio.*

From figures 7.8 and 7.9 the stress for any given reduction was found to decrease linearly with increasing copper : steel thickness ratio, typical results for a true strain of 0.2 and 1.0 are shown in figure 8.25. These results differ from those of Davies<sup>(12)</sup>, who found, in his study of the plane strain compression of aluminium/copper/aluminium composites, that for any given reduction, there was an optimum clad to core thickness ratio which gave a minimum deformation load.

In Davies' work an optimum clad to core thickness ratio was only obtained when he used composites of varying total thickness. Davies' results are not, however, reliable because it has already been shown that his test parameters did not give plane strain conditions.

Optimum clad to core thickness ratios have also been reported by Arnold and Whitton<sup>(23)</sup> and Afonja and Sansome<sup>(24)</sup> in their studies of sandwich pack rolling. None of these workers have produced strong experimental evidence for the existence of optimum clad to core thickness ratios, this having been discussed in section 2.2.

The rolling load for various first-pass rolling reductions were determined on samples of the roll bonded three layer composites. Both roll load and the total work done for any reduction were found to decrease linearly with increasing copper to steel thickness ratios, the results for a 30% first-pass reduction are shown in figure 8.26. The differences between these results and those obtained by Arnold and Whitton<sup>(23)</sup> or Afonja and Sansome<sup>(24)</sup> (see figure 2.6 Page 19) may be explained in the following way:

The roll load for a given reduction of a thin strip of metal may be reduced by cladding that metal, the reduction in roll load being associated with:—

(a) A geometrical effect: In the rolling of thin strip the redundant work zones often overlap, increasing the thickness, by cladding, may result in these zones being separated. Separation of the redundant work zones makes deformation easier and so, for a given reduction, the roll load decreases.

(b) tensile effect: During deformation, tensile stresses are set up in the "hard" component at the interfaces with the "soft" component, these stresses making



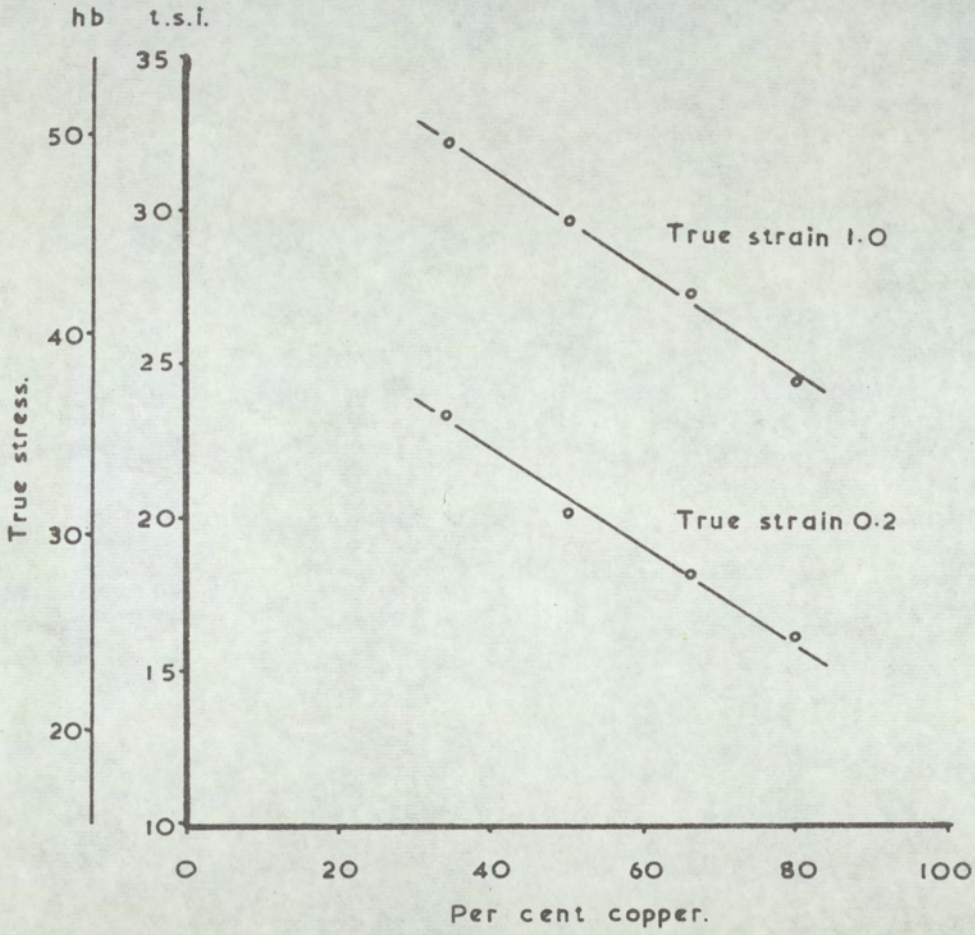


Figure 8.25 The variation of true stress (in plane strain compression) with per cent copper at true strain levels of 0.2 and 1.0.



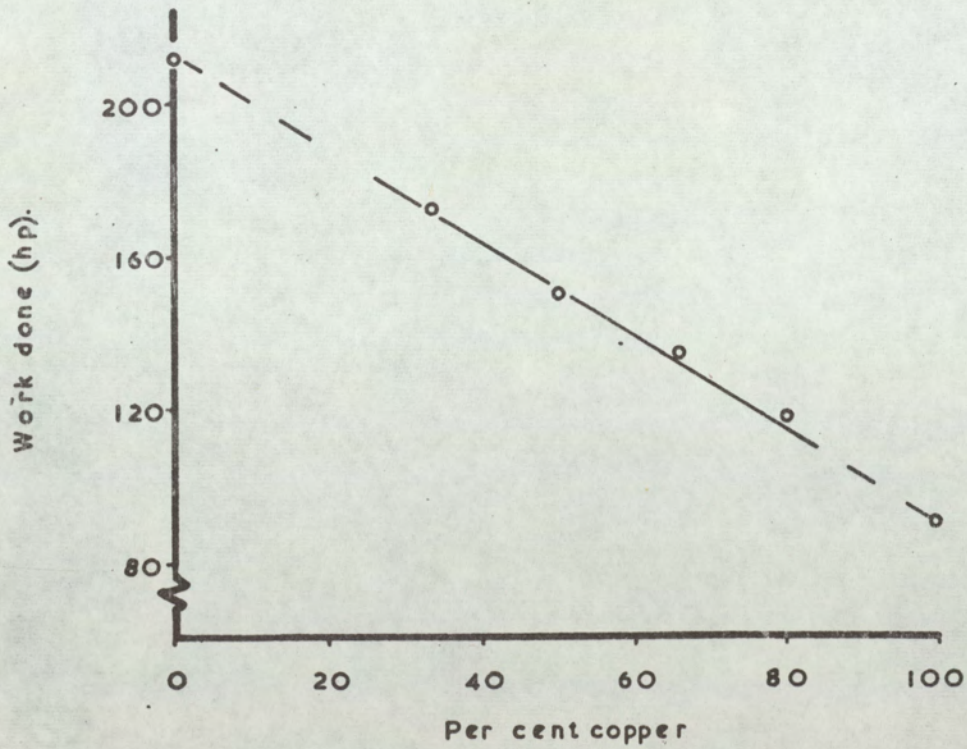
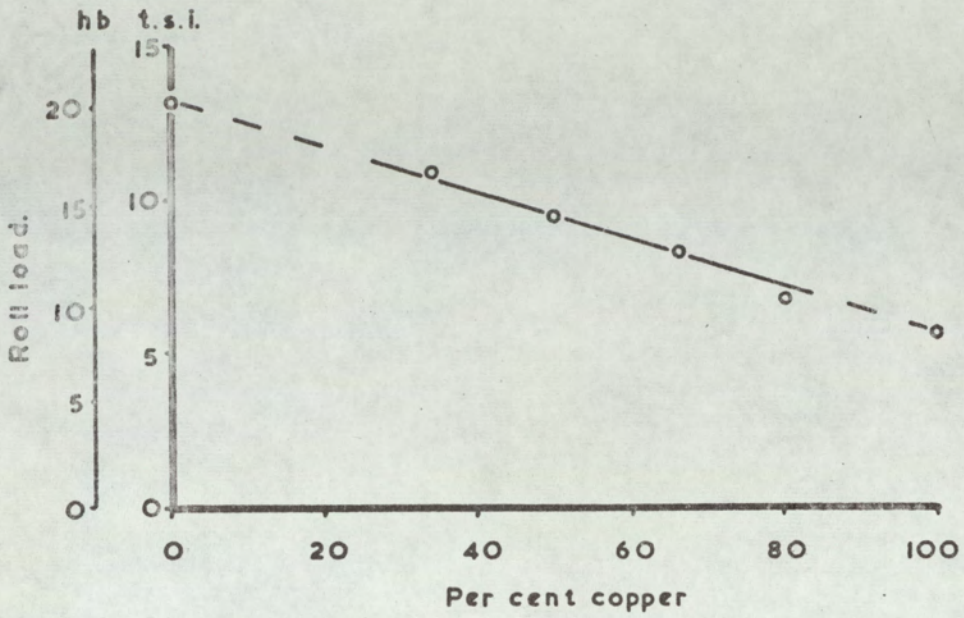


Figure 8.26 The variation of roll load and work done with per cent copper for a first pass rolling reduction of 30%.



deformation of the "hard" component easier, so that the roll load is again decreased.

However, as the thickness of the material is increased, the arc of contact is increased so that, for a given reduction, the roll load will increase.

The results of Arnold and Whitton<sup>(23)</sup> and Afonja and Sansome<sup>(24)</sup> may now be explained. The initial reduction in the curves of roll load against clad: core thickness ratio is attributed to the combined effect of factors (a) and (b), but a stage is reached when this decrease is offset by the increased roll load resulting from the increased arc of contact. As the thickness of the material is increased beyond this point, the increase in the arc of contact between the rolls and the composite, becomes the dominant factor and the roll load increases.

It may be seen that the clad: core thickness ratio, which will give a minimum roll load for a given reduction, will be determined by the relative magnitudes of the three factors that have been discussed. This explains why Alexander<sup>(33)</sup> found it impossible to theoretically determine the optimum thickness ratio. If the arc of contact remains constant for the varying clad: core thickness ratios, as was the case for the composites used in this work, no optimum thickness ratio is observed; roll load decreasing continuously as the thickness ratio of the "hard" to "soft" component, decreases.

#### 8.8 APPLICATION OF THE EQUAL STRAIN HYPOTHESIS TO THE PLANE STRAIN COMPRESSION PROPERTIES.

Plane strain compression tests were not made on either the copper or steel components of the composites because of lack of time and material. The plane strain compression properties of the composites were, therefore, predicted by the equal strain hypothesis from the properties of the 100% copper and 100% steel samples. The properties of these samples were not strictly comparable with those of the appropriate components of the composites, the use of these in predicting the tensile properties (table 8.1 Page 111) gave greater differences than was obtained when the correct properties of the composite components were used.



The percentage differences between the calculated and experimental results are shown in table 8.9 for both types of test pieces and at two strain levels. The differences between calculated and experimental results were found to decrease with strain; the maximum differences being + 34.7% at a true strain level of 0.1 and + 14.0% at 0.8 true strain.

The observed differences between the calculated and experimental results is somewhat greater than those observed for the tensile properties, particularly at low strain levels. Compressive stresses may be converted to their tensile equivalents by multiplying by the factor  $\sqrt{3}/2$ , so that it may be seen that the compressive properties of the composites should be predicted to the same degree of accuracy as were the tensile properties. The greater differences are, therefore, attributed to the use of the properties of the 100% copper and 100% steel samples, instead of the properties of the appropriate copper or steel components.



Table 8.9. The differences between calculated and experimental values of true stress for testpieces with  $dE_y = 0$  and for those with  $dE_z = 0$ .

Composite		% Difference at a true strain of 0.1 :		% Difference at a true strain of 0.8 :	
% Copper	% Steel	Test piece $dE_y = 0$	Test piece $dE_z = 0$	Test piece $dE_y = 0$	Test piece $dE_z = 0$
20	80	30.8	33.8	12.7	14.0
33	67	22.1	27.0	6.5	8.5
50	50	24.3	24.0	14.3	11.0
67	33	25.9	20.4	11.4	11.7
80	20	24.4	15.6	10.6	10.1
34	2 x 33	17.8	34.7	5.1	12.0
50	2 x 25	22.9	31.9	3.5	12.0
80	2 x 10	22.4	29.4	8.3	10.5
2 x 25	50	23.4	28.2	7.9	10.5
2 x 33	34	15.8	17.5	7.7	8.5



## 9.0 SUGGESTIONS FOR FURTHER WORK:

As there has been no previous investigations of the mechanical and press forming properties of clad material, it is suggested that similar investigations, to the one now reported, are made on combinations other than copper and steel. In particular the following points need further clarification:

1. the influence of the hardness ratio of the two composite components. For this it may be necessary to use adhesive bonded composites or to make a limited investigation using electro-deposited coatings. This investigation could also be extended to include metal/non-metal combinations e.g. plastic coated steel.
2. the relationship between the earing behaviour of the composites and its components. The components used for such an investigation should have greater earing potentials than had the copper and steel components of the composites used in this work, so that greater differences in earing behaviour would be observed. If the components were sufficiently thick to withstand the tendency to wrinkle, the investigation could be based on unbonded composites and the influence of combining materials having different earing potentials and/or strengths and with matched or mismatched rolling directions could be determined.
3. the relationship between properties and per cent clad in the regions of 0–20% and 80–100%. This relationship is of particular interest in stretch forming, greater penetrations having been obtained when the more ductile component was on the outer surface. If similar results were obtained in the ranges specified above, then, cladding could be used practically to improve stretch formability, especially if unbonded clads could be used.
4. the behaviour of composites, particularly of bilayer composites, under conditions of biaxial tension using the hydraulic bulge tester.



## 10.0 CONCLUSIONS:

1. During the tensile tests curling, about the longitudinal axis was observed, the degree of curling increasing with strain. Qualitatively it has been shown that curling is dependent upon the R values of the composite components. This behaviour may be utilized practically, e.g. in bending, by arranging the composite such that the component of lower R value forms the outer radius of the bend. If tension is applied during bending, the composite will have a natural tendency to bend in the required direction and, consequently, the bending load will be reduced.
2. The results have shown that the equal strain hypothesis may be used to predict the stress strain characteristics of the composites, both in tension and compression; mechanical properties such as proof stress, U.T.S., uniform elongation and R; the punch loads for deep drawing or stretch forming and mean cup heights. The degree of accuracy of results, predicted by the equal strain hypothesis, was generally improved when the appropriate properties of the composite components were used rather than those for the 100% copper and 100% steel samples. Properties such as U.T.S. and punch loads could be more accurately predicted than could properties such as R and uniform elongation, where the experimental values were difficult to accurately determine.
3. The work hardening indices ( $n$ ) of the composites could not be predicted by the equal strain hypothesis, although a function has been derived that enable 'n' to be calculated from the stress - strain characteristics of the composite components.
4. With the adhesive bonded composites the properties of the Redux were unknown so that it was not possible, with confidence, to include Redux in the equal strain hypothesis and, as a result, the calculated results were not as accurate as were those for the roll bonded composites.
5. No attempt was made to calculate the limiting draw ratios of the composites by means of the equal strain hypothesis because the experimental results were found to be influenced by tool geometry; especially the ratio of punch profile radius: sheet thickness.



6. In the deep drawing tests on the bilayer composites, greater mean cup heights and ear heights were obtained when the composites were deformed so that the copper was on the outer surface of the drawn cups. The greater mean cup heights have been attributed to the frictional conditions over the punch nose, whereas the differences in ear heights have been attributed to differences in the degree of radial drawing—in of the two components.
7. If the drawing of unbonded composites is to be practicable, relative slip of the composite components must be prevented, e.g. by adhesive bonding, or alternatively the components should be of a thickness where wrinkling is not likely to be a problem.
8. The theoretical analysis of draw stress has been modified to enable the calculation of the draw stress for the composites to be made using the stress—strain characteristics of the composite components. Using this modified analysis the maximum draw stresses for the composites have been calculated with similar accuracies as can those for single metals.
9. The stretch formability of the composites was found to be dependent upon the ductility of the outermost component, rather than on that of the composite.
10. A relationship between  $\beta$  and R has been suggested for material exhibiting planar anisotropy. This relationship has been shown experimentally to be more accurate than the relationship previously suggested.<sup>(65)</sup>
11. Using the results of the plane strain compression tests anomalies in the published results on composites have been clarified.



11.0 ACKNOWLEDGMENTS

The author would like to thank his supervisor, Professor J. C. Wright of the University of Aston in Birmingham, for helpful discussions, advice and encouragement.

The author gratefully acknowledges the assistance of the following for the supply of materials studied in this report:

I.M.I. (Kynoch)

Steel Company of Wales

Texas Instruments (Massachusetts)

Finally, the author would like to thank Mr. J. Booth of the British Steel Corporation (Midland Division) for carrying out the chemical analysis of the steel samples used in this work.



## 12.0 REFERENCES

1. Du Pont de Nemours Chem. & Eng. News 1963, 41, 50.
2. Durst, G., Jnl. of Metals, 1956, (March), 328
3. Agers, B.M., Ph.D. Thesis, Univ. of Wales, Sept., 1962 "Mechanisms of Pressure Welding".
4. Donelan, J.A., Sheet Met. Ind., 1963, 40, 863
5. Rollason, E.C., Ibid (Discussion)
6. Krivonosov, Y.I., et al Tsvet Metally, 1966, (12), 8.
7. Bianchi, L.M., Met. Prog., 1965, 87, (3), 127.
8. Rathbone, A.M., Blast Fnce. & Steel Plant, 1968, 56, 575.
9. Smirnov, V.S., et al Stal (in English), 1966, (11), 901.
10. Kameda, I., et al Mitsubishi Heavy Indust. Tech. Rev., 1967, 4, (2), 55.
11. Meandrov, L.V., et al Stal' In English, 1963, (4), 296.
12. Davies, D.H., M.Sc. Thesis, Univ. of Wales, Sept., 1965, "A Study of the Compression of Aluminium - Copper Laminates".
13. Holliday, L., "Composite Materials", Elsevier, 1966 Ed. Holiday, L., Ch.I, p.16
14. McDanel, D.L., et al Met. Prog. 1960, 78, (6), 118.
15. Broughtman, L.J., "Modern Composite Materials", Addison - Wesley 1967 Ed. Broughtman, L.J., & Krock, R.H., Ch.13 p.337
16. Cratchley, D., Met. Reviews, 1965, 10, 37, 79
17. Krock, R.H., Proc. A.S.T.M., 1963, 63, 605.
18. Krock, R.H., Proc. A.S.T.M., 1964, 64, 712.
19. Gurland, J., & Bardzil, P., Trans. A.I.M.E., 1955, 203, 311.
20. Krock, R.H., "Modern Composite Materials", Addison - Wesley 1967 Ed. Broughtman, L.J., & Krock, R.H., Ch. 16, p.455
21. Delagi, R.G., Machine Design, 1968, 40, (27), 133.
22. Holmes, E., Ph.D. Thesis, Univ. of Birmingham, 1955. "Formation of Ply-metals by Rolling"
23. Arnold, R.R., & Whitton, P.W., Proc.I. Mech. E., 1959, 173, (8), 241.
24. Afonja, A.A., & Sansome, D.H., TO BE PUBLISHED
25. Pomp, A., & Leug, W., Kaiser Wilhelm Inst. Iron Res., 1942, 24, 123.
26. Weinstein, A.S., & Pawelski, O., Advances in Machine Tool Design & Research, 8th Int. M.T.D.R. Conference, Sept. 1967, p.961.
27. Walker, R., Final year B.Sc. project report Univ. of Aston in Birmingham, 1970. "The plane strain compression properties of cold roll bonded copper/steel composites.
28. Bland, D.R., & Ford, H., Proc. I. Mech. E., 1948, 159, 145.
29. Cook, M., & Larke, E.C., J. Inst. Met. 1948, 74, 55.
30. Cook, M., & Parker, R.J., J. Inst. Met., 1953, 82, 129.
31. Watts, A.B., & Ford, H., Proc. I. Mech. E., 1952, 1B, 448.
32. Watts, A.B., & Ford, H., Proc. I. Mech. E., 1955, 169, 1141.



33. Alexander, J.M., Proc. I. Mech. E., 1959, 173, 241 (Disc.)
34. Edwards, R.D., J. Inst. Met., 1955, 84, 199.
35. Wright, J.C., Sheet Met. Ind., 1965, 42, 814.
36. Alexander, J.M., & Brewer, R.C., "Manufacturing Properties of Materials" Van Nostrand, London, 1963. p.303
37. Pearce, R., Sheet Met. Ind., 1964, 41, 567.
38. Chung, S.Y., & Swift, H.W. Proc. I. Mech. E., 1951, 165, 199.
39. Barlow, D.A., Engineering, 1956, 181, 329, 366, & 393.
40. Mintz, B., Internal Report, Univ. of Aston in Birmingham, Aug. 1968. "The Stretch formability and Deep drawability of Maraging Steel".
41. Wright, J.C., Sheet Met. Ind., 1961, 38, 649, 731, 813.
42. Kaftanaglu, B., & Alexander, J.M., J. Inst. Met., 1962, 90, 457.
43. King, F., & Turner, A.N., Inst. of Metals, Monograph & Report Series 1954, No.20, 45.
44. Svahn, O., J.I.S.I. 1954, 177, 129.
45. Willis, J., & Blade, J.C., Sheet Met. Ind., 1966, 43, 316.
46. Plevy, T.A.H., M.Sc. Thesis, Univ. of Aston in Birmingham 1968. "Planar Variations in Normal Anisotropy in Mild Steel Strip".
47. Jevons, J.D., "The Metallurgy of Deep drawing & Pressing", Chapman & Hall Ltd., London, 1940.
48. Pearce, R., Sheet Met. Ind., 1960, 37, 647.
49. Lloyd, D.H., Sheet Met. Ind., 1962, 39, 82.
50. Considère, A., Ann. ponts et chaussées, 1885, 9, ser.6, 574.
51. Voce, E., Metallurgia 1955, 51, 219.
52. Lankford, W., Snyder, S.C., & Bauscher, J.A., Trans. A.S.M., 1950, 42, 1197.
53. Butler, R., B.D.D.R.G. Colloquium "Fundamental Considerations in Sheet Metal Forming", London, March, 1964.
54. Whiteley, R.L., Trans. A.S.M., 1960, 52, 154.
55. Holcomb, R.T., & Backofen, W.A., Sheet Met. Ind., 1966, 43, 476.
56. Hosford, E.F., & Backofen, W.A., 9th Sagamore Ordnance Materials Research Conference, New York, 1962.
57. Duckett, R., Barry, B.T.K., & Robins, D.A., Sheet Met. Ind., 1968, 45, 666,
58. Nelson, P.G., Met. Prog., 1960, 78, 93.
59. Rathbone, A.M., Iron Age, 1967, 200, (Nov. 16th), 70.
60. Chung, S.Y., Sheet Met. Ind., 1951, 28, 453.
61. Griffiths, A.J., Ph.D. Thesis, Univ. of Aston in Birmingham 1967, "The press forming behaviour of austenitic & metastable stainless steels".
62. Euronorm 14-58 1958, C.D.620, 162-2.



## Services des Publications des Communiqués Européennes, Luxembourg

- |     |   |  |
|-----|---|--|
| 63. | CIBA (A.R.L.) Ltd.,                                 | Instruction Sheet No. A15d, June, 1967                                     |
| 64. | Roberts, W.T.,                                      | Sheet Met. Ind., 1966, 43, 237.  |
| 65. | Bonded Structures Divisions,<br>CIBA (A.R.L.) Ltd., | Redux 775, Advance Information Sheet (R775 – D3/X1), March, 1967.          |
| 66. | Ebert, L.J., Hecker, S.S., &<br>Hamilton, C.H.,     | J. Composite Materials 1968, 2, (4), 458.                                  |
| 67. | Metals & Controls                                   | Information Sheet IND-3B   |
| 68. | Metals & Controls                                   | Information Sheet IND-61   |
| 69. | Hill, R.,   | "The Mathematical Theory of Plasticity".<br>Clarendon Press, Oxford, 1950. |



**APPENDIX 1.**     *ANALYSIS OF THE DEEP DRAWING PROCESS FOR THE DRAWING OF  
FLAT BOTTOMED CYLINDRICAL CUPS.*

The draw stress may be calculated by summing the stresses necessary to produce:

- a.     radial drawing of the flange
- b.     bending over the die profile
- c.     overcome friction over the die profile
- d.     unbending over the die profile

In the analysis it is assumed that draing of the punch nose is negligible and that the tendency to form ears is also negligible. Drawing off the punch nose is unlikely to significantly influence the accuracy of predicting the maximum draw stress but will significantly influence the punch load—punch travel diagram. With respect to the earing tendency Chung and Swift<sup>(38)</sup> found that the accuracy of their predicted punch load — punch travel diagram decreased as the tendency to form ears increased.

1.     *RADIAL DRAWING OF THE FLANGE*

The stress required to draw in the flange may be determined by considering the forces acting on an element of material in the flange of radius,  $r$ ; width  $\delta r$ ; and initial thickness,  $t$ .

Acting on this element we have:

- |            |                                  |
|------------|----------------------------------|
| $\sigma_r$ | radial stress                    |
| $\sigma_c$ | compressional stress             |
| $\sigma_t$ | axial stress due to blank holder |

The stresses acting on a segment of the flange are shown in figure A.1.:



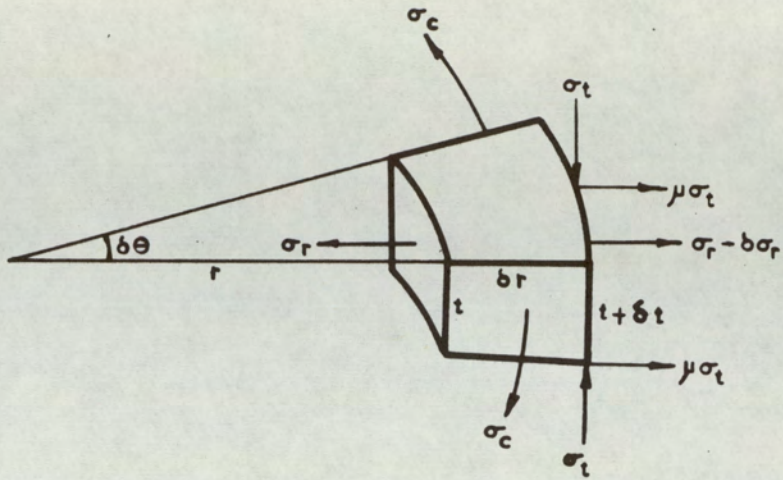


Figure A.1. The stresses acting on an element of the flange during radial drawing.

If the forces acting on this element are resolved radially and it is assumed that  $\delta\theta$  is so small that  $\sin \delta\theta = \delta\theta$  then:

$$\sigma_r t r \delta\theta - (\sigma_r - \delta\sigma_r) (r + \delta r) (t + \delta t) \delta\theta + 2 \left( \sigma_c \frac{\delta\theta}{2} \right) \left( t \delta r + \frac{\delta r \delta t}{2} \right) = 0 \quad \dots\dots\dots A.1$$

or  $\sigma_r t r - (\sigma_r - \delta\sigma_r) (r + \delta r) (t + \delta t) + \sigma_c \left( t \delta r + \frac{\delta r \delta t}{2} \right) = 0$  \dots\dots\dots A.2

Although considerable thickening of the flange occurs during drawing, Chung and Swift<sup>(38)</sup> found that at any instant the variation was less than 5%, so that the variation in thickness may be neglected (i.e.  $\delta t \approx 0$ ) and equation A.2. becomes:

$$\sigma_r r - \sigma_r r + r \delta\sigma_r - \sigma_r \delta r + \delta\sigma_r \delta r + \sigma_c \delta r = 0 \quad \dots\dots\dots A.3$$

If  $\delta\sigma_r$  and  $\delta r$  are themselves small their product may be neglected, so that equation A.3 becomes:



$$r\delta\sigma_r - \sigma_r\delta r + \sigma_c\delta r = 0 \quad \dots\dots\dots .A.4$$

$$\text{or } \frac{\delta\sigma_r}{\delta r} = \frac{(\sigma_r - \sigma_c)}{r} \quad \dots\dots\dots .A.5$$

Using the Tresca yield criterion ( $\bar{\sigma} = \sigma_{\max} - \sigma_{\min}$ )  
for the case under consideration  $\sigma_r > \sigma_t > \sigma_c$

$$\therefore \bar{\sigma} = \sigma_r - \sigma_c \quad \dots\dots\dots .A.6$$

The Tresca yield criterion is not however, as accurate as that of Von Mises which, if it is assumed that the through thickness stress ( $\sigma_t$ ), may be written as:

$$\bar{\sigma}^2 = \sigma_r^2 - \sigma_r \sigma_c + \sigma_c^2 \quad \dots\dots\dots .A.7$$

The difference between the two yield criterion never exceeds about 15% <sup>(36)</sup> in terms of the stresses and can be reduced by multiplying the left hand term of equation A.6 by a factor 'm', where m has a value between 1 and  $2/\sqrt{3}$ , say 1.1. The error in using the modified Tresca yield criterion rather than the more accurate Von Mises' criterion will be small.

Equation A.6 is rewritten as:

$$m\bar{\sigma} = \sigma_r - \sigma_c \quad \dots\dots\dots .A.8$$

Substituting equation A.8 into A.5:

$$\delta\sigma_r = m\bar{\sigma} \frac{\delta r}{r} \quad \dots\dots\dots .A.9$$

and integrating between limits of R and  $r_p$ , (where R = current radius of rim of blank and  $r_p$  = mean radius at the cup walls).

$$\sigma_r = m \bar{\sigma} \ln \frac{R}{r_p} + C \quad \dots\dots\dots .A.10$$

where C = integration constant.

The integration constant may be determined if it is assumed that the blank holder force acts only on the periphery of the blank, so that C depends on the frictional forces at this point:



$$C = \frac{\mu H}{\pi r_p t_p} \dots \dots \dots .A.11$$

where H = blank holder load.  
 $t_p$  = thickness at the mean cup wall radius.

In practice the blank holder load is distributed over an annulus of material rather than being concentrated at the periphery of the flange. The stress increment due to the blank holder load will be higher than the value predicted from A.11, but this increment is so very much smaller than the stress  $\sigma_r$  that the error arising from the use of equation A.11 will be negligible so that:

$$\sigma_r = m\bar{\sigma} \ln \frac{R}{r_p} + \frac{\mu H}{\pi r_p t_p} \dots \dots \dots .A.12$$

II *STRESS DUE TO BENDING AND UNBENDING OVER the DIE RADIUS:*

Chung<sup>(60)</sup> has shown that the radial stress,  $\sigma_B$ , required to bend or unbend the sheet over the die profile radius using the modified Tresca yield criterion is :

$$\sigma_B = \frac{m \bar{\sigma} t}{4 R_D} \dots \dots \dots .A.13$$

where  $R_D$  = radius to neutral axis of sheet = die profile radius + 1/2 sheet thickness.

t = current sheet thickness.

Barlow<sup>(39)</sup> found that a comparison of Chung's analysis with the more accurate and more complex formula of Chung & Swift<sup>(38)</sup> gave an error of about 3%. The stress due to bending and unbending is only 10–15% of the total stress so that the error arising from the use of Chung's analysis will be negligible.

III *STRESS DUE TO FRICTION:*

In allowing for friction Barlow<sup>(39)</sup> simplified Chung & Swifts<sup>(38)</sup> complex analysis by neglecting axial symmetry so that the problem could be solved using the slow speed transmission belt design formula:

$$T_1 = T_2 e^{\theta \mu} \dots \dots \dots .A.14$$



- where  $T_1 =$  applied tension  
 $T_2 =$  back tension  
 $\Theta =$  total angle of contact.

For the case under consideration:

- $T_1 =$  total stress due to radial drawing ( $\sigma'_{TR}$ )  
 $T_2 =$  summation of stress due to radial drawing, blank holder stress and stress due to bending over the die radius

i.e.  $T_2 = m \bar{\sigma} \ln \frac{R}{r_p} + \frac{\mu H}{\pi r_p t_p} + \frac{m \bar{\sigma} t}{4 R_D}$

$\Theta = \pi/2$

Substituting for  $T_1$ ,  $T_2$  and  $\Theta$  in equation A.14

$\sigma'_{TR} = \left( m \bar{\sigma} \ln \frac{R}{r_p} + \frac{\mu H}{\pi r_p t_p} + \frac{m \bar{\sigma} t}{4 R_D} \right) e^{\mu \pi / 2} \dots \dots \dots .A.15$

Total draw stress:

After being drawn over the die radius the sheet is unbent so that the total draw stress ( $\sigma_{TR}$ ) is

$\sigma'_{TR} + \frac{m \bar{\sigma} t}{4 R_D}$

or  $\sigma_{TR} = e^{\mu \pi / 2} \left( m \bar{\sigma} \ln \frac{R}{r_p} + \frac{\mu H}{\pi r_p t_p} \right) + \frac{m \bar{\sigma} t}{4 R_D} \left( e^{\mu \pi / 2} + 1 \right) \dots \dots \dots .A.16$



## APPENDIX 2. *SELECTION OF AN ADHESIVE FOR THE PRODUCTION OF THE ADHESIVE BONDED COMPOSITES*

### 1. *INTRODUCTION*

Adhesives for metal cladding should have high shear strengths so that, during deformation processes, the adhesive is capable of withstanding, and transmitting, the applied and induced stresses from one component to the other. In addition the adhesive should also be capable of plastically deforming with the metal components during deformation.

In section 2.1.3. it was stated that adhesives, for metal cladding applications, would be either those based on thermo-setting polymers, e.g. epoxy resins or those produced by a blend of the thermo-setting and thermo-plastic polymers e.g. vinyl-phenolic. A review of the trade literature on adhesives of these types revealed that there were numerous adhesives that could be used in metal cladding. A preliminary investigation was made to determine which, if any, of the commercially available adhesives would be suitable for metal cladding.

### 2. *ADHESIVES USED*

From the commercial adhesives available, three samples of high shear strength adhesives were chosen. Two of the three adhesives were based on thermo-setting polymers, epoxy and modified epoxy, whilst the third was a vinyl-phenolic resin, a blend of thermo-setting and thermo-plastic polymers. Data for the selected adhesive is shown in table A.1. The overlap shear strengths included in table A.1 were determined using aluminium alloy samples.

### 3. *MATERIALS USED*

0.057" thick commercial purity copper and 0.068" super purity aluminium were used for the experimental work. The copper was coated with a primer, as recommended by CIBA<sup>(63)</sup>, dried at 80°C for 30 minutes, cured at 150°C for 30 minutes and lightly abraded. Aluminium / copper composites were produced, the samples being bonded using the adhesives shown in table A.1. The adhesives were mixed, if necessary, and cured in accordance with the manufacturers instructions which are summarised in table A.1.



Table A.1. Adhesives examined

Adhesive	AZ15	EC2214	Redux 775
Supplier	CIBA	3M's	Bonded Structures Div. (CIBA)
Base	Epoxy	Modified Epoxy	Vinyl Phenolic
Consistency: Resin	Med. visc. liq <sup>d</sup>	) Soft paste	) 1 part
Hardener	Low visc. liq <sup>d</sup>	) (One part adhesive)	) film 0.020" thick
Mixing ratio: Resin	10	"	"
(parts by wt.) Hardener	3		
Cure cycle: Time (mins)	60 *	40	30
Temp. <sup>o</sup> (°C)	200 *	120	150
Pressure (p.s.i.)	Contact	Contact	10 – 100
Overlap Shear strength (p.s.i.)	4000	> 3000	4500

\* The composite components were coated with adhesive and dried at 100°C for 30 mins., prior to assembly and curing.



#### 4. *TENSILE AND DEEP DRAWING TESTS ON ADHESIVE BONDED COMPOSITES*

Tensile and deep-drawing tests were made on the composites to determine whether or not the adhesive would withstand severe deformation under simple and complex stress systems respectively.

All the adhesives performed satisfactorily in the deep drawing tests, no breakdown of the adhesive was observed in successfully drawing cups from 61 m.m. diameter blanks. However, in the tensile tests, where the adhesives were subjected to higher strain levels, only Redux performed satisfactorily. Adhesives AZ15 and EC2214 failed prematurely, and, in both cases, the aluminium component also failed prematurely.

#### 5. *CONCLUSIONS*

Only Redux of the three adhesives examined had sufficient strength and ductility to transmit the applied and induced stresses and strains, so that relative movement of the sandwich components was prevented in both the tensile and the deep drawing tests.

It would appear that the adhesives based on the epoxy or modified epoxy resins, e.g. AZ15 and EC2214, although possessing high shear strengths, are too brittle for metal cladding applications when the composites are to be subjected to severe deformation.



**APPENDIX 3. THE THEORETICAL CALCULATION OF DRAW STRESS**

Notation:

$R_o$	=	original radius of rim of blank
$R$	=	current radius of rim of blank
$r_p$	=	mean radius of cup walls = punch radius + $\frac{1}{2}$ sheet thickness
$r_o$	=	initial radius of element
$r_i$	=	current radius of element
$R_i$	=	original radius of the element at the mean cup wall radius.
$t$	=	original sheet thickness
$t_m$	=	mean blank thickness at the considered stage.

Other symbols have the same meaning as was assigned in Appendix I.

Consider the drawing of a flat bottomed cup from a 65 m.m. diameter blank of mild steel, using a 33 m.m. diameter punch, the original sheet thickness being 1.83 m.m. and the blank holder load 500 kg. We have therefore:

$R_o$	=	32.5 m.m.
$r_p$	=	17.4 m.m.
$t$	=	1.83 m.m.
$H$	=	500 kg.

Let us now consider an element of the flange which is close to the rim of the blank, say 32 m.m., and that the cup has been partially drawn such that the current radius of the rim of the blank is 30 m.m.

i.e.	$r_o$	=	32 m.m.
	$R$	=	30 m.m.



The stress due to plane radial drawing may be calculated using equation A.12 of Appendix 1. (page 171) :

$$\sigma_r = m \bar{\sigma} \ln \frac{R}{r_p} + \frac{\mu H}{\pi r_p t_p}$$

The quantities  $R$ ,  $r_p$ ,  $\mu$  and  $H$  are known; it remains to calculate  $t_p$  and  $\bar{\sigma}$  (the mean flow stress).

Chung and Swift's<sup>(38)</sup> results indicate that the thickness at the mean cup wall radius is not much greater than the original sheet thickness, and, as the stress due to the blank holder force is very much smaller than the stress  $\sigma_r$ , the error in using  $t$  will be small.

The mean flow stress may be calculated by taking a mean value between that for the metal at the rim (which has received the least work) and that for the metal at the mean cup wall radius at the considered instant (because this has received the greater work in the early stages of the draw where the maximum load is reached.)

At any instant, each element of the flange has been extended in the radial direction and compressed in the circumferential direction. Hill<sup>(69)</sup> has pointed out that the effective strain in any element during radial drawing for ratios  $< 2$  never differs from the absolute magnitude of the circumferential strain by more than 3% i.e. the current yield stress of any element corresponds to the circumferential strain received.

At the considered instant, the circumferential strain of the rim is known and that of the element at the mean cup wall radius may be calculated if its initial radius is known. The initial radius may be calculated from constancy of volume, being given by:—

$$R_i = \frac{\sqrt{R_o^2 - (R^2 - r_p^2)} \frac{tm}{t}}{t} \dots\dots\dots A.16$$

All the quantities in this expression are known, with the exception of  $t_m$ . Chung and Swift<sup>(38)</sup> calculated the development of thickness strain due to plane radial drawing and found that thickness was affected only slightly by changes in work hardening characteristic, blank holder load or friction so that the mean thickness at any



stage of the draw may be read with sufficient accuracy from their results shown in figure A.2

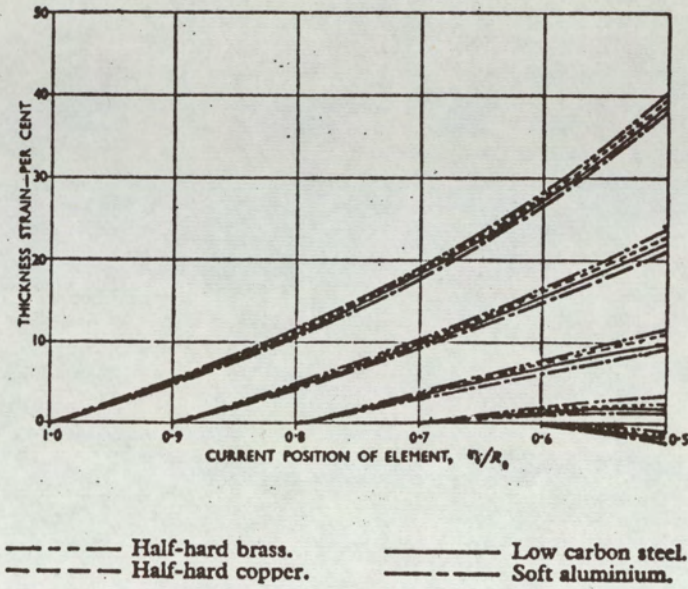


Figure A.2. The development of thickness strain due to radial drawing<sup>(38)</sup>

The value of  $t_m$  at the considered instant may be read from Figure A.2 if the current radius of the element,  $r_i$ , is known.  $r_i$  may be calculated, if it is assumed that the thickness of the flange is constant across the flat portion and that there is constancy of volume between  $r_i$  and  $R$ , using the following formula:—

$$r_i = R_o \sqrt{\left(\frac{R}{R_o}\right)^2 - \left[1 - \frac{r_o}{R_o}\right] \sqrt{\frac{R}{R_o}}} \dots\dots\dots A.17$$

At the considered instant  $R = 30$  m.m. so that

$$r_i = \underline{29.5} \text{ m.m.}$$

$$\begin{aligned} \text{The current position of the element} &= \frac{r_i}{R_o} \\ &= \underline{0.91} \end{aligned}$$

so that from figure A.2  $t_m = \underline{1.047} t$



Substituting for  $R_o$ ,  $R$ ,  $r_p$  and  $t_m$  in equation A.16

$$R_i = \underline{20.76} \text{ m.m.}$$

The radial strain of the rim and of the element at the mean cup wall radius may now be calculated:

$$\text{Radial strain of the rim} = \ln \frac{R_o}{R} \quad \dots\dots\dots \text{A.18}$$

$$= \underline{0.0798}$$

$$\begin{aligned} \text{Radial strain of element at the} \\ \text{mean cup wall radius} &= \ln \frac{R_i}{r} \quad \dots\dots\dots \text{A.19} \end{aligned}$$

$$= \underline{0.1782}$$

The corresponding stresses may be calculated from the true stress — true strain curve :

$$\sigma = k\delta^n \quad \dots\dots\dots \text{A.20}$$

$$\text{For the mild steel: } k = 56.2 \text{ kg/mm}^2 \quad (57.3 \text{ hb})$$

$$n = 0.159$$

$$\therefore \sigma_{\text{Rim}} = 37.3 \text{ kg/mm}^2 \quad (38.1 \text{ hb})$$

$$\sigma_{\text{cupwall}} = 42.7 \text{ kg/mm}^2 \quad (43.6 \text{ hb})$$

$$\bar{\sigma} = \frac{\sigma_{\text{rim}} + \sigma_{\text{cupwall}}}{2}$$

$$\bar{\sigma} = \underline{40.0} \text{ kg/mm}^2 \quad (40.8 \text{ hb})$$



The radial tensile stress at the mean cup wall radius due to the blankholder load is

$$\frac{\mu H}{\pi r_p t_p}$$

According to Chung and Swift<sup>(38)</sup> at the maximum load the thickness at the mean cup wall radius is not much greater than the original blank thickness so that  $t_p \simeq t$ .

If the coefficient of friction ( $\mu$ ) is assumed to be 0.02 all the quantities in equation A.12 are now known so that  $\sigma_r$  may be calculated.

$$\sigma_r = m\bar{\sigma} \ln \frac{R}{r_p} + \frac{\mu H}{\pi r_p t_p}$$

$$\sigma_r = 24.1 \text{ kg/m.m.}^2 \quad (24.6 \text{ hb})$$

The stress due to bending and unbending over the die radius may be calculated using equation A.13 (page 171.)

$$\sigma_B \simeq \frac{m\bar{\sigma} t}{4R_D}$$

In equation A.13 the thickness of the sheet at the mean cup wall radius has again been assumed to be approximately equal to the original sheet thickness. For simplicity the flow stress for the material at the mean cup wall radius can be taken for bending, this will give slightly high results as the metal at the beginning of the die profile radius will have a slightly lower yield stress than that at the mean cup wall radius.

Substituting these values of  $t$  and  $\sigma$  in equation A.13, with a die profile radius of 3 m.m.:

$$\sigma_B = 5 \text{ kg/mm}^2 \quad (5.1 \text{ hb})$$



The total draw stress may now be calculated using equation A.16:

$$\sigma_{Tr} = e^{\mu\pi/2} \left( m \bar{\sigma} \ln \frac{R}{r_p} + \frac{\mu H}{\pi r_p t_p} \right) + \frac{m \sigma_t}{4R_D} (e^{\mu\pi/2} + 1)$$

$$\sigma_{Tr} = 34.8 \text{ Kg/mm}^2 \quad (35.5 \text{ hb})$$

In order to calculate the maximum draw stress the calculations were repeated for several draw ratios and also for several elements in the flange. The maximum draw stress determined in this way was compared with the experimental maximum draw stress.

The experimental draw stress was determined by assuming that the load bearing cross sectional area of the cup walls was given by:

$$2\pi R_p t \quad \text{where } R_p = \text{radius of the punch}$$

The region of the cup wall near the punch profile radius is locally thinned, so that its load bearing area is reduced, as a result of being bent and unbent over the punch-profile radius. This localised thinning is accompanied by an increase in strength as a result of this region work hardening more than the surrounding regions, so that its effective load bearing capacity is greater than is suggested by its thickness alone. For this reason the original sheet thickness was taken as being representative of the load bearing capacity of the cup walls.